MITIGATION OF THE INFLAMMATORY RESPONSE TO BIOPROSTHETIC HEART VALVE TISSUE THROUGH ANTIGEN-DIRECTED MASKING

by

Engela Helena du Plessis

B.Sc.(HONS)

Student number: VMRENG003

SUBMITTED TO THE UNIVERSITY OF CAPE TOWN

In dissertation fulfilment of the requirements for the degree

M.Sc.(Med) in Cardiothoracic Surgery

Faculty of Health Sciences

UNIVERSITY OF CAPE TOWN

Date of submission: 13 February 2009

Supervisor: Dr Paul Human

Cardiovascular Research Unit

Chris Barnard Division of Cardiothoracic Surgery

University of Cape Town

Acknowledgements

My sincere thanks and appreciation to:

- Dr Paul Human, without whose guidance, dedication and encouragement this thesis would not have been possible. His most valued comments and suggestions throughout the project as well as his time and effort with editing this thesis were greatly appreciated.

- Mrs Helen Ilsely for preparations of the histology slides and operating the TEM. Her expertise and comments with regards to the interpretation of the histology contributed to my understanding of the results.

- Mrs Melanie Black for teaching me most of the histology and immunohistology techniques.

- Mr Noel Markgraaf of UCT Animal unit for his support and assistance with the care of the animals.

- All members of the Cardiovascular Research Unit for their contribution, expertise, assistance and support with this project

- My husband, Louis for all his patience, motivation and support.

Table of contents

A. Abstract

Patients requiring heart valve replacement surgery due to rheumatic or congenital heart valve disease have the option of receiving either a mechanical valve, a homograft human cadaver or a chemically treated bioprosthetic heart valve from animal tissue. Each valve has its limitations. The latter has a limited lifespan in younger patients with calcification the major cause of failure. Recently the significance of inflammatory response to these valves has been highlighted as well as the role that it may play in calcification and therefore contributing to the failure of these valves.

This research was firstly directed to characterise the immune response to bioprosthetic heart valves in patients as well as in animal models. The study further demonstrated that the glutaraldehyde concentration applied to commercial heart valves is insufficient to mask the antigenicity of the tissue, therefore an method of masking antigens to mitigate the inflammatory response is needed.

Rabbits were immunised with porcine aortic wall, decellularised porcine aortic wall and porcine plasma fibronectin. Tissue specific immunoglobulin was isolated and the Fc fragment removed to produce immunoglobulin fragments which were used to mask porcine aortic tissue against Fc receptor mediated adherence inflammatory cells.

The finding of this thesis was that bioprosthetic heart valve tissue elicits an immune response in patients and animal models. The concept of applying antigen-directed antibody fragments to porcine aortic tissue clearly was shown to mask the antigens and mitigate binding of intact antibodies to the tissue *in vitro*. A rabbit pilot *in vitro* study did not show a clear benefit when the antibody fragments were tethered onto the tissue. The *in vitro* results were nevertheless encouraging and its potential should still be further investigated.

B. Introduction

B1. Heart Valves

The heart consists of four chambers with a valve at every exit of the chamber, namely the aortic, pulmonary, mitral and tricuspid valves, which are essential to the physiological functioning of the heart. These valves (see figure B-1) permit unidirectional flow of blood through the heart without obstruction or regurgitation. The valve function is pressure driven. When the blood pressure below the valve is greater than the pressure above, the leaflets are forced towards the outside, causing the valve to open. When the blood pressure above the valve is greater than the pressure below, the valve closes by pushing the leaflets toward the centre. Blood flows from the body into the right atrium through the open tricuspid valve (ventricular relaxation) into the right ventricle. The pulmonary valve opens (ventricular contraction) and the blood is pushed into the pulmonary trunk towards the lungs. The left atrium receives the oxygenated blood from the lungs and the blood flows through the open mitral valve (ventricular relaxation) into the left ventricle. The aortic valve opens (ventricular contraction) and the oxygenated blood is pushed into the aorta and flows to the rest of the body.

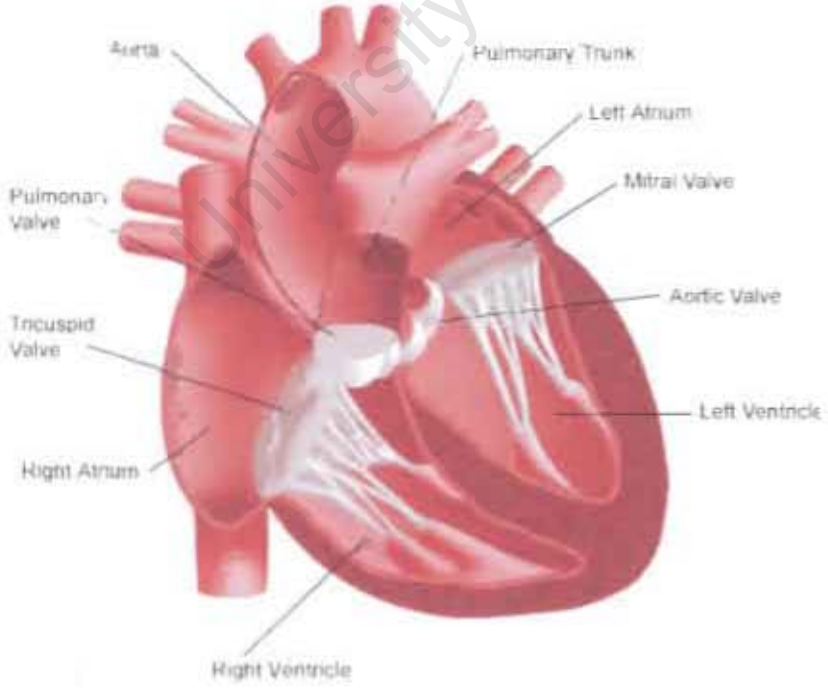

Figure B-1 Anatomy of the heart

B1.1. Anatomy of Heart Valves

The aortic valve has cup-like leaflets composed of thin sheets of soft tissue anchored in the aortic wall. A cross-section of the leaflet shows three distinct layers[1] (see figure 2), each with specific extracellular matrix components. The top layer of the leaflet on the outflow side is the fibrosa[2], which is composed of densely packed collagen bundles and fibres with a matrix of elastin surrounding the collagen bundles. It is the primary structural layer that provides strength and prevents the leaflet from sagging. The layer on the inflow side is the ventricularis[2]. This layer has dense collagen with elastic fibres and is less stiff than the fibrosa, allowing the leaflet to stretch when closed[3]. The middle layer connecting the fibrosa and ventricularis together is the spongiosa. This layer is composed of loosely arranged collagen and abundant glycosaminoglycans. The glycosaminoglycans are capable of absorbing a large amount of water within the tissue matrix. This matrix serves to decrease the shear stresses associated with continuous bending, rearranging, straightening, and rotating during valve function[4-10]. The valvular interstitial cells such as fibroblasts, as well as endothelial cells and resident macrophages are present in abundance in the valve tissue. Fibroblasts synthesise the several types of valvular extracellular matrix molecules. The valve undergoes constant physiological remodelling that entails the synthesis, degradation, and reorganization of its extracellular matrix[11, 12]. Thus, heart valves are specialised components of the heart that rely on balanced homeostatic activities for their mechanical and biological functions.

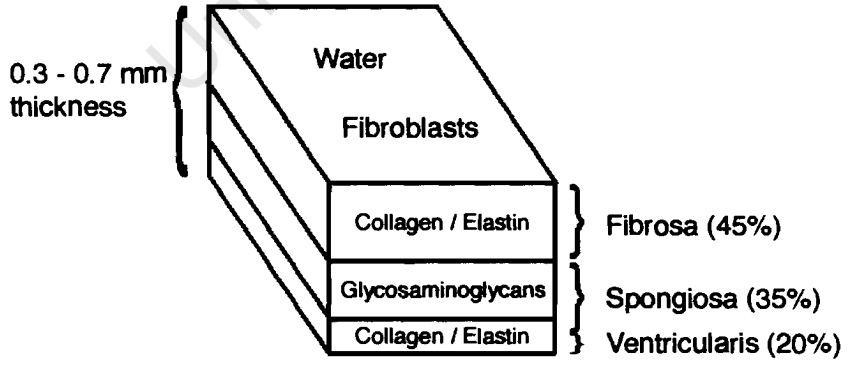

Figure B-2 Schematic cross-section of the leaflet

B1.2. Pathology

Heart valve diseases are typically associated with either acquired calcific disease, degeneration of congenitally abnormal valves, atherosclerosis, infections

(endocarditis), or rheumatic heart disease and results in progressively defective valves[12]. Valve dysfunction limits the valves to open and close properly. This results in imperfect closure, permitting back flow (insufficiency or regurgitation) or incomplete opening, limiting forward blood flow (stenosis) or both. Either process critically influences the performance of the heart, possible hampering the heart's ability to pump blood adequately through the body. Damaged heart valves lack the ability to spontaneously regenerate[13] and the only treatment option presently available is open-heart surgery, in which the diseased valve is either repaired or removed and replaced with a prosthetic one. Endovascularly deployed valves may offer and alternative to open-heart surgery, but would similarly rely on the introduction of a tissue based valve prosthesis.

B2. Prosthetic heart valves

Heart valve disease is a worldwide problem and ultimately leads to most patients with the disease needing heart valve replacement surgery. It entails surgical removal of the diseased valve and suturing in its place a prosthetic valve made of non-living, biocompatible biomaterials to resume valvular mechanical functions. Heart valve replacement is often lifesaving and improves recipient's quality of life[14]. The first heart valve replacements performed in 1960 were mechanical devices[15, 16]. In 1962 the first biological heart valve was used when Ross replaced an aortic valve with a freeze-dried valve from human cadavers (homograft)[17], and in 1965 the first bioprosthetic valves from porcine aortic tissue were used[18]. The porcine prosthesis was the valve of choice in the 1970s and early 1980s[19]. However, the increasing incidence of structural valve degeneration of these porcine valves[20, 21] resulted in an increased used of mechanical valves[22] with biological valves being limited to patients in whom anticoagulation was contraindicated or to elderly patients[14, 19, 23]. The second generation of tissue valves improved their durability, but structural valve degeneration was still the limiting factor. Worldwide, over 275,000 heart valve replacement operations are performed annually[24]. Presently, over 50% of implanted prosthetic heart valves are mechanical valves, approximately 45% are bioprosthetic valves and the remainder are pulmonary autograft valves and human cryopreserved homografts[25]. The use of mechanical heart valves is increasing at a rate of 3 – 5 % per year compared to bioprosthetic heart valves increasing at 8 – 11%[26].

The ideal replacement valve should have the following characteristics[27-29]:

- Replicate the function of the natural valve, have good hemodynamic performance, open to allow unimpeded flow and close preventing regurgitation, and have limited resistance to blood flow while moving;
- Include living cellular components with the ability to repair structural injury, renewal of the cell population; remodel the extracellular matrix, and potentially grow;
- Be biocompatible, **non-immunogenic, non-inflammatory,** non-calcifying and with a substrate not supportive of infections;
- Have non-thromobogenic blood-contacting surfaces;
- Be chemically stable, non-leachable, and with non-cytotoxic components;
- Provide ease of implantation using minimally invasive surgery and integration into host tissue with minimal host healing response;
- Be durable to withstand 40 million cardiac cycles each year, resistant to wear and maintain structural properties throughout lifetime;
- Ensure that the patient's daily activities are uncompromised by the valve;
- Have a long-term shelf life without changes in properties and sterility;
- Be available in all sizes with design features adaptable to individual patients requirements; and
- Be reasonable priced.

There is currently no prosthetic heart valve that meets all of the criteria listed above. With respect to bioprosthetic tissue valves immunogenicity remains a key determinant of their potential for success or failure and our exploration aimed at modifying and/or masking residual antigens capable of eliciting a host response is justified in the quest to prolong the life of a bioprosthetic heart valve.

B2.1. Mechanical heart valves

Mechanical heart valves are constructed of rigid supporting materials and mobile components using only inert, biocompatible materials such as pyrolitic carbon, polyester (Dacron)-covered polymers, or metals[26]. All mechanical valves have a similar basic structure with three essential components: (1) the occluder, (2) the housing and (3) the sewing ring. The occluder is one or more moveable part, which

may be a ball, a disc, or a hinged leaflet. The occluder fits in the housing, which help the occluder to move by guiding and restricting its movement. The fabric-sewing cuff is attached to the housing, to allow implantation of the device[26]. Blood pressure differences within the chambers of the heart enable these mechanical valves to function properly.

There are three general designs for mechanical valves, ball-in-cage valves, tilting-disc valves, and bileaflet valves[26, 29, 30]. Currently, the most commonly used mechanical valves are the bileaflet valves. Mechanical valve complications include design or material failure, infections, and tissue overgrowth. Structural failure of mechanical valves is almost nonexistent and they can be expected to perform properly for at least 20 years[29]. Imperfect blood flow through some of these devices can create non-physiological patterns that may induce the formation of blood clots. Furthermore, the surfaces exposed directly to blood flow are not entirely non-thrombogenic and mechanical valves are prone to thrombosis[30]. Thus, patients are required to take anticoagulation medications for the rest of their lives[27].

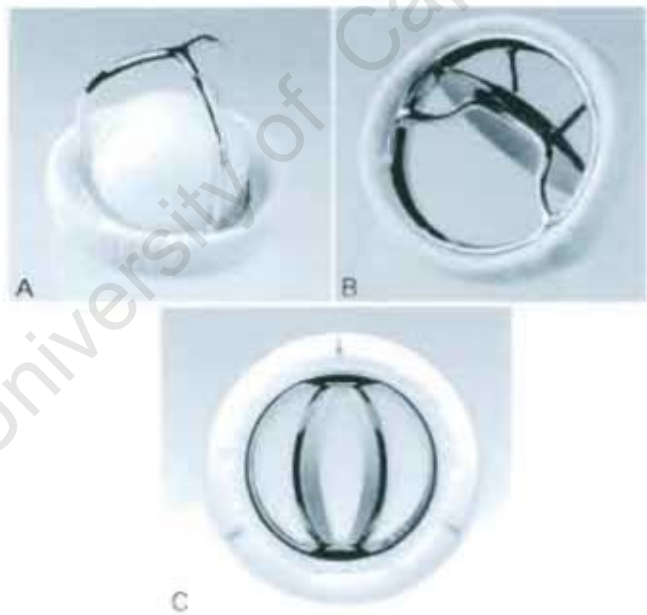

Figure B-3 The general designs of mechanical valves: A) ball-in-cage valves, B) tilting-disc valve and C) bileaflet valves.

Anticoagulation treatment is associated with bleeding complications[29]. The consequence in first world countries is overregulated, whereas in developing or third world countries suboptimal anticoagulating is the norm, often resulting in fatal acute thromboembolic events. Patients with contraindication for anticoagulation and in

developing countries with limited access to healthcare facilities should therefore ideally have a bioprosthetic heart valve implanted, although currently the trend is towards the use of mechanical valves in these countries due to a resistance by surgeons who are fearful of having to perform complicated and high risk redo valve replacements at a later stage. Mechanical valves are not recommended for pregnant women, or women considering pregnancy, because Warfarin (anticoagulation treatment) is associated with embryopathy (a developmental disorder in an embryo), spontaneous abortions, stillbirths, and less commonly, central nervous system defects and fetal bleeding with exposure beyond the first trimester[31].

B2.2. Biological heart valves

Biological heart valves may be divided into two groups. The one group are tissue heart valves prepared from human tissue specifically homografts or autografts. The second group are bioprosthetic heart valves prepared from chemically treated animal tissue such as porcine aortic valve tissue or bovine pericardial sheets. Currently, 45% of heart valve replacements are bioprosthetic valves[25]. Bioprosthetic heart valves are the prosthesis of choice in elderly patients since anticoagulation is avoided[14, 32-35]. These valves are contraindicated in children and adolescents, however, as they produce severe short-term calcification[36-38] with acute hemodynamic deterioration necessitating urgent valve replacement[33, 39, 40]. Homografts are a popular choice but its use is restricted to less than 5% of cases because of their limited availability.

B2.2.A Autografts (Ross procedure)

Autografts were first used in 1967[41]. The Ross procedure is a procedure for patients requiring aortic valve replacement[42-45]. In the Ross procedure[41] the diseased aortic valve is replaced by the patient's own pulmonary valve (autograft). The patient's pulmonary valve is replaced by an aortic homograft. This procedure is attractive for children, athletes and woman of childbearing age because it eliminates the use of anticoagulation and has the potential for somatic growth[46].

The major concern is the complexity of insertion technique and the long-term consequence of trading one diseased valve for the possibility of two diseased valves. There is a risk of dilation and consequently insufficiency in the pulmonary autograft[43, 47] and is the leading cause of late reoperation. Homograft stenosis is the primary reason for reoperation of the homograft valve[42, 48, 49]. Structural valve degeneration and calcification do not appear to be common complications with pulmonary

autografts. Freedom from reoperation 20 years after the Ross procedure can be expected to be 75% for the autograft and 80% for the homograft[49, 50]. Autografts have excellent durability after implantation, but are not readily available for all patients[8].

B2.2.B Homografts

Homografts were first used in 1962[17] and involve valves harvested from human cadavers. In 1962 Ross performed the first homograft replacement of the aortic valve using a freeze-dried valve from a cadaver[17]. Preservation of valves harvested from cadavers to increase storage times improved availability and access to homograft valves. The standard storage technique for homograft valves is cryopreservation using cryoprotectants and storage in liquid nitrogen vapour at -180°C. Cryopreserved homograft valves have morphologically intact tissue structure at the time of implantation[51] and are superior to fresh homograft valves[52-54]. Cryopreservation allows storage of homograft heart valves for years while maintaining graft viability[53].

Cryopreserved homograft valves nevertheless have been shown to elicit a host immune response[55-59]. These valves have decreased durability in younger children, which has been attributed to an accelerated immune response-mediated valve failure[58, 60]. The graft contains viable interstitial cells[61, 62] and endothelial cells[51, 63] that may contribute to the immune response[64]. Specifically the viable cells present in cryopreserved homograft human valves are capable of expressing human leukocyte antigen class I and II antigens and induce alloantibodies[60, 65], which could damage transplanted tissue and contribute to early degradation of homograft function[59, 60]. In homograft implants blood group incompatibility between recipient and donor may also play a role in homograft dysfunction and fibrocalcification, particularly in very young patients (3 years old or younger)[51, 55, 66]. Cryopreserved homograft valves have viable cells at the time of implantation, but experimental studies showed early cell death from metabolic depletion[67, 68]. Currently, decellularised homograft valves are also used and clinical studies indicate a reduced immune response and the potential to repopulate with host cells[69].

B2.2.C Bioprosthetic heart valves

Porcine aortic valves were first used in 1965[18]. These valves are composed of animal tissues that have been chemically treated to improve their biocompatibility. Cross-species implantation of untreated animal tissues is prone to severe immune

rejection and rapid tissue degeneration and resorption. For this reason, bioprosthetic heart valve tissues are treated with glutaraldehyde, which covalently cross-links protein[70] to suppress immunogenicity[71, 72] and stabilise the tissue against proteolytic degradation once implanted[73, 74]. Porcine bioprostheses for valve replacement was first used in 1965[18]. In the 1970s, bovine pericardial valve constructs were also used[75]. Currently, the predominantly used bioprosthetic valves are made from glutaraldehyde treated porcine aortic valve tissue or bovine pericardial tissue, designed to imitate the flow and material properties of the human heart valve.

Bioprosthetic valves have central flow, good hemodynamics and good thrombo-resistant surfaces. Glutaraldehyde fixation is often believed to be directly responsible for calcification of bioprosthesis[76], the main reason for structural valve deterioration[77]. The xenograft material is antigenic and must nevertheless be cross-linked to prevent acute rejection. As a result glutaraldehyde is used at lower concentrations (0.2% – 0.6%) to reduce the risk of calcification, with minimal regard for the risk of inflammation and immune responses.

B2.2.C(1) Stented versus non-stented valves

The three main designs of bioprosthetic valves are stented porcine valves, stented pericardial valves and non-stented porcine valves[25]. Stented valves are made from either glutaraldehyde treated porcine aortic valve tissue or glutaraldehyde treated flat sheets of bovine pericardial tissue mounted on a stent made of metal or plastic and covered with synthetic fabric[25]. The stent facilitates handling, insertion and attachment of the prosthesis to the recipient aortic root, but it adds a bulky, nonbiological component to the bioprostheses. The non-stented porcine valves overcame this problem, using whole porcine aortic root fixed in glutaraldehyde, with minimal or no fabric cover[78]. Although promising improved hemodynamics, these valves are more difficult to implant and are ignored by the majority of surgeons.

Second generation pericardial valve designs have better hemodynamics over stented porcine valves and similar hemodynamics to non-stented porcine valves. The fundamental advantage of stentless valves over stented valves is greater orifice area. These have very low to zero residual gradient[79] and excellent hemodynamics[79]. However, non-stented valves have similar structural valve deterioration rates and may fail at the same rate as stented valves[80].

B2.2.C(2) Failure modes of bioprosthetic valves

The first generation porcine aortic valves suffered from structural valve degeneration due to calcification and bovine pericardial valves had design-related problems with shorter lifetimes due to leaflet tears than porcine aortic valves [81, 82]. These valves were fixed at high-pressure giving very stiff, noncompliant leaflet material and cause flexure fatigue-related valve leaflet damage[83]. In the 1980s, high-pressure fixation was abandoned in favour of low-pressure fixation and anti-mineralization treatments were applied to improve the durability of second-generation valves[84]. Second generation bioprosthetic valves though have similar structural valve deterioration rates[32].

The limitation of bioprosthetic heart valves is durability in the long-term. The leading cause of bioprosthetic heart valve dysfunction is structural valve deterioration, which begins to increase 5 to 6 years after implantation[33, 39].

B3. Structural valve deterioration

The major two determinants of bioprosthetic heart valve structural degeneration that receive the most attention in literature are dystrophic calcification and mechanical damage with minimal emphasis on inflammatory and immune processes, which only now are being recognized.

After implantation bioprosthetic heart valves undergo a complex, time-dependant process of structural changes, resulting in the dysfunction of the valve. Repeat surgery for replacement of bioprosthetic heart valves is a relatively common event. Clinical follow-ups indicate that more than 50% of patients with artificial heart valve implants develop complications within 10 years[12]. The major cause of repeat surgery for bioprosthetic heart valves is structural valve deterioration, which refers to dysfunction of the valve resulting from any intrinsic degenerative change causing stenosis or regurgitation[33, 39, 85].

Bioprosthetic heart valve degeneration is a complex process. In clinical studies of the failure of bioprosthetic heart valves, the term structural valve deterioration is used without clearly classifying the cause of failure as either calcification, primary tearing, pannus outgrowth, leaflet dehiscence or a combination of causes. Tearing of leaflets was due to calcification, which leads to higher stress and secondary collagen fibre damage and leaflet tearing. Vesely et al[86] studied this hypothesis and found leaflet tears develop independent of calcification as a result of mechanical damage.

Bioprosthetic heart valves constructed from porcine aortic valves or bovine pericardial sheets, which are obtained from the abattoir, begin to degrade immediately. Major degenerative changes already occur during tissue preparation of these heart valves. The cells lose their viability, the endothelium is largely denuded and extracellular matrix components are modified[9]. The material is cross-linked primarily to mask antigenic properties[87] and secondly to stabilise the tissue, resulting in a nonviable material that at best maintains the original structural and some degree of mechanical integrity of the tissue. Biological integrity is however, lost.

B3.1. First versus second generation valves

First-generation bioprosthetic heart valves were valves from porcine aortic tissue and bovine pericardium tissue fixed with glutaraldehyde at high pressure without any anti-mineralization treatment. Calcification was the major cause of failure for first-generation porcine bioprosthetic heart valves[88]. Primary leaflet tears were the major problem for first-generation bovine pericardium bioprosthetic heart valves[89].

Porcine and pericardial tissue valve designs were revised and second-generation valves were fixed in glutaraldehyde at low pressure and treated with anti-mineralization agents. They have comparable long-term freedom from thromboembolism, endocarditis, and nonstructural valve complications[90].

The ten year study of Butany et al[91] found that structural valve degeneration neverthless still remains the major problem. Prosthetic valves explanted after failure showed high rates of stent deformation, calcification, and pannus overgrowth. Analysis of explanted mechanical and bioprosthetic valves revealed overall causes of failure which included perivalvular leaks, thrombosis, host tissue overgrowth, degeneration or mechanical failure, and susceptibility to infections[92]. Complications related to thrombogenicity are the major problems of mechanical valves, whereas tissue-derived valves are mainly affected by the degeneration and calcification of the tissue components.

B3.2. Calcification of bioprosthetic heart valves

The failure of bioprosthetic heart valves is mainly due to tissue valve calcification[8, 88, 90, 91, 93-96]. Calcium deposits increase stiffness, weaken the tissue, reduce the pliability of the leaflets, tearing, and results in stenosis or insufficiency, or both. The mechanisms of calcification and the factors that induce the calcium hyroxyapatite crystal formation are not fully understood and many hypotheses are proposed. The

cross-linking process and the presence of foreign proteins and cells appear to play a key role in calcification of tissue heart valves.

B3.2.A Factors that influence bioprosthetic heart valve calcification

Many independent factors determine calcification and can be summarised as 1) implant composition, 2) chemical treatment, 3) mechanical factors, and 4) host factors.

B3.2.A(1) Implant composition

The main tissue types used for bioprosthetic heart valves are from bovine pericardium and porcine aortic valves. The valve leaflets and aortic walls are used to construct either a stentless valve (part of the aortic wall tissue with the leaflets and a small fabric covering) or a stented valve (valve mounted on a stent with fabric sewing ring covering the valve orifice at the base). Bioprosthetic tissue consists of cells embedded in an extracellular matrix composed mainly of varying proportions of collagen, elastin and glycosaminoglycans (GAGs) (see table 1). Pericardial tissue is mainly composed of collagen[97]. The major difference between leaflets and aortic wall tissue is the composition of the extracellular matrix components. Collagen type I is a major component of leaflets extracellular matrix whereas elastin is the major extracellular matrix component of post-sinotubular junction aortic wall[98].

Examination of explanted bioprostheses indicates that calcification is associated with mitochondria, membrane fragments and cell debris of all glutaraldehyde fixed tissues used for bioprosthetic heart valves[99, 100]. However, collagen calcifies readily in leaflets and pericardium, and elastin calcifies independently in the aortic walls irrespective of glutaraldehyde treatment[97, 98]. Thus, cells or cellular materials are not solely responsible for calcification of bioprosthetic tissue. Collagen and elastin can serve as nucleation sites for calcium phosphate minerals, independent from cellular components[8, 96]. Collagen and elastin calcification is poorly understood. Elastin is hydrophobic and may adsorb cellular material.

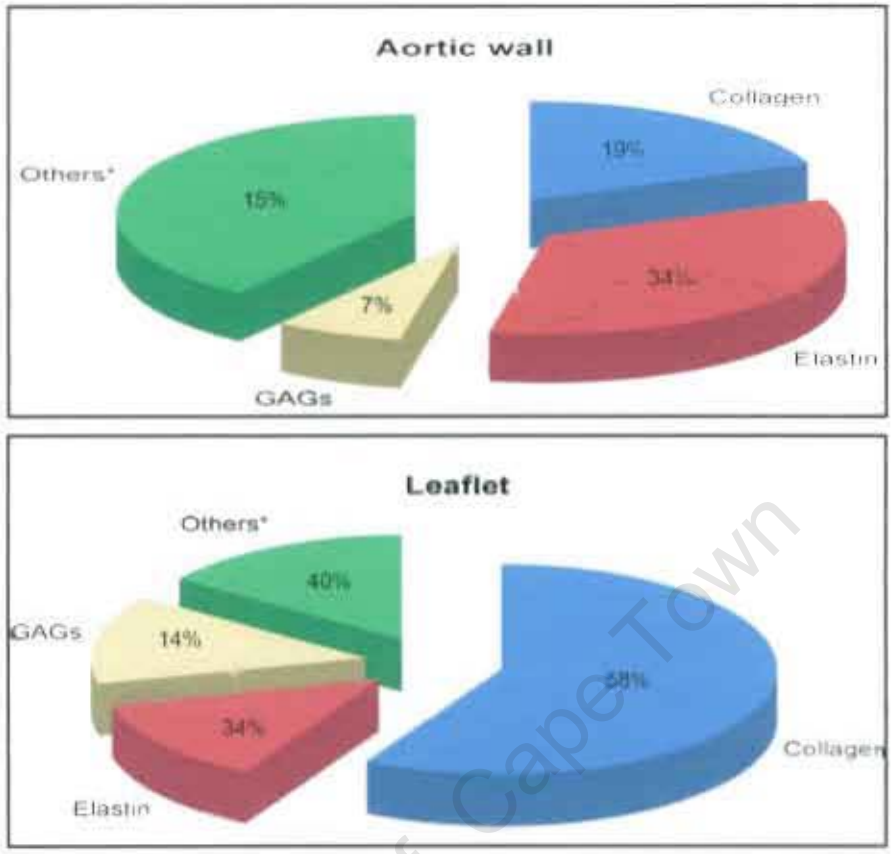

Figure B-4 Porcine aortic valve tissue composition

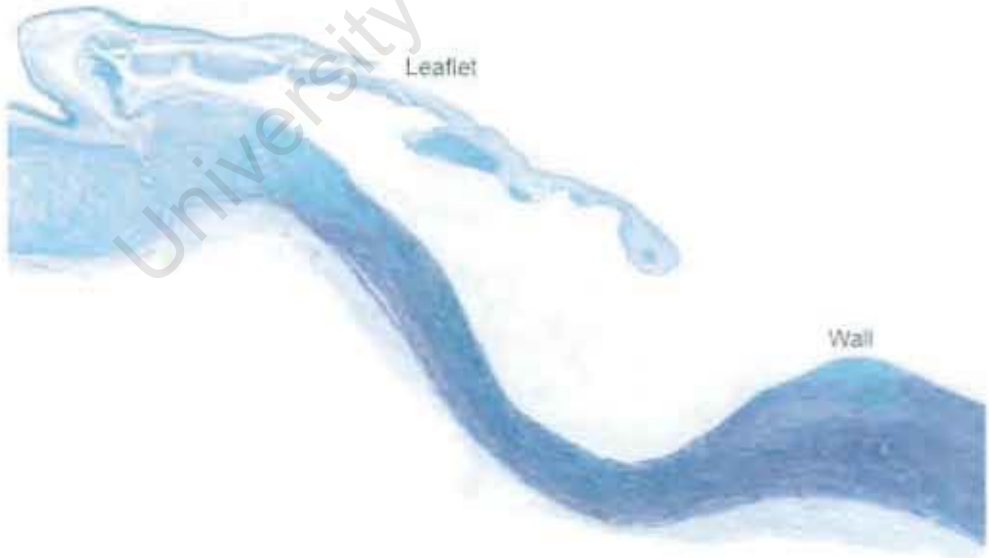

Figure B-5 Porcine aorta valve (leaflet and wall) stained with ELMAS. The collagen stained blue and the elastin black.

B3.2.A.1(i) Cellular components

Cells are the major sites of initiation of mineral deposits[99-102]. Glutaraldehyde treatment does not remove nonviable connective tissue cells. Although the mechanism of calcification of the cells is yet to be fully understood, one hypothesis for the mechanism of calcification of bioprosthetic tissue is that nonviable cells lack the ability to maintain local calcium concentration gradients across the cell membrane. In living cells calcium uptake occurs through gradient dependent passive channels. Calcium is released from the cell via Ca^{2+}-ATPase pumps to maintain calcium homeostasis. There is a 10,000-fold calcium ion concentration gradient across the plasma membrane with intracellular calcium lower than the calcium rich extracellular fluid[103-105]. Thus, calcium is passively transported into the cell and actively pumped out with the ATP-pump. This regulation mechanism is disrupted in bioprosthetic tissue where calcium ions flood nonviable energy-depleted cells with disrupted membranes[102, 106].

Plasma membranes and membrane-bound organelles, such as mitochondria, are rich in phospholipids and provide phosphorous for apatite formation[96]. The cell membrane has trans-membrane proteins, imbedded in a double-layer lipid membrane, with acidic phospholipids exposed inside the cells. There is an electrostatic attraction between the acid phospholipids of the connective tissue and calcium[107]. Calcium floods the cell and nucleation of calcium-phosphate crystals occurs at the phospholipid-rich membranes and calcium-binding proteins[8]. The inorganic phosphate ions combine with the calcium ions and the continuous influx of calcium ions lead to the formation of hydroxyapatite[97].

Cunanan et al[107] found a statistically significant direct correlation between phospholipid levels and calcification; lower phospholipid levels being associated with lower calcium levels. The cellular role in calcification is supported by the prevention of calcification by lipid extraction from biological tissue, especially of phospholipids, which are present in cell membranes[100].

Native human heart valves are covered by a monolayer of endothelial cells, which act as an effective barrier between the blood and the tissue. During the fixation process the bioprosthetic heart valves lose this endothelial barrier[101, 108]. Structural alterations on the surface of leaflets from explanted porcine bioprosthetic valves involved loss of endothelial cells, exposure of large areas of basement membrane material, fibrin depostion and insudation, presence of activated leucocytes, adherent

platelet aggregates and focal accumulation of crystalline deposits[108]. A confluent endothelial lining may suppress plasma insudation, extrinsic calcification of mural microthrombi and immune responses in the underlying tissue. There is however little or no spontaneous, natural endothelialisation of bioprosthetic heart valves through outgrowth of host endothelial cells[109]. Unless the tissue is quiescent with regard to an inflammatory response, endothelial seeding or overgrowth is inefficient at avoiding an, often severe, inflammatory response at the tissue interface.

B3.2.A.1(ii) Collagen

Collagen fibres are a major constituent of leaflet extracellular matrix and pericardium (see table 1). They provide the architectural framework and mechanical reinforcement needed for function in a bioprosthetic heart valve[97]. A collagen molecule consists of three polypeptide chains arranged in a triple helix configuration ending in non-helical carboxyl and amino terminals, one at each end. These non-helical ends are believed to contribute to most of the antigenic properties of collagen. Calcification patterns, observed in both *in vitro* and explanted valve tissue, show that collagen plays a role in valve calcification. Firstly, calcification was seen to align longitudinally along collagen fibre bundles, secondly, calcification occurs perpendicular to the fibre bundles in banded patterns and thirdly, large, dense focal deposits damage the underlying collagen structure[110]. Fixation of the tissue changes the morphology and the charges on the collagen molecules[111] which might facilitate complex formation with calcium ions. Collagen is present in the matrices of all three major skeletal tissue calcification structures: bone, cartilage and dentin[112].

Purified type I collagen sponges prepared with increasing concentrations of glutaraldehyde implanted subcutaneously for 21 days in rats calcified, but the degree of calcification did not correlate with the extent of assumed cross-linking. However, purified type I collagen gels resorbed without evidence of calcification[113]. The investigators concluded that cross-linking with glutaraldehyde promotes the calcification of collagen sponge implants made of pure collagen. Vincentelli et al[114] suggested that collagen type I sponges resorbed without evidence of calcification may demonstrate that the immunologic rejection of the collagen sponge did not leave time for calcification to occur.

Simonescu et al[115] demonstrated that collagen and elastin degrading enzymes are active in glutaraldehyde-fixed aortic leaflets and wall tissues and that these proteases are able to degrade glutaraldehyde-fixed collagen and elastin.

Progressive collagen breaks, independent of calcification[86], also contribute to the limited durability of bioprosthetic valves.

B3.2.A.1(iii) Elastin

Elastin, a structural protein of the extracellular matrix, is a major component of elastic fibres in connective tissue and in contrast with leaflets, the major component of aortic wall tissue (see table 1). Aortic wall calcification seems to differ from bioprosthetic heart valve leaflet calcification. Contrary to leaflets, elastin appears to be the major site of extracellular calcific deposits in aortic wall tissue[116]. Elastin is highly hydrophobic, insoluble, is rich in non-polar amino acids and has very few free lysine groups to react with glutaraldehyde[117]. The lack of reactivity of glutaraldehyde with elastin suggests that elastin is not protected against the activity of degradative enzymes, such as matrix metalloproteinases (MMPs)[118]. The elastin-associated microfibrils are disrupted during the preparation of bioprosthetic aortic wall tissue leaving the elastin core exposed[9]. Elastin degradation products could possibly elicit immune responses and trigger unwanted reactions in host cells such as protease release[119, 120]. Degradation and fragmentation of elastin fibres appears to cause increased elastin-orientated calcification[98]. Inhibition of matrix metalloproteinase activity significantly inhibits elastin calcification when implanted subcutaneously in rats[121] Lee et al[122] found MMP-mediated (MMP-9 and MMP-2) elastin degradation is involved in initiation and progression of pure porcine aortic elastin calcification. Thus, elastin degradation may be the primary step in pathologic elastin calcification. Vyavahare et al[117] used pure elastin to study elastin calcification independent from the effects of structural components of the aortic wall (cells, phospholipids, glycosaminoglycans, intrinsic enzymes and other extracellular matrix proteins). They demonstrated that purified elastin calcifies in a rat subdermal model independent of glutaraldehyde. Thus, glutaraldehyde treatment is not a prerequisite for aortic wall calcification.

B3.2.A.1(iv) Glycosaminoglycans and proteoglycans

Glycosaminoglycans are long, hydrophilic, anionic, unbranched polymeric molecules consisting of disaccharides[4], present in valves and pericardium tissue[123]. They bind to a core protein as large polymers to form proteoglycans. They are distributed in the extracellular matrix of leaflets (particularly within the spongiosa) and aortic wall tissues, and are also associated with the surfaces of collagen and elastic fibres[9]. Proteoglycans reside in empty areas created in collagen fibres and it has been

suggested that they protect collagen from calcification. Proteoglycans and glycosaminoglycans reduce calcification by chelating calcium ions[124], thereby preventing hydroxyapatite nucleation and thus effective inhibitors of mineralization[123-125]. Glycosaminoglycans are capable of absorbing water and swell to form a gel to resist compression forces and play an important role in maintaining proper mechanical functions within bioprosthetic heart valves[5-7, 10]. Glycosaminoglycans lack amine groups necessary for cross-linking by glutaraldehyde and are lost *in vitro* during bioprosthetic heart valve preparation, fixation and storage as well as when implanted[4, 9, 10], suggesting insufficient stabilisation by glutaraldehyde. Matrix metalloproteases[115] and glycosaminoglycans-degrading enzymes[126] can degrade proteoglycans and may contribute to bioprosthetic heart valve degeneration. Lovecamp et al[4] did a comprehensive study of glycosaminoglycans' role in porcine bioprosthetic heart valves. They found the loss of glycosaminoglycans may impact on the mechanical durability of bioprosthetic heart valves, but plays a minor role in the calcification of valves implanted in the rat subdermal model.

B3.2.A.1(v) Fibronectin

Fibronectin (Fn) is a large extracellular glycoprotein found in body fluids (mostly plasma), soft connective tissue matrices, and most basement membranes. There are at least two types of Fn termed plasma and cellular Fn. They are structurally and functionally very similar, but not identical. The two forms are indistinguishable in the biological activities in assays but in contrast the effects of these molecules on cell morphology are sometimes substantially different [127]. As an insoluble multimer, it is a key component of the extracellular matrix [128]. Fn is usually formed as a dimer, consisting of similar but not identical chains, and each polypeptide chain is approcimately 250 kDa in size. A pair of disulfide bonds joins the carboxy-terminal end of the chains [129]. Proteases cleave Fn in regions to generate separate, structured domains of the molecule containing specific binding sites for ligands such as collagen, heparin sulfate, fibrin as well as a cell binding domain (see Figure B-6, which is applicable of both forms of Fn) [127].

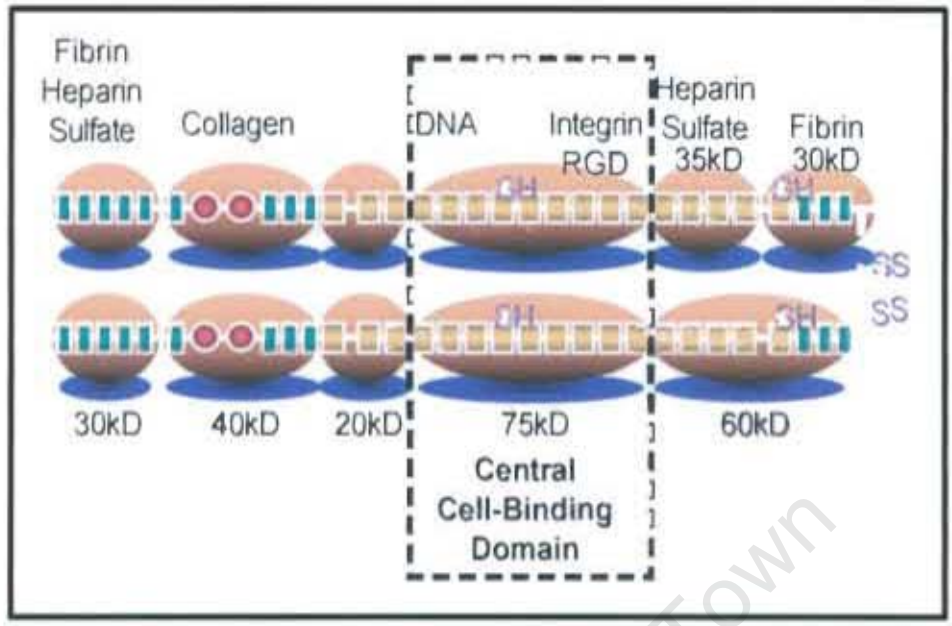

Figure B-6 A modular structure of fibronectin with the different binding domains.

B3.2.A.1(vi) Non-collagenous components

Non-collageneous proteins of the extracellular matrix, such as osteopontin, osteocalcin and osteonectin are normally present and expressed at specific stages of bone development and regulate calcification in bone matrix[130]. Thus, non-collageneous components play important roles in calcium homeostasis within the extracellular matrix. Non-collagenous bone proteins, osteopontin, osteocalcin and osteonectin, and extracellular bone matrix proteins have been reported in bioprosthetic tissue calcification[131-133]. The exact functions of these proteins are yet unknown, if they are a cause or a consequence of the calcification process. These proteins may play a significant role in the regulation of calcification. It is hypothesised that osteopontin regulates calcification in bioprosthetic tissue by binding to hydroxyapatite and that it physically inhibits crystal growth[134]. Osteocalcin and osteonectin may serve to regulate crystal growth and mineral resorption[133]. Macrophages and smooth muscle cells synthesize non-collagenous matrix proteins[135]. Srivatsa et al[133] found osteopontin, osteocalcin, and osteonectin protein adjacent to and within regions of mineralization of bioprosthetic valves. Macrophage cell infiltration was also observed surrounding calcified areas.

B3.2.A(2) Chemical treatment

Chemical treatments that stabilise bioprosthetic heart valve tissue influence the degrees of degradation and calcification. Glutaraldehyde treatment is commercially used to create chemically stable cross-links in collagen fibres of bioprosthetic tissue to improve durability. Glutaraldehyde treated materials calcify to a large extent[106], which might be due to the cross-linking process. Glutaraldehyde fixation of xenografts can lead to several biochemical and structural determinants that plays a detrimental role in bioprosthetic heart valve tissue calcification[136, 137]. The role of glutaraldehyde in calcification is not clearly defined.

In normal leaflets, valvular interstitial cells and resident macrophages actively participate in maintaining tissue architecture via constant remodelling[97]. Glutaraldehyde treatment devitalises tissues, cross-links nonviable cells but does not remove them leaving cell debris that can serve as nucleation sites for calcification[8, 96, 101, 138]. Kim et al[139] showed that glutaraldehyde fixation leads to influx of Ca^{2+} into cells followed by apatite nucleation. Tissue injury during harvesting of the valves and a delay in glutaraldehyde fixation was shown to intensify calcification of bioprosthetic heart valves in the subcutaneous rat model[140, 141].

Incomplete glutaraldehyde binding to tissue proteins, loosely bound glutaraldehyde, or free aldehyde groups result in cytotoxic reactive aldehyde group residuals and polymeric glutaraldehyde cross-links that can depolymerise[142]. Depolymerization of polymeric glutaraldehyde cross-links has been reported, which releases monomeric and highly cytotoxic glutaraldehyde into the recipient[142]. The free aldehyde groups seem to be involved in bioprosthetic heart valve calcificiation[94, 97]. Glutaraldehyde treatment changes the morphology and charges on the collagen molecules[111], which may be responsible for calcification. Neutralising (chemical treatment with amino compounds to reduce residual glutaraldehyde released from fixed tissue) and excess rinsing after glutaraldehyde fixation minimise cytotoxicity and reduce calcification potential[143]. Higher glutaraldehyde concentrations (3%) reduces tissue calcification in both the circulatory sheep model[144] and subcutaneous models[141]. Better cross-linking improves ultrastructural tissue preservation[145], reduces macrophage activation[146], and suppresses the immune response[147].

Glycosaminoglycans are natural inhibitors of calcification[4] but fail to be stabilised within the glutaraldehyde cross-linked heart valve tissue and as a result are lost from bioprosthetic heart valves[4, 9, 10]. Thus, fixation of bioprosthetic tissue alters structural

and biochemical characteristics of the tissue significantly. These changes play a direct or indirect role in calcification of the bioprosthetic heart valve.

B3.2.A(3) Host-related factors

The role of the host in calcification is unclear. Certainly, the age of the recipient does play a role in the time period for structural valve deterioration. Bioprosthetic heart valves calcify at an accelerated rate in young children[36-38, 148] and growing adults with active immune responses and rapid growth[14, 39]. The small sized valves used in children result in increased pressure gradients and stress on the leaflets, which may enhance early tissue fatigue. Calcium turnover is high in children who maintain a positive calcium balance[149]. Patients with abnormal calcium metabolism such as patients with renal failure and patients with bone tumours have soft tissue calcification[97, 150]. Accelerated degeneration and calcification of bioprosthetic valves in these patients with a high calcium turnover suggests that calcium metabolism[148] may play a role in bioprosthetic heart valve calcification.

The donor and recipient species influences the onset and degree of calcification. Carpentier et al[151] found pig a favourable donor of bioprosthetic tissue. The donor species order of calcification was the highest in bovine, then sheep and lowest in pig when implanted subcutaneously in rats. Subcutaneous implantation of glutaraldehyde-treated porcine and bovine leaflets showed the highest ratio of calcification in rabbits compared to rats, with no calcification in cow and hen. Even the different strains of animals can affect the calcification response. The highly inbred immune-tolerant Fischer-344 rat calcifies bioprosthetic tissue much less than other strains such as Long-Evans, Wistar and Sprague-Dowley rats[106].

The host immune response to bioprosthetic tissue remains highly debated in the literature. Untreated vascularised xenograft tissue triggers a hyperacute rejection within minutes of implantation. The chemical cross-linking of bioprosthetic heart valve tissue dramatically masks the tissue's antigenicity but standard commercial glutaraldehyde fixation does not eliminate the immune response[152-154] and bioprosthetic heart valves continue to fail albeit over many years rather than days. The mild inflammatory response to the tissue nevertheless results in slow degradation of the tissue. Implantation of bioprosthetic heart valves certainly has been shown to induce a foreign body type response[92, 107].

Early clinical studies suggested the host's immune response to bioprosthetic heart valves might also contribute to calcific degeneration[155, 156]. Investigators found

infiltration of plasma cells, histiocytes and an immunoglobulin response in failed bioprosthetic heart valves in children[157]. In the 1980s, Levy's group investigated the possible contribution of the immune response. In a study which involved subcutaneously implanted Millipore diffusion chambers containing glutaraldehyde-treated porcine valve leaflets they suggested that normal T-lymphocyte function nor "immunologic processes" contributed to the process of bioprosthetic heart valve calcification[158] since the Millipore diffusion chambers, which allow extracellular fluid infiltration but prevent host cell migration, did not affect calcium accumulation, whether in the presence or absence of host cells. Indeed, the morphologic appearance of calcium in glutaraldehyde-treated tissue in normal and nude mice (T-lymphocyte deficient) were identical 21 days after implantation. This suggested a passive, rather than cell-mediated calcification process. However, they failed to address the role of a T-lymphocyte independent immune response. Many investigators believe this evidence suggests that neither specific nor non-specific immune responses play a role in bioprosthetic heart valve degeneration and that no contributory immunologic basis has been demonstrated for bioprosthetic valve calcification or failure. Schoen and Levy[8] suggest in their review of tissue heart valve calcification that circulating antibodies to valve tissue detected in experimental and clinical studies may be a secondary response to valve damage rather than a cause of failure. Similarly one could argue that macrophage infiltration is a consequence of collagen degeneration rather than its cause, although studies have demonstrated phagocytosis of intact collagen by macrophages. Liao et al[159] compared autograft, allograft and xenograft tissue implanted in the subcutaneous Sprague-Dawley rat model. Tissue was either untreated or treated with 0.625% glutaraldehyde for different time periods. Calcification increased with fixation time in treated groups whereas untreated tissue did not calcify. They concluded that calcification was not related to the antigenicity of the implants, but the glutaraldehyde treatment.

Magilligan et al[160] found no second-set rejection in patients with bioprosthetic heart valves replaced by a second bioprostheses. Some investigators suggested that the immune mechanisms contributing to bioprosthetic heart valve failure may not lead to dramatic immediate rejection, but may play a significant role in the degeneration of the valve over time. Nimni et al[153] showed commercial fixation with glutaraldehyde only achieves 59% reduction in antigenicity as opposed to 92% reduction through enhanced fixation using diamine bridges.

The potential role of inflammatory and immune processes is still unclear but a growing number of researchers provided evidence for immune-mediated bioprosthetic heart valve degeneration:

- The presence of circulating graft-specific antibodies in clinical and experimental studies[73, 94, 154, 157]
- Experimental animals can be sensitized to both fresh and cross-linked bioprosthetic valves tissues[152, 154, 161]
- Failed bioprosthetic heart valves have mononuclear inflammation with macrophages identified as the main invading and collagen-degrading inflammatory cell[101, 162].
- Eishi et al[163] observed a decrease in calcific degeneration of bioprosthetic heart valve patients with steroid therapy for aortitis (inflammation of the aorta).
- Dahm et al[152] indicated that glutaraldehyde-tanned bovine pericardium elicit both a cellular and humoral immune response.
- Vincentelli et al[114] found a possible link between inflammation and bioprosthetic heart valve failure. They compared 0.6% glutaraldehyde treated autologous and heterologous pericardial samples implanted subcutaneously in sheep. The heterologous group calcified 35 times more than the autologous group, suggesting that an immune response may be responsible for the changes and not the glutaraldehyde treatment.
- Human and Zilla[161] directly linked bioprosthetic tissue specific antibodies and calcification. They incubated glutaraldehyde treated porcine aortic wall in serum containing high levels of graft-specific antibodies before subcutaneous implantation in rabbits. The tissue calcified three times more than tissue incubated in pre-immune serum.

B3.2.A(4) Mechanical stress

Mechanical stresses in the heart contribute to calcification of bioprosthetic heart valves[164-166]. The right side of the heart supplies blood only to the lungs, while the left side of the heart must supply blood to the rest of the body. Therefore, the left side develops pressure ten times higher than in the right side of the heart. Bioprosthetic heart valves calcify less after being implanted in the left (aortic and mitral valve) side of the heart as compared to the right side (pulmonary and trileaflet

valve)[97]. Greater incidence of valve degeneration for mitral valves is likely due to a higher closing pressure[33].

Leaflet calcification appears to be concentrated in areas of high stress. There is a relation between the distribution of mechanical stress in the leaflet and calcification. Distribution of mechanical stresses in the leaflet is highest near the commissures, then at the free margin and lowest at the base of the leaflet. Calcification is most frequently observed near the commissures, less in the body of the leaflet and free margin, and least at the base of the leaflet[167].

Intrinsic and extrinsic mineralization is observed at sites of intense mechanical deformation generated by motion, such as the points of flexion in heart valves[95]. Pericardial bioprostheses calcify where the highest stress occurs, particular in the areas of flexion of the leaflets. Mechanical stress damages the structural integrity of the leaflet tissue[166].

Modification of design and tissue properties to duplicate those of natural aortic valves may improve the durability of bioprosthetic valves.

B3.2.B Prevention of calcification

Calcification is the primary reason for bioprosthetic heart valve failure. Therefore bioprosthetic heart valve treatments are directed at prevention of calcification. The treatments target different factors involved in calcification. Combinations of the approaches may be more effective in preventing calcification. Nimni et al[106] suggested the ideal treatment should include removal of non-covalently bound glutaraldehyde, neutralisation of free aldehyde residues, removal of lipids and non-collagenous proteins and the inclusion of calcium phosphate inhibitors. Glutaraldehyde has been branded the villain[158] and most strategies target glutaraldehyde by incorrectly decreasing concentrations used rather than avoiding the problem of slowly leaching glutaraldehyde monomers due to labile bonds through appropriated detoxification.

B3.2.B(1) Inhibitors of calcium phosphate mineral formation

B3.2.B.1(i) Biphosphonates

Biphosphonates act as a crystal 'poison'[106] by binding to developing hydroxyapatite crystals, and thereby preventing further crystal growth[168], and as a result inhibiting calcification. Biphosphonates can be administered systemically or locally. Systemic administering has been associated with significant adverse effects[169]. Rats receiving subcutaneous injections daily showed severe somatic growth retardation and

elevation of the serum calcium levels. Locally systematic delivery of biphosphonates using controlled-release delivery systems or pre-treatment of the leaflets with biphosphonates prevented these effects and animals had normal somatic growth and serum calcium levels[170]. Biphosphonates significantly inhibit bioprosthetic aortic wall calcification[116] and calcification of bioprosthetic leaflets implanted subcutaneously in young rats[170].

B3.2.B.1(ii) Trivalent metal ions (Al^{3+} or Fe^{3+})

Trivalent metal ions can bind at phosphorous-rich loci of devitalised cells[171, 172]. The Al^{3+} or Fe^{3+} ions inhibited calcification by forming a phosphate complex, thereby preventing calcium phosphate formation or arresting crystal growth[173]. These ions also inhibit alkaline phosphatase[171, 173], an important enzyme involved in bone formation activity and this may be related to their ability to prevent initiation of calcification. Aluminium ions bind irreversibly to elastin, inducing permanent alteration in the elastin structure such that it resists calcification[117]. Aluminium ions also partially stabilise pure elastin against matrix metalloproteinase-mediated elastolysis, and protect it from degeneration and calcification when tested in animal models[174]. Fe^{3+} and Al^{3+} significantly inhibit bioprosthetic heart valve leaflet as well as aortic wall calcification[116, 171, 172, 175]. Calcification of purified elastin in a rat subdermal implantation model is also inhibited by aluminium chloride pre-treatment[117].

B3.2.B(2) Removal or modification of calcifiable material

B3.2.B.2(i) Surfactants

Detergents, such as sodium dodecyl sulfate (SDS)[176], Tween 80[177], and Triton X-100[86] are used to inhibit mineralization in bioprosthetic heart valves. Detergents reduce calcification by removing acidic phospholipids, which result in suppression of the initial cell membrane oriented calcification[176]. The detergent pre-treatment could also be responsible for extracting proteins, removing cell debris or interfering with adsorption of proteins, thereby reducing the capacity to adsorb non-collagenous bone proteins[103]. Detergents reduce calcification in subcutaneous implantation models, but the results are not as favourable in circulatory models[177, 178]. SDS is not an efficient anti-mineralization treatment[177].

B3.2.B.2(ii) Ethanol

Ethanol extracts phospholipids and cholesterol from glutaraldehyde fixed leaflets and induces permanent alteration to collagen conformation[179]. The collagen conformational changes increase collagen resistance to collagenase digestion[180]. Ethanol pre-treatment reduces the water content of the leaflet and affects leaflet interactions with water and lipids. The changes to proteins could affect short-term mechanical properties of the valve. Ethanol pre-treatment prevents calcification of leaflets in rat subdermal implants and sheep mitral valves (circulatory model) but is not particularly effective in preventing aortic wall calcification[103, 175, 176]. Elastin is the prominent protein in aortic wall and is not affected by ethanol pre-treatment[179]. Thus, the mechanism of inhibition is probably based on lipid extraction and collagen structural changes.

B3.2.B.2(iii) Tannic acid

Glutaraldehyde is unable to stabilise elastin and elastin is susceptible to degradation and calcification after implantation in animal models[118, 174]. Tannic acid is a plant polyphenol belonging to the galloylglucose family. It forms multiple bonds with proteins, particularly those rich in proline such as elastin and collagen[181]. Tannic acid is commonly used in electron microscopy for ultrastructural demonstration of elastin fibres. Tannic acid binds to pure elastin protecting it from enzymatic attack[118, 181]. Isenburg et al[181] treated porcine aortic wall samples with glutaraldehyde and tannic acid. Calcification in the subdermal rat model was three times less in the group with tannic acid than the group with glutaraldehyde alone.

B3.2.B(3) Improvement or modification of glutaraldehyde fixation

Neutralisation of free aldehyde groups with compounds that have reactive primary amines and rinsing of tissue after glutaraldehyde fixation reduce calcification in animal models[97]. Increased cross-link density inversely correlates with tissue calcification[95, 141, 144]. However, tissue fixed using higher concentration of glutaraldehyde has higher tissue stiffness[182] which may compromise the mechanical performance of the bioprosthetic heart valve. The following treatments neutralise and detoxify glutaraldehyde treated bioprostheses.

B3.2.B.3(i) Amino compounds

Amino compounds such as L-lysine[182], L-arginine[183] and L-glutamic acid[143] neutralise and detoxify glutaraldehyde fixed bioprosthetic tissue. Amino compounds create

bridges between glutaraldehyde molecules by binding to free aldehyde groups with reactive primary amines to improve the cross-link density[8, 182]. Urazol, a secondary amine group, removes residual glutaraldehyde molecules from tissue under acid conditions[184, 185]. Neutralisation of free aldehyde groups of glutaraldehyde treated bioprosthetic tissue reduces calcification in the subcutaneous rat model[143] and detoxification of glutaraldehyde fixed aortic wall tissue achieves long-term cell growth after implantation[185].

B3.2.B.3(ii) Alpha-Amino oleic acid (AOA®)

AOA is an active neutralisation agent blocking or reducing free aldehyde residues. The 2-amino group of AOA covalently binds to free aldehyde groups of glutaraldehyde fixed tissue[186] and reduces the influx of calcium ions into bioprosthetic tissue[186-188]. This results in slowing down the initial calcium phosphate formation[186]. AOA also functions as a surfactant to extract phospholipids from the cell membranes which reduces the initial nucleation sites for crystallization of calcium phosphate. Compared with aortic walls, AOA penetrates more easily into the relatively thin and less dense collagenous leaflet tissue[186]. The AOA level in aortic walls is not sufficient to prevent the calcium influx into aortic wall tissue, explaining why AOA effectively mitigates calcification of bioprosthetic leaflets and pericardial tissue in the rat subdermal model and the circulatory sheep model, but not aortic wall tissue[186]. AOA is used in FDA-approved non-stented[189] and stented porcine aortic valves[190].

B3.2.B(4) Tissue fixatives other than glutaraldehyde

Studies have demonstrated that glutaraldehyde is directly responsible for calcification of bioprosthetic heart valves[76, 77, 142]. Thus, even if this is a misinterpretration of the truth, the use of tissue fixatives other than glutaraldehyde may have better long-term results in bioprosthetic heart valves.

B4. Hypothesis

The hypothesis under investigation:

1. Conventional chemical fixation of antigen reduction through decellularisation of bioprosthetic heart valve tissue fails to adequately mask/remove all immunogens resulting in both a significant humoral immune response and persistent inflammatory response as a direct result thereof.

2. Targeted masking of these residual immunogens by application of immunoglobulin specific for epitopes contained on these immunogens together with modification thereof to abolish their opsonising potential prior to implantation will mitigate both the host immune response and thus the proinflammatory potential of such tissue.

3. Modification of specific immunoglobulin by enzymatic removal of the Fc fragment and application of the resulting antigen binding fragments (Fab and/or $F(ab')_2$) prior to treatment of the tissue as one scenario will avoid Fc receptor mediated adherence of phagocytes.

The results of this study will provide a better understanding of the mechanism involved in the granulocyte and macrophage/foreign body giant cell dominated destruction of bioprosthetic heart valve constructs. Finally, it offers to provide an antigen-targeted solution in the quest for the elusive quiescent bioprosthetic heart valve.

C. Proof of Concept

C1. Characterisation of response against bioprosthetic heart valves

C1.1. Immune response to bioprosthetic heart valves in patients

C1.1.A Introduction

Patients suffering form valvular heart disease typically may undergo heart valve replacement surgery to replace their diseased valves. The options for prosthetic heart valves involve either mechanical or tissue valves. Tissue valves include autografts, homografts or bioprosthetic valves. The homografts and autografts are currently the best tissue valves to use, but have limited availability. Of all prosthetic heart valves currently implanted, only a third are bioprosthetic heart valves. The disadvantage of bioprosthetic valves are that they cannot be used regularly in younger patients, because they have a limited lifetime and the patients will have to come back for redo operations. In patients over 65 the lifetime of the prostheses is generally between 10 [191-194] and 15 years [33, 91] which may outlast the life of the patient. These valves usually fail due to structural valve damage caused by calcification or leaflet tears [93], but immune and inflammatory processes are increasingly being implicated in the pathology associated with these failed implants.

Bioprosthetic heart valve 'rejection' is not similar to the hyperacute rejection of transplanted vascularised solid organs, such as hearts, from animal donors and yet these prostheses too represent donor-recipient mismatching across the species barrier. Bioprosthetic heart valves fail over years and not over days or even minutes as in the case with hyperacute rejection. This is largely due to the fact that the bioprosthetic valve relies on its structural rather then biological integrity. Heart valves are treated with a cross-linking agent such as glutaraldehyde to improve biocompatibility by masking non-self immunogens and inducing a full out response. The delays in processing as well as the handling of tissue during dissection and further processing of the valves results in complete denuding of the endothelium. Thus, the subendothelial extracellular matrix, in particular the basement membrane, is exposed to a host immune system response when implanted. The initial burst of inflammatory cells, usually neutrophils and macrophages, may damage the tissue exposing the extracellular matrix even further. After a while the initial immune response tapers off to only a few polymorphonuclear leukocytes (PMNs), macrophages and foreign body giant cells that persist. These inflammatory cells are

phagocytes [195, 196] which have the ability to engulf, digest and remove particles from the body as well as fulfil their primary role which is to present antigens [197] to other cells of the immune system. Often phagocytes in their attempt to engulf the bioprosthetic tissue, will undergo frustrated phagocytosis [198]. This process occurs when phagocytes fail to digest the indigestible cross-linked prostheses. These inflammatory cells have mechanisms to release enzymes and other constituents[199-201] (nitric oxide, superoxide, hypochlorite and other products of activated oxygen and nitrogen metabolism) in the extracellular matrix that may serve to slowly degrade the extracellular matrix and further expose more collagen and elastin. These exposed and damaged structures of the extracellular matrix may lead to calcification. The weakened tissue and structural deterioration of the valves may over time lead to leaflet tears and subsequently structural failure of the valve.

In most studies of explanted bioprosthetic heart valves the investigators do not give a detailed report on the inflammatory response and only briefly comment on the presence of inflammatory cells [33, 91, 93, 189, 192-194]. This may be due to the fact that valves typically only fail after 5 years or longer and the early inflammation may have 'burnt out' and is often undetected when the valves fail. This early inflammation may leave behind 'latent' damage, which may not be identified as failure due to inflammation but rather due to structural wear-and-tear. It is only recently that Butany et al[202] reported on stentless porcine valves where an inflammatory reaction may have lead to aortic tissue damage and eventually heart valve failure and suggested that it might be a consequence of cellular graft rejection. Only nine explanted Freestyle™ porcine aortic valves were identified representing a small percentage of the Freestyle™ valves implanted annually worldwide. Freestyle™ valves are porcine aortic valves cross-linked with glutaraldehyde and treated with alpha-amino oleic acid (AOA) as an anti-mineralization treatment. Inflammatory cells (lymphocytes, macrophages and plasma cells) were found in all nine explants, mostly on the abluminal (adventitial) surface of the porcine aortic wall and the interface between the native and the porcine aortic tissues. Inflammatory cells (mostly macrophages) were also seen on the inflow and outflow surface of the leaflets. A chronic inflammatory infiltrate was associated with structural damage to the aorta and the leaflets, a phenomenon observed relatively soon after implantation (4 months) and seen to persist for up to at least 10 years.

In order to investigate if inflammation played a role in the failure or structural damage of bioprosthetic valves, the histopathology of a small cohort of bioprosthetic porcine valves explanted from patients at Groote Schuur Hospital was evaluated.

C1.1.B Materials and methods

Five valves explanted at Groote Schuur hospital were used to evaluate the inflammatory response. The explanted heart valves selected were from different manufacturers and which failed after different time periods. The valves were all stented porcine aortic valves treated with glutaraldehyde and implanted in the mitral valve position. The manufacturers employed different anti-calcification treatments.

Standard histological sections were stained with haematoxylin and eosin (HE) (see Appendix A21). Immunohistochemistry for CD68 (macrophage marker) and CD15 (granulocyte marker) were performed (see Appendix A20). The sections were examined to determine if any inflammatory cells were present. The valves were also stained to for IgG, IgM and C3 to investigate the presence and extent of a humoral immune response (IgG, IgM and C3).

The valves investigated were as follows:

- Medtronic Mosaic
    - Porcine aortic stented valve fixed with glutaraldehyde and treated with AOA (anti-mineralization agent)
    - Two valves explanted after 109 days and 3 years. The valve explanted after 3 years was implanted in a 37 year old male and the valve explanted after 109 days was implanted in a 77 years old patient.
- Carpentier-Edwards
    - Porcine aortic stented valve fixed with glutaraldehyde
    - One valve explanted after 11 years from a 34 year old female patient.
- Medtronic Hancock
    - Porcine aortic stented valve fixed with glutaraldehyde and treated with T6 (SDS Surfactant – anti-mineralization treatment)
    - Two valves explanted after 19 and 24 years. The patient with the valve explanted after 19 years was a 32 year old female at the time of the valve replacement. The valve explanted after 24 years was implanted in a female patient 26 year old.

C1.1.C Results

Figure C-1 Hancock valve (A) before implant and the inflow (B) aspect of the valve after 24 years.

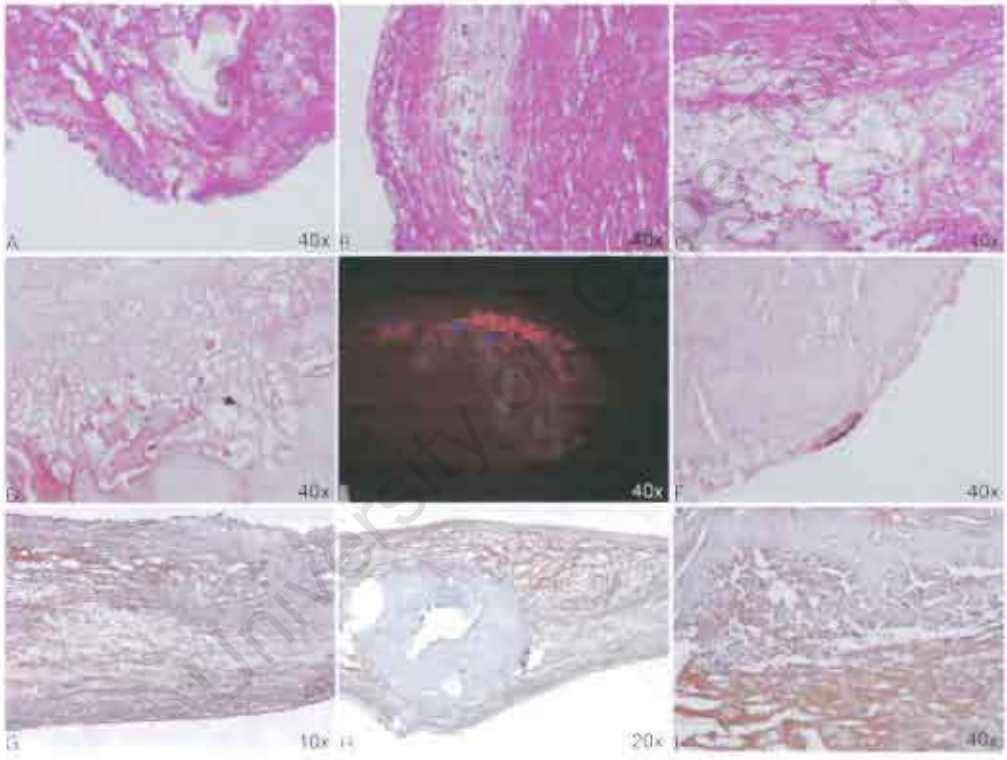

Figure C-2 Hancock Porcine valve failed after 24 years. A-C: HE stain; D-F CD68 stain (E was a fluorescent stain where red is positive); G-I IgG stain.

Case 1: A Hancock valve was explanted after 24 years from the mitral position. The patient was a 26 year old female at the time of the implant. The inflammatory cells (see Figure C-2) were mostly macrophages on the fibrosal side of the leaflet. A few PMNs were visible on the fibrosal side and a few infiltrated into the spongiosa. There were a few lymphocytes present on the fibrosal side of the valve. The valve stained positive for IgG throughout the leaflet, but it was the lowest intensity of the valves stained.

Figure C-3 Hancock valve (A) before implant and the outflow (B) aspect and the inflow (C) of the valve after 19 years.

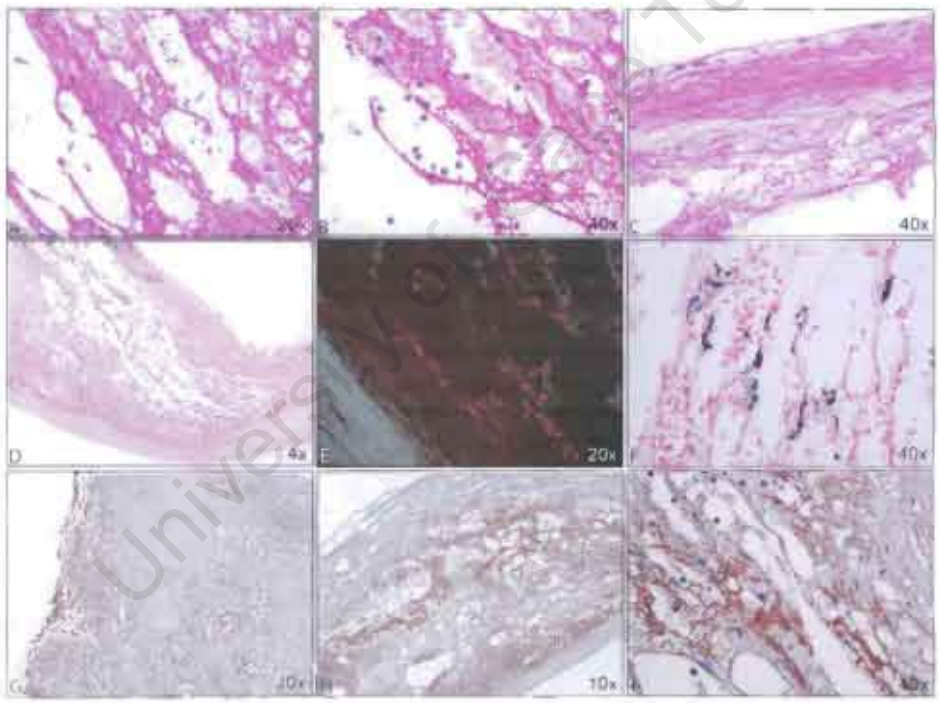

Figure C-4 Hancock Porcine valve failed after 19 years. A-C: HE stain. D-F CD68 stain; G-I IgG stain.

Case 2: The second Hancock valve was explanted after 19 years. The valve was implanted in the mitral position of a 32 year female patient. This valve did not present with many inflammatory cells, but those present were mainly infiltrated into the spongiosa of the valve (see Figure C-4). The inflammatory cells involved a combination of macrophages and granulocytes. The spongiosa stained positive for IgG and was mostly associated with the extracellular matrix, but not with the cells.

Figure C-5 Carpentier-Edwards valve (A) before implant the outflow (B) aspect and the inflow (C) of the valve after 11 years.

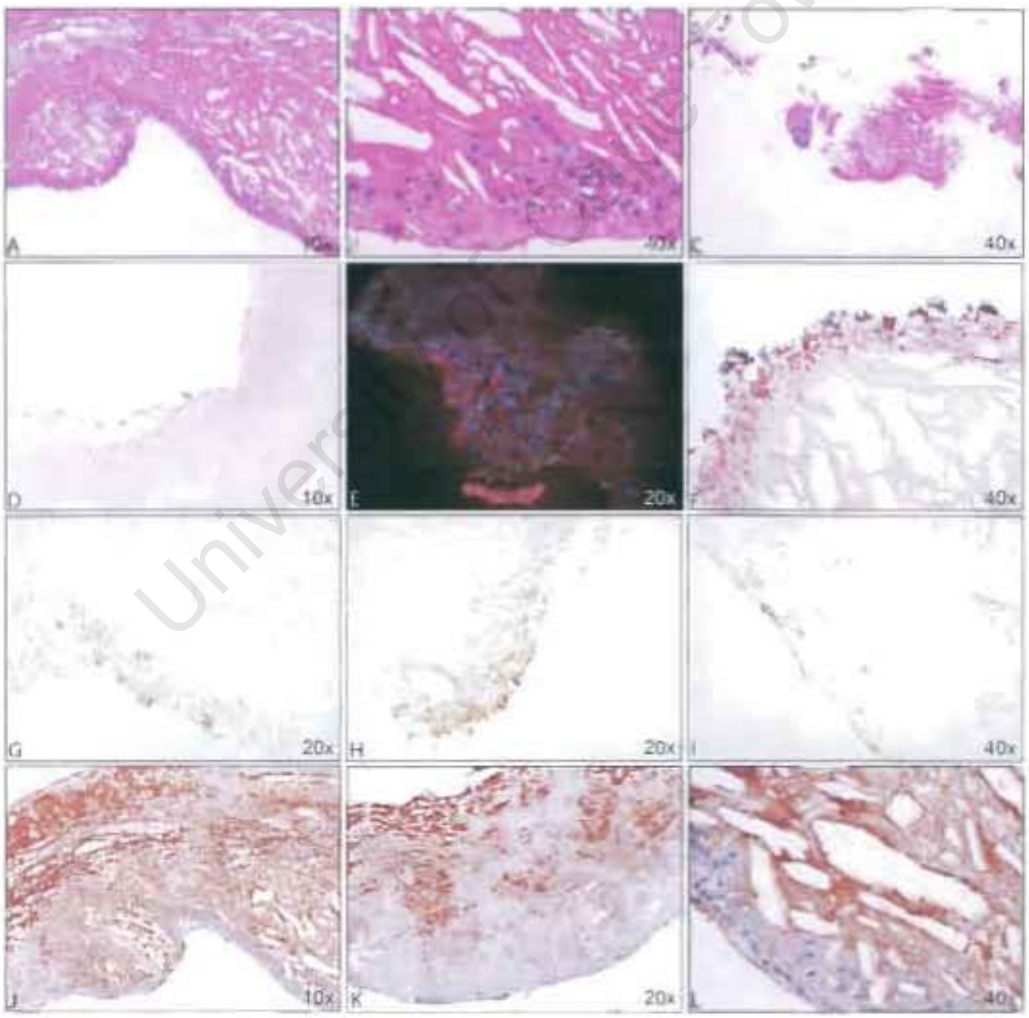

Figure C-6 Carpentier-Edwards porcine valve failed after 11 years. A-C: HE stain; D-F CD68 stain; H-I: Ham56 stain, J-L IgG stain.

Case 3. A 23 year female patient, with a Carpentier-Edwards valve implanted in the mitral position and explanted after 11 years. The fibrosa had inflammatory cells (see Figure C-6) all along the edge that consisted of PMNs, macrophages, foreign body giant cells, lymphocytes and plasma cells. The leaflet stained positive for IgG on the ventricularis edge and also within the tissue of the spongiosa. There was no clear IgG staining on the edge of the fibrosa.

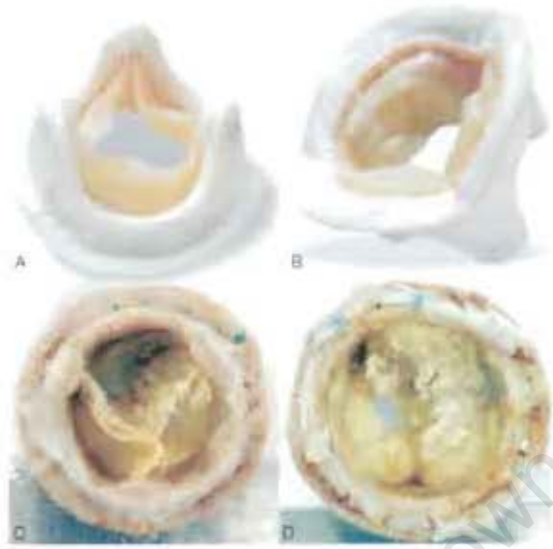

Figure C-7 Mosaic valve (A, B) before implant and the outflow (C) and inflow (D) aspects after 3 years.

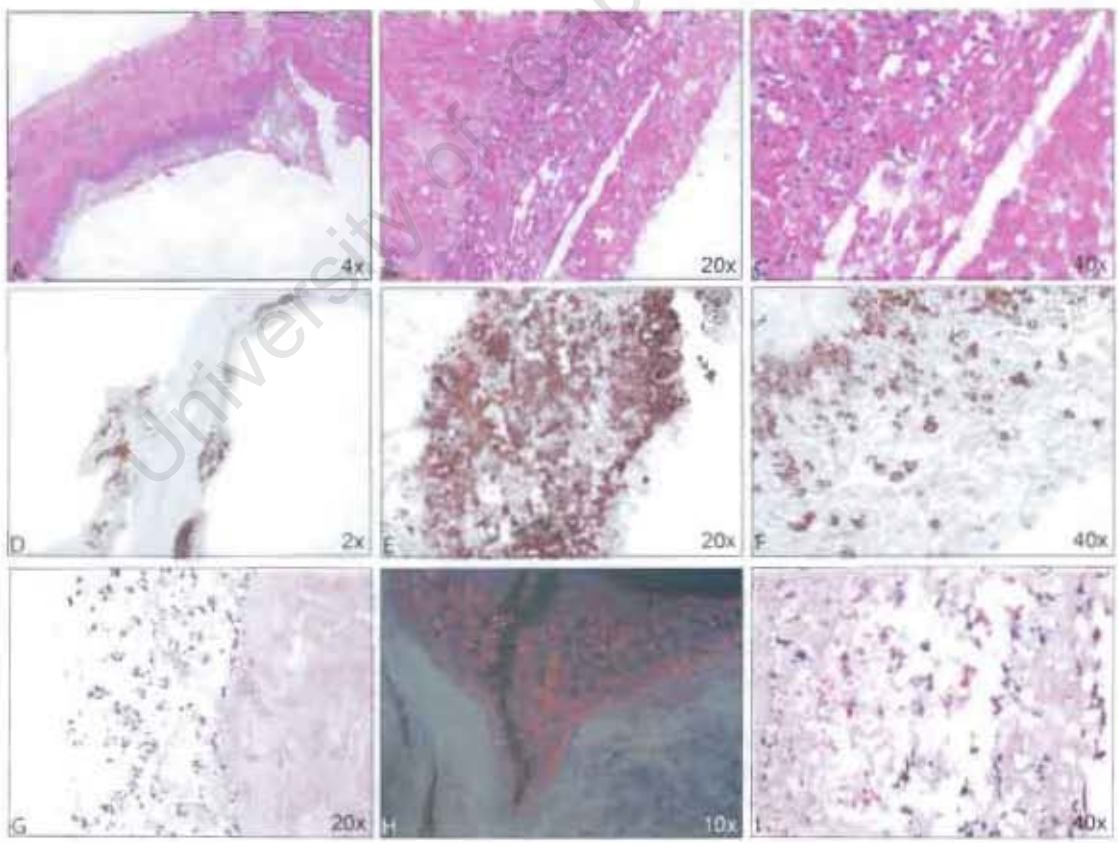

Figure C-8 Mosaic Porcine valve failed after 3 years. A-C: HE stain; D-F CD15 stain; G-I CD68 stain.

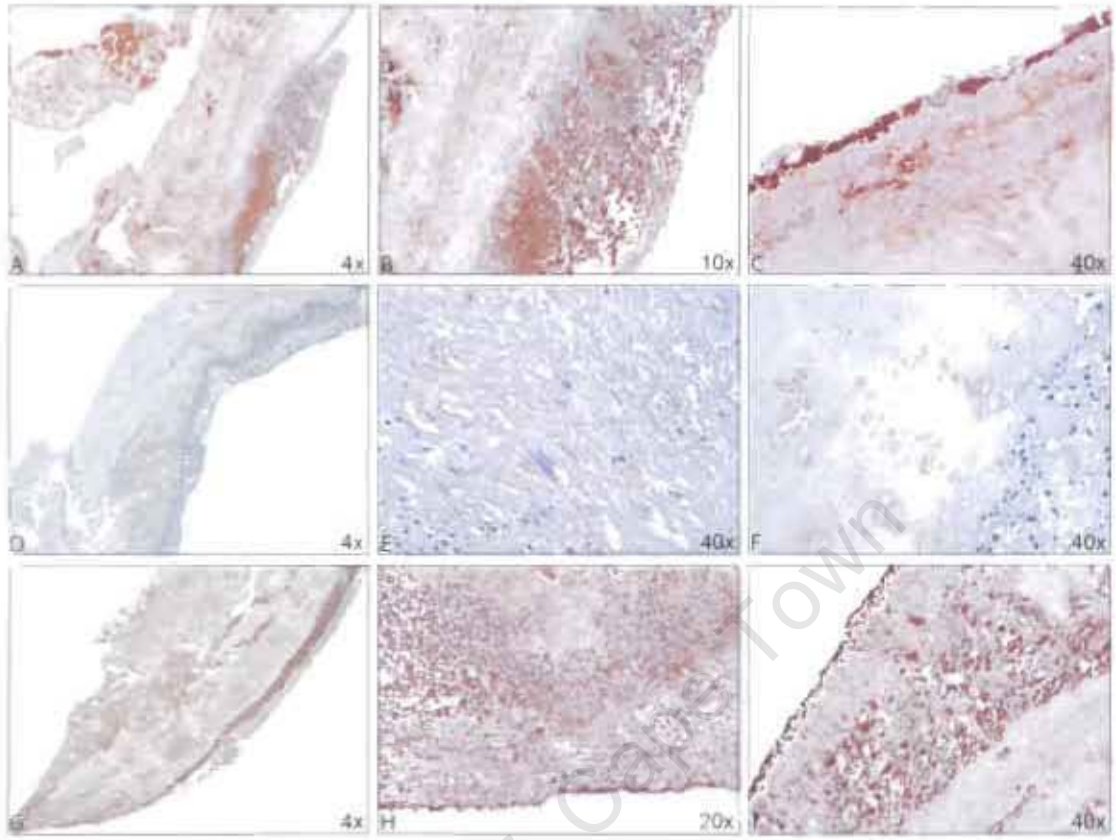

Figure C-9 Mosaic Porcine valve failed after 3 years. A-C IgG stain; D-F IgM stain; G-I C3 stain.

Case 4: A Mosaic valve was explanted after 3 years from a male patient aged 37 years at the time of implant. The valve had marked numbers of inflammatory cells on the fibrosal surface of the leaflet (see Figure C-9). Most of the inflammatory cells were granulocytes but also included plasma cells, lymphocytes and macrophages. A few foreign body giant cells were also observed on the outside of the inflammatory rim. The ventricularis had less inflammation but all of the above inflammatory cells were present. The valve leaflet stained strongly positive in all three layers for both IgG and C3 (complement) (see Figure C-9). There was no positive staining for IgM, suggestive of an acquired rather than a preformed antibody response against the porcine tissue.

Figure C-10 Mosaic valve (A, B) before implant and the outflow (C) aspect of the valve after only 109 days.

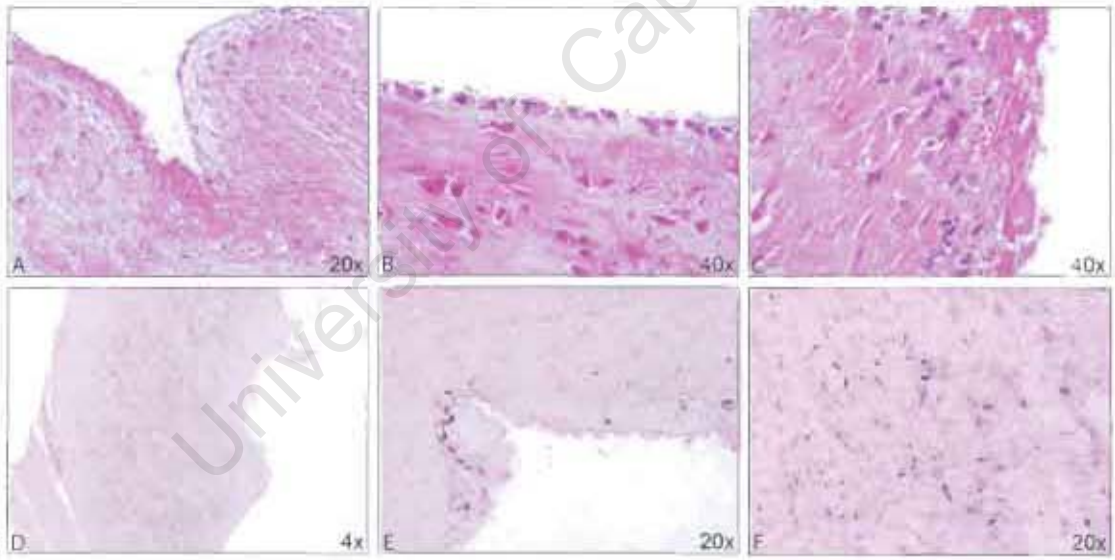

Figure C-11 Mosaic valve that failed after 109 days. A-C: HE stain; D-F CD68 stain.)

Case 5: The valve was explanted after only 109 days because one leaflet was sutured onto the sewing ring (see Figure C-10). The valve had only scanty inflammatory cells (see Figure C-11). Macrophages, lymphocytes and granulocytes were present in the spongiosa and towards the fibrosal side of the leaflet, but not on the fibrosal surface of the leaflet. This valve was included because it showed the inflammation of the valve after only 109 days.

Table 1 Inflammation of the leaflets of explanted bioprosthetic heart valves from patients

Valve	Inflammatory cells	Fibrosa	Spongiosa	Ventricularis
Hancock (24 years)	PMNs	+	+	-
	Macrophage	+	+	-
	Foreign body giant cell	-	-	-
	Lymphocyte	+	-	-
	IgG	+	+	+
Hancock (19 years)	PMNs	-	+	-
	Macrophage	-	+	-
	Foreign body giant cell	-	-	-
	Lymphocyte	-	-	-
	IgG	-	+	-
Carpienter Edwards (11 years)	PMNs	+	+	-
	Macrophage	+	-	-
	Foreign body giant cell	+	-	-
	Lymphocyte	+	-	-
	IgG	-	+	+
Mosaic (3 years)	PMNs	+	+	+
	Macrophage	+	+	+
	Foreign body giant cell	+	-	-
	Lymphocyte	+	+	+
	IgG	+	+	+
Mosaic (109 days)	PMNs	+	-	-
	Macrophage	+	-	-
	Foreign body giant cell	-	-	-
	Lymphocyte	-	-	-
	IgG	N	N	N

(N: not stained for IgG) (+: cells present, -: cells absent)

C1.1.D Summary

Clinical studies have shown that macrophages are the main invading phagocyte which may play a role in degrading collagen. In another study the initial steroid therapy after heart valve replacement in patients also lowered the occurrence of calcification of the bioprosthetic valves[163]. The steroid therapy may have reduced the initial inflammatory response to the valves and thus protected the valves from structural damage. Graft-specific antibodies were present in patients confirming that there is a humoral response to the tissue as well[73, 94, 157, 163]. It is only recently that it has been reported that an inflammatory reaction may have lead to aortic tissue damage and eventually heart valve failure and suggested that it might be a consequence of cellular graft rejection[202]. In this study the small cohort of bioprosthetic valves explanted at Groote Schuur hospital showed that inflammation might have played a role in their failure.

The inflammation of the valves explanted at different time periods showed that initially the valves had an innate type inflammation dominated by neutrophils. There was a strong humoral response as seen with the strong positive staining for IgG. The IgM response was less obvious suggesting that the response was not simply a preformed antibody response as is the case with hyperacute rejection of vascularised xenogenic organ transplants. Bioprosthetic tissue is typically denuded of its endothelial lining as a consequence of processing and thus the porcine vascular endothelial xenoantigen, galactose-[alpha]-1,3-galactose (alpha-Gal), is depleted, at least with respect to the valve's lumenal surface. Preformed alpha-Gal antibody which is mostly responsible for early hyperacute rejection seen in vascularised discordant donor-recipient solid organ transplants between pigs into human (or primates) as a result does not play a similar role in heart valve replacement. Chen et al[203] showed that although cardiac microvascular endothelium strongly expressed the galactose [alpha]-1,3-galactose antigen, galactose [alpha]-1,3-galactose was not detected on the endothelium of porcine aortic and pulmonary valves and this may also result in porcine valves being protected from xenograft rejection in primates. In contrast another group reported the presence of the immunogenic alpha-Gal-epitope on fibrocytes interspersed in the connective tissue of porcine valves. They also showed that glutaraldehyde-fixation at concentrations used for commercial use did not diminish the response to the alpha-Gal epitope. Their finding of a significant

increase of alpha-Gal IgM antibodies in patients after implantation with bioprosthetic heart valves suggested a response specific against the xenograft. [204].

The inflammatory cells were mostly found on the fibrosal aspect of the leaflets. This surface is more protected against the shear stress exerted by the blood flow than is the case with that of the ventricularis. In some cases the inflammatory cells infiltrated into the spongiosa continuing inflammatory cell degradation of the tissue. In contrast there were only a few inflammatory cells on the blood surface of the inflow side of the valve. The ventricularis is exposed to a more laminar blood flow compared to the fibrosa and it is therefore more difficult for the inflammatory cells to adhere. This is similar to what is seen on the blood surface of the aortic wall compared to its adventitial surface.

Inflammation included neutrophils, macrophages, lymphocytes and plasma cells with only a few foreign body giant cells. The types of cells found suggest that the response was not limited to an initial non-specific acute response, but that it had evolved into a more specific form. The presence of IgG on all of the layers of the leaflet indicated that there was a clear well-defined humoral response against the bioprosthetic tissue. Most of the inflammatory cells also present have Fc receptors [205] capable of recognising the Fc part of the IgG bound to, and thus opsonising, the tissue and leading to a stronger and more specifically targeted response.

Even though this was only an anecdotal study of a limited number of clinically explanted valves, it nevertheless demonstrated that fixation of porcine heart valve tissue with the low concentration of glutaraldehyde used in contemporary bioprostheses was not adequate to sufficiently mask the antigens from the host immune system and that a clear cellular inflammatory response was present long after the valves were implanted.

C1.2. Immune response to bioprosthetic tissue implants in animal models

C1.2.A Introduction

Animal models used to investigate the biocompatibility of bioprosthetic heart valves are typically either circulatory [206] or noncirculatory, as in this case a subdermal model. In the circulatory model the whole valve may be implanted and its performance can therefore be investigated in a blood flow environment, thus simulating how it will be used clinically. In the subdermal model only the host response and calcification potential can be investigated. Indeed subdermal models are regularly used to test different anti-calcification treatments [207], but not the full biocompatibility or functionality of the design of the valve.

In this study we examined the immune response to bioprosthetic valves in both circulatory and subdermal animal models to compare inflammatory responses to bioprosthetic tissue.

C1.2.B Materials and methods

C1.2.B(1) Circulatory models

Chacma baboon

Pig aortic wall was harvested from healthy pigs at the abattoir (see Appendix A3) and treated with 0.2% glutaraldehyde (see Appendix A12) after a 48 hour delay at 4°C. The treated pig aortic wall tissue was used to fabricate vascular tubes, size approximately 2 cm, small enough to implant end-to-end in the iliac position of the baboon (see Figure C-12). These tubes were retrieved after 42 days.

Figure C-12 The baboon iliac model. The top right picture shows the graft implanted in the graft position. The bottom right picture shows the graft explanted and split longitudinally.

The explanted tissue was fixed in 4% paraformaldehyde, processed and wax embedded in blocks for sectioning (see Appendix A19) and stained with HE (see Appendix A21). Immunohistochemistry (see Appendix A20) for CD68 (macrophage marker), Abcam (macrophage marker), and IgG were also performed. The sections were investigated to determine the extent and type of inflammation present.

Vervet monkey

Porcine arteries, sized approximately 3 cm, were harvested at the abattoir from healthy pigs (see Appendix A3) and treated with 0.2% glutaraldehyde (see Appendix A12) after a 48 hour delay at 4°C. After treatment the porcine arteries were implanted end-to-end in the iliac position of the vervet for 42 days (see Figure C-13).

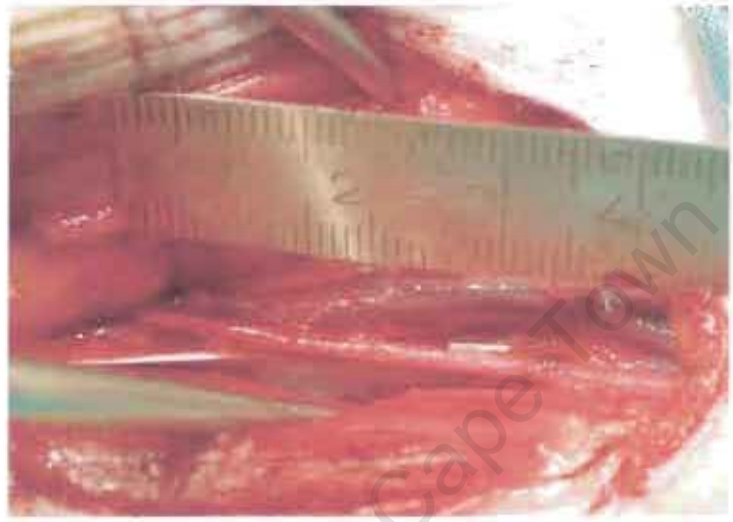

Figure C-13 The porcine artery implanted in the iliac postion of the vervet monkey.

Retrieved arteries were fixed in 4% paraformaldehyde. The samples were processed and blocked in wax (see Appendix A19). Sections were stained with HE and Brown and Brenn (BB) (see Appendix A21). The BB stain is normally used to determine bacterial loading of the tissue but also provides good definition of the nuclei of inflammatory cells, thus aiding in their identification.

C1.2.B(2) Subdermal implant models

Porcine aortic tissue was harvested at the abattoir from healthy pigs (see Appendix A3). Coupons, size 12 mm, were cut from the porcine aortic wall and treated with 0.2% glutaraldehyde (see Appendix A12) after a 48 hour delay at 4°C. The coupons were implanted subdermally into pouches created by blunt dissection on the ventral aspect of the abdomen of the Vervet monkey, and the dorsal subscapular region of rabbits and rats.

The coupons were retrieved and fixed in 4% paraformaldehyde after 42 days. The samples were processed and blocked in wax (see Appendix A19). Different immunohistochemistry stains were performed for the different subdermal models.

Vervet monkeys

Sections were stained with HE (see Appendix A21) and immunohistochemistry (see Appendix A20) for IgG and C3 (complement) was performed.

New Zealand White rabbits

Sections were stained with HE and BB (see Appendix A21) and immunohistochemistry (see Appendix A20) for C3 (complement), IgM and IgG was performed.

Long Evans rats

Sections were stained with HE and BB (see Appendix A21)

C1.2.C Results

C1.2.C(1) Circulatory models

C1.2.C.1(i) Chacma baboon

The inflammatory cells on the intimal side (see Figure C-16) of the implants were predominantly foreign body giant cells that lined up against the luminal surface. There was also host tissue overgrowth (pannus) on the intimal side (see Figure C-16) overgrowing the foreign body giant cells. The pannus tissue itself included PMNs, plasma cells and lymphocytes. On the blood surface side of the pannus, repopulation of endothelial cells was seen.

The inflammatory rim (see Figure C-14) on the adventitial side was dominated with PMNs, eosinophils, macrophages, plasma cells, lymphocytes and foreign body giant cells. In contrast with the intima and adventitial surfaces of the artery, were there no inflammatory cells in the media.

IgG staining (see Figure C-16) was observed on the both the intimal and adventitial surfaces respectively but did not penetrate into the media. IgG staining was mostly colocalised with the macrophages on the adventitial side and with some infiltration into the media. On the intimal surface the staining was mostly on the surface area with limited infiltration into the media. There was not positive staining for IgG in the media.

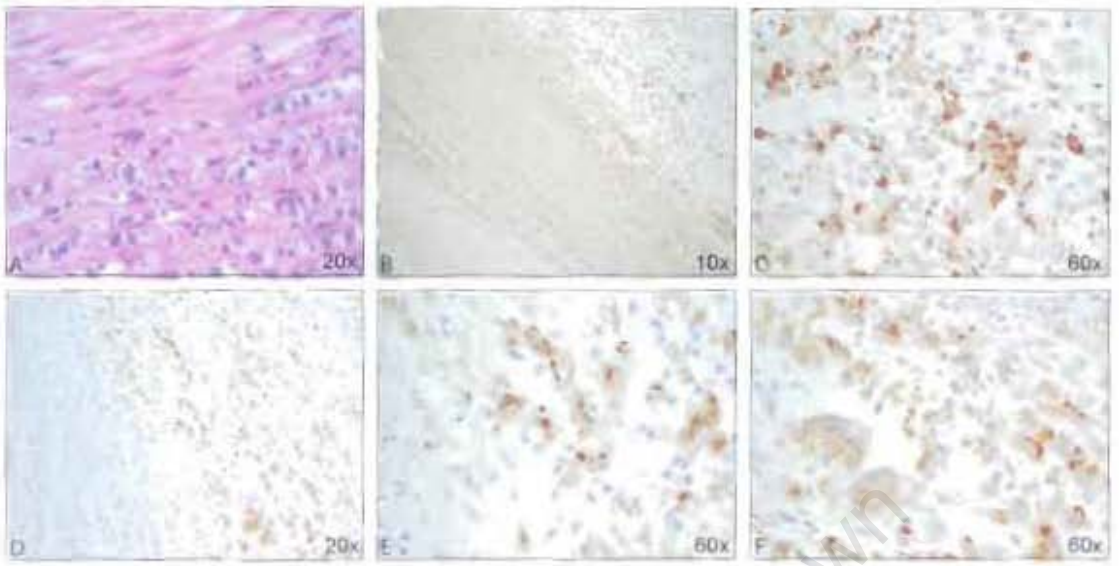

Figure C-14 Baboon adventitial side of the porcine aortic tubes: A: HE stain, B and C: Abcam stain, D - E: CD68.

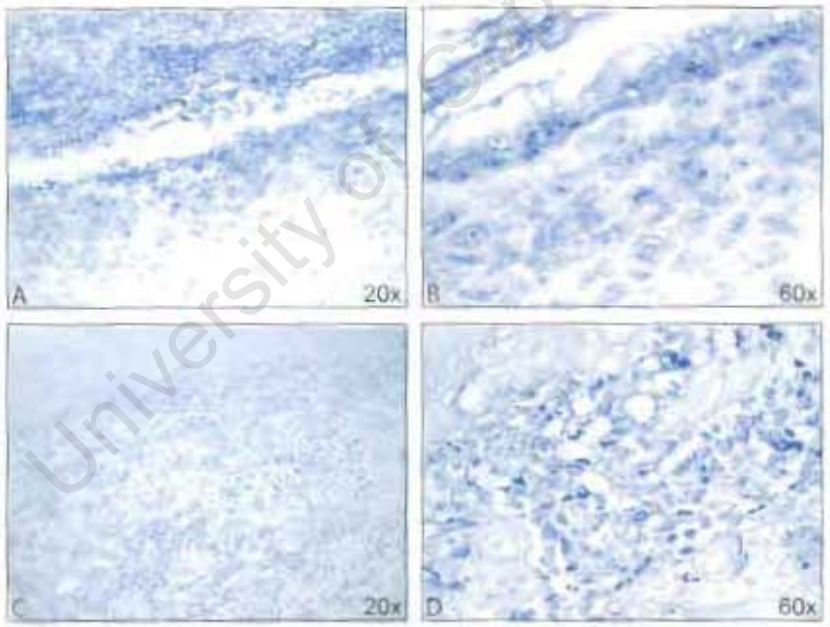

Figure C-15 Baboon model stained for IgG. A and B is on the intimal side and C and D is staining on the adventitial side.

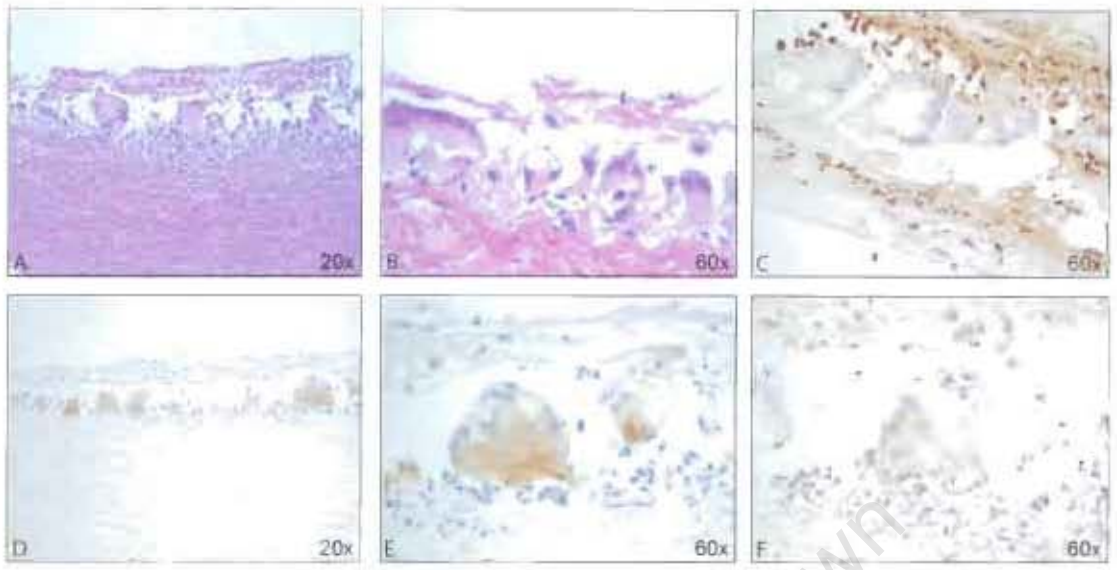

Figure C-16 Baboon intimal side of the porcine aortic tube. A and B: HE stain. C: Abcam 60x. D - F: CD68 stain.

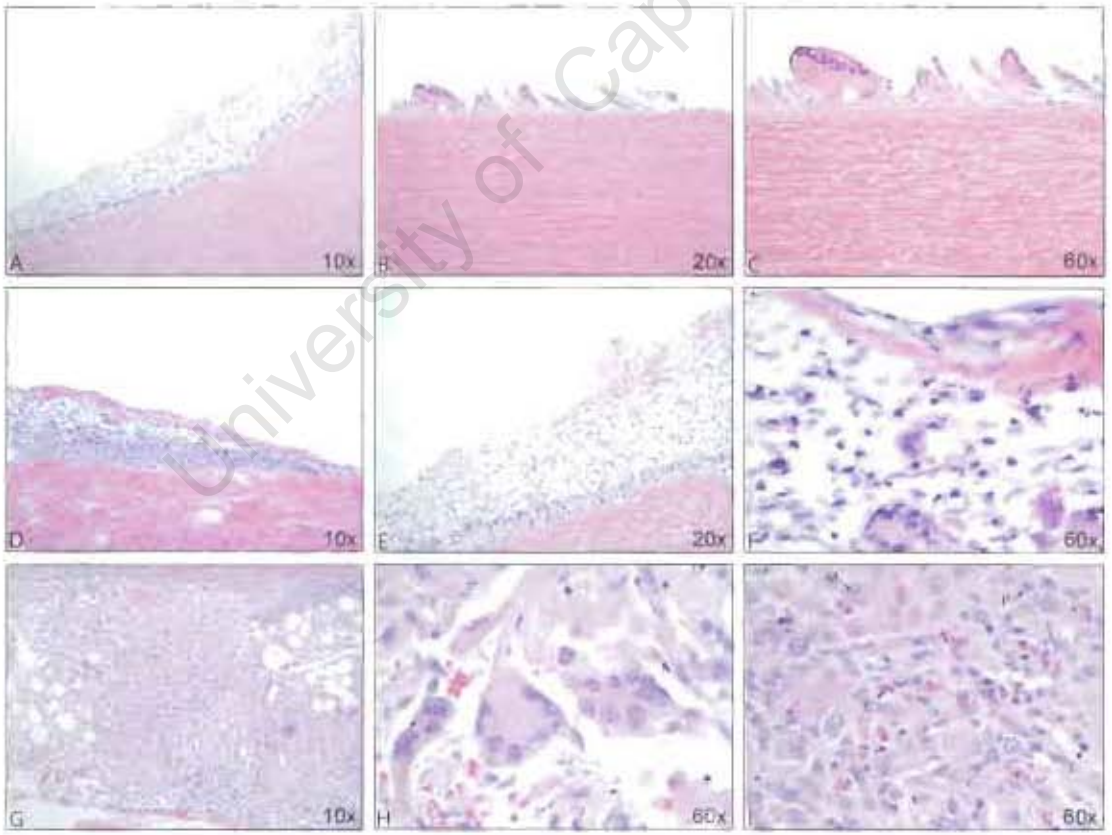

Figure C-17 Porcine aortic tube explanted from the baboon after 42 days histology sections stained with HE. A to C is on the intimal side of the tube, D to E is the pannus on the intimal side of the tube and G to I is the adventitial side of the tube.

C1.2.C.1(ii) Vervet monkey

There were only a few macrophages and foreign body giant cells on the intimal surface without any pannus overgrowth (see andFigure C-18 and Figure C-19).

There was no observed infiltration of inflammatory cells in the media, but there was some degradation of tissue on the adventitial side.

The inflammatory cells (see Figure C-18 and Figure C-19) on the adventitial side were a combination of PMNs, macrophages, lymphocytes, plasma cells and foreign body giant cells.

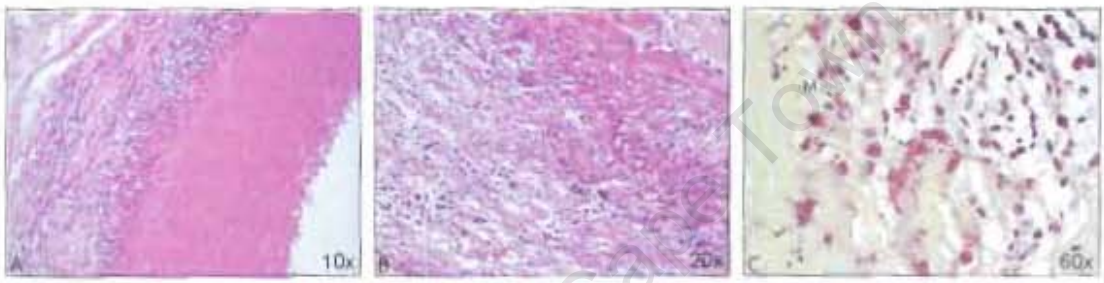

Figure C-18 Vervet artery stained with HE (A and B) and BB (C). A: Whole graft, B and C: Adventitial side. (M – Macrophage, F – Foreign body giant cell; L – Lymphocyte).

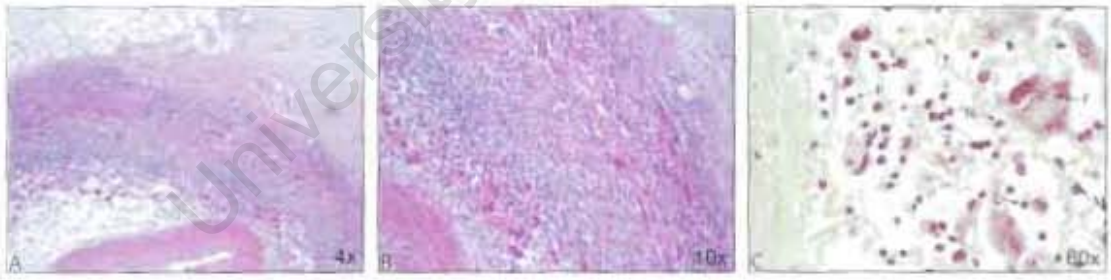

Figure C-19 Vervet artery stained with HE (A and B) and BB (C). A: Whole graft , B and C: Adventitial side (M – Macrophage, F – Foreign body giant cell; L – Lymphocyte, P – Plasma cell, N- Neutrophil)

C1.2.C(2) Subdermal implant model

C1.2.C.2(i) Vervet monkey

The inflammatory cells on the intimal surface were PMNs, lymphocytes, macrophages and foreign body giant cells. IgG and C3 stained positive on the edge of the media.

On the cut edge of the coupon there were some macrophages and IgG positive staining associated with these cells. There was only scattered positive staining for C3 throughout the media.

The foreign body giant cells were observed lined up directly against this adventitial surface of the tissue. The inflammatory rim outside the foreign body giant cells included PMNs, macrophages, lymphocytes and plasma cells. There was also positive staining for C3 at the medial interface.

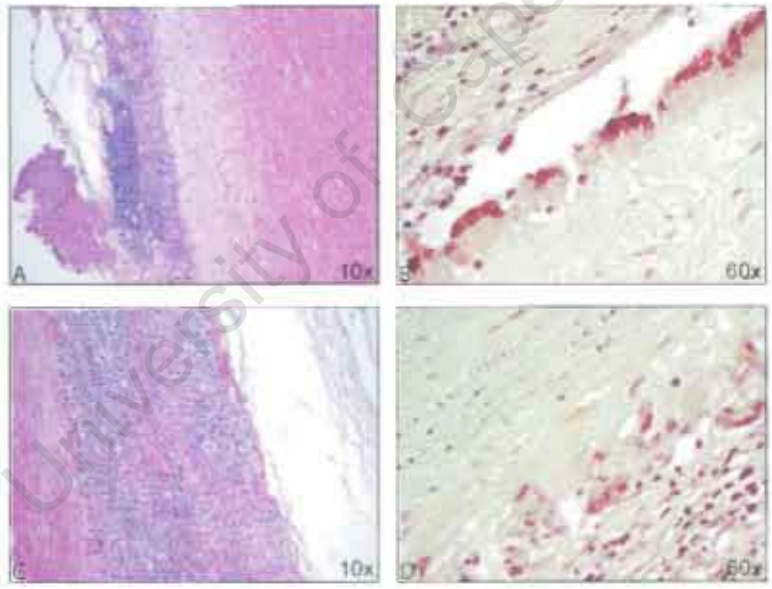

Figure C-20 Glutaraldehyde fixed porcine aorta coupons explanted from vervet monkeys. A and C: HE stains; B and D: BB stains. A and B: intimal side, C and D: adventitial side.

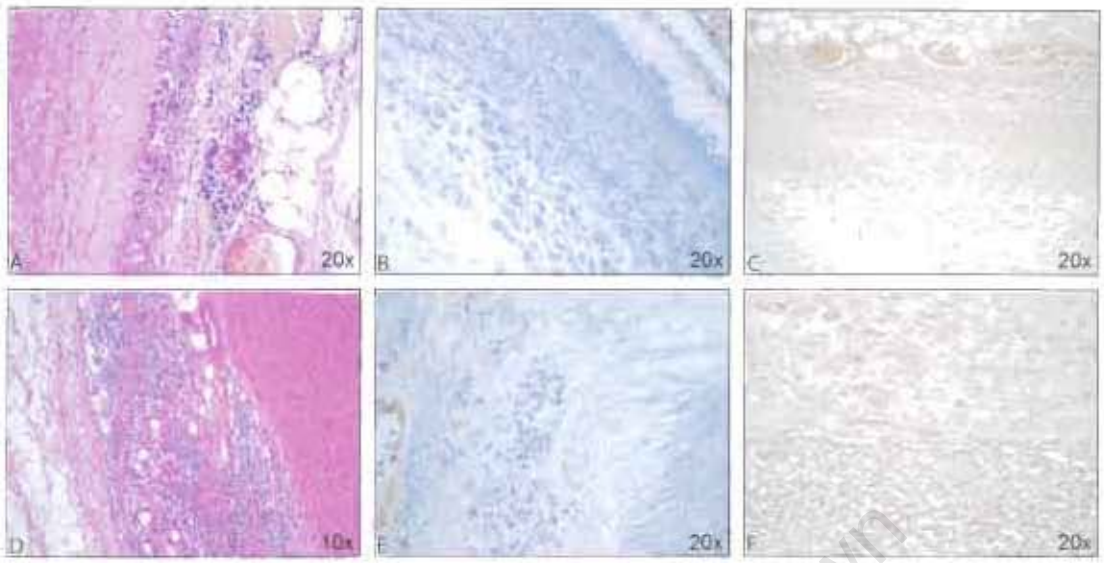

Figure C-21 Glutaraldehyde fixed porcine aorta coupons explanted from vervet monkeys. A and D: HE stain; B and E: IgG stain and C and F: C3 stain. A to C intimal side and D to F: adventitial side.

C1.2.C.2(ii) New Zealand White rabbit

On the intimal surface macrophages with a few foreign body giant cells formed the main inflammation on the edge of the tissue. Only a few PMNs and plasma cells were seen on the intimal side. There was IgG and IgM positive staining on the surface of the tissue. IgG and IgM staining was mostly colocalised with inflammatory cells. IgM was specifically associated with plasma cells and PMNs. The IgM may be an artefact of the IgM staining the plasma cells surface immunoglobulin or it may be due to binding to the Fc receptor of the PMNs.

There were no inflammatory cells in the media and no IgM positive staining. The C3 stained in association with cells in the media. The IgG positive staining in the media was associated with calcification deposits in the coupons.

Macrophages and foreign bodies lined the edge of the adventitial side of the coupon. The inflammatory cells included also PMNs, lymphocytes and plasma cells. IgG, IgM and C3 stained positive on the surface of the adventitial tissue.

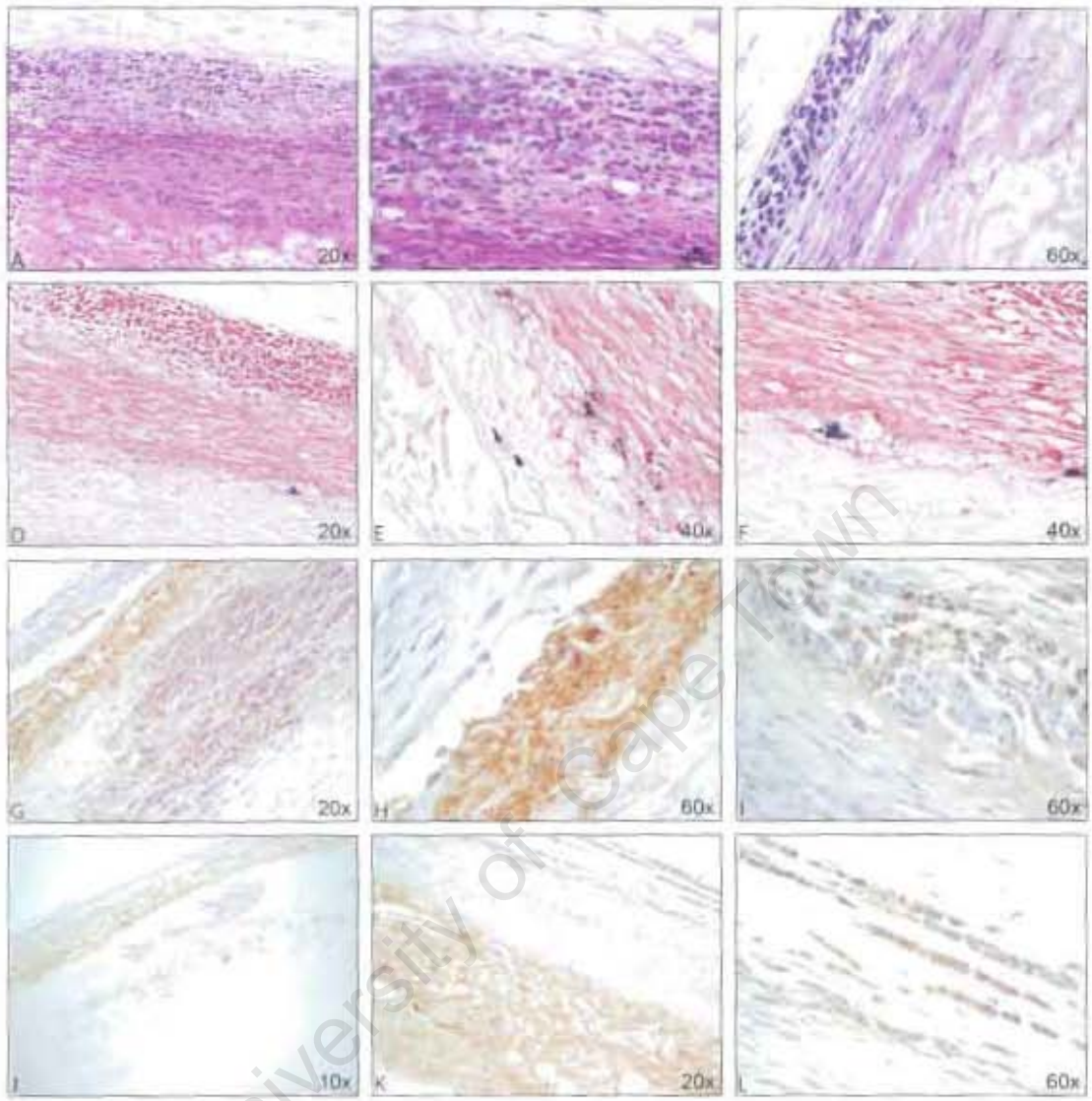

Figure C-22 Adventitial side of glutaraldehyde fixed porcine aorta coupons explanted from rabbits: A to C: HE stain. D to F: Macrophage stain. G to I: IgG stain. J to L: IgM stain.

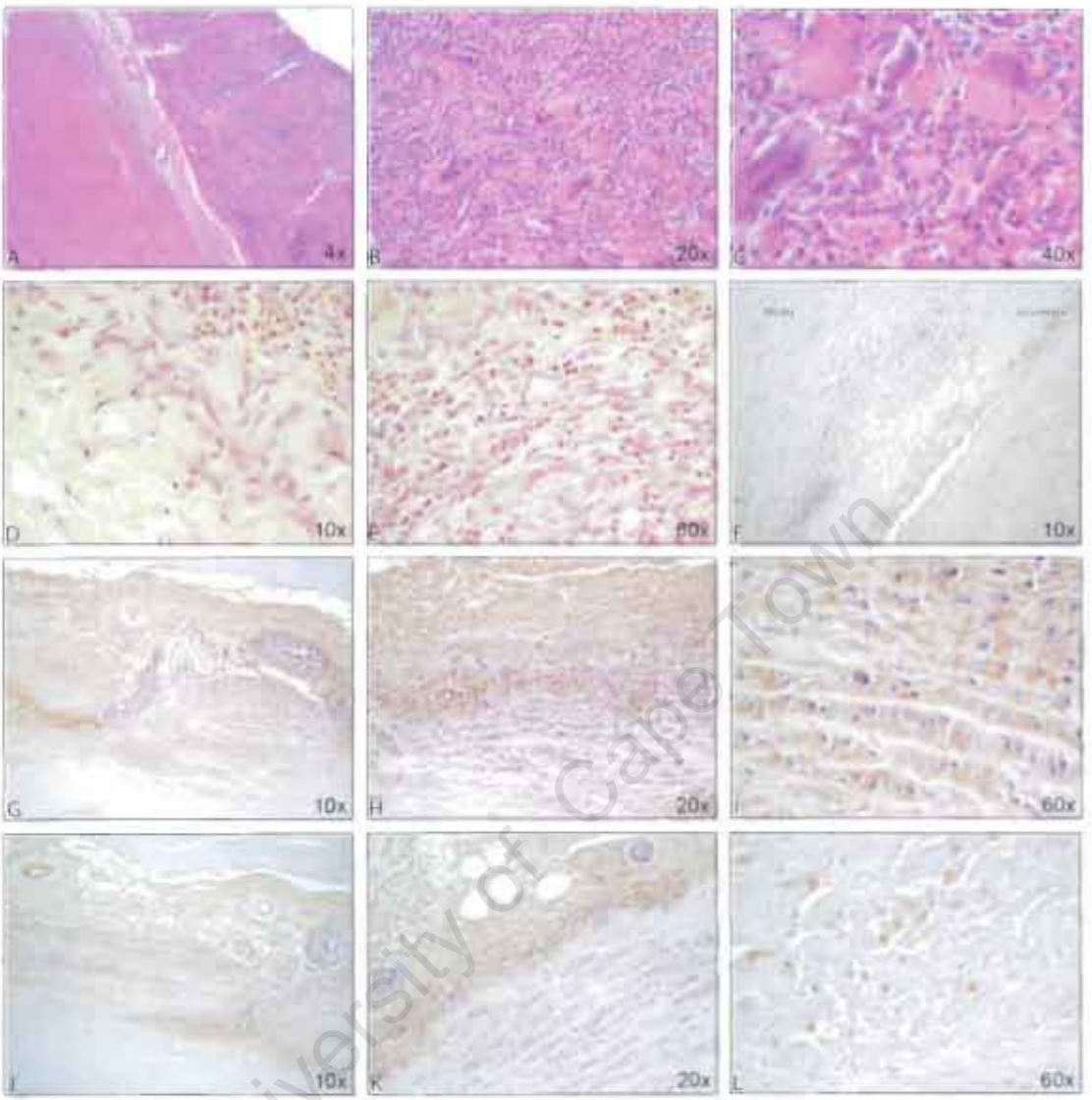

Figure C-23 Adventitial side of glutaraldehyde fixed porcine aorta coupons explanted from rabbits. A to C: HE stain. D to E: BB stain. F: C3 stain. G to I: IgG stain. J to L: IgM stain.

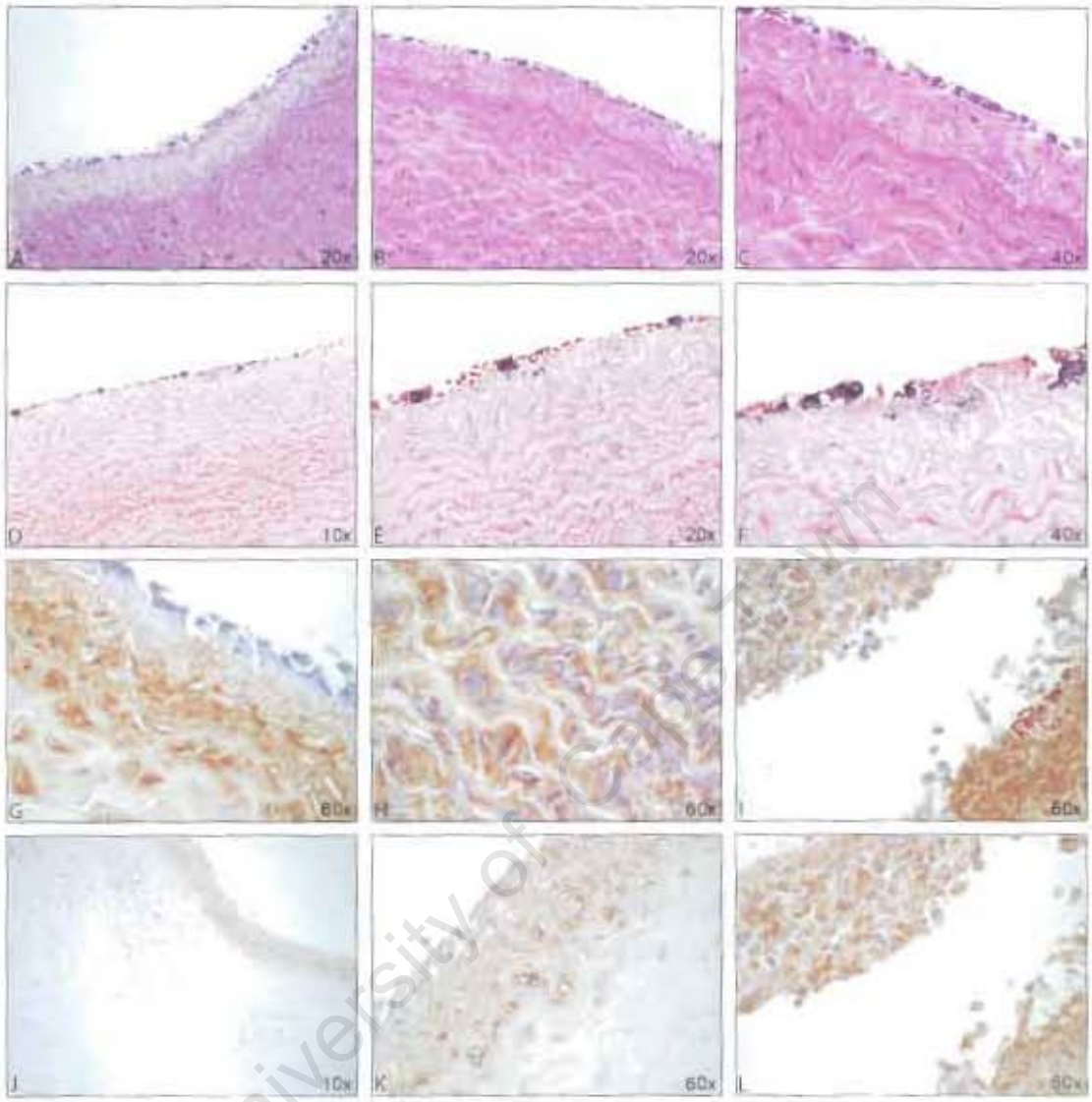

Figure C-24 Intimal side of glutaraldehyde fixed porcine aorta coupons explanted from rabbits. A to C: HE stain. D to F: Macrophage stain. G to I: IgG stain. J to L: IgM stain.

C1.2.C.2(iii) Long Evans rat

The inflammatory cells mostly observed were lymphocytes with a few macrophages and PMNs on both sides of the coupon. There were no inflammatory cells within the media and no infiltration of the inflammatory cells into the media.

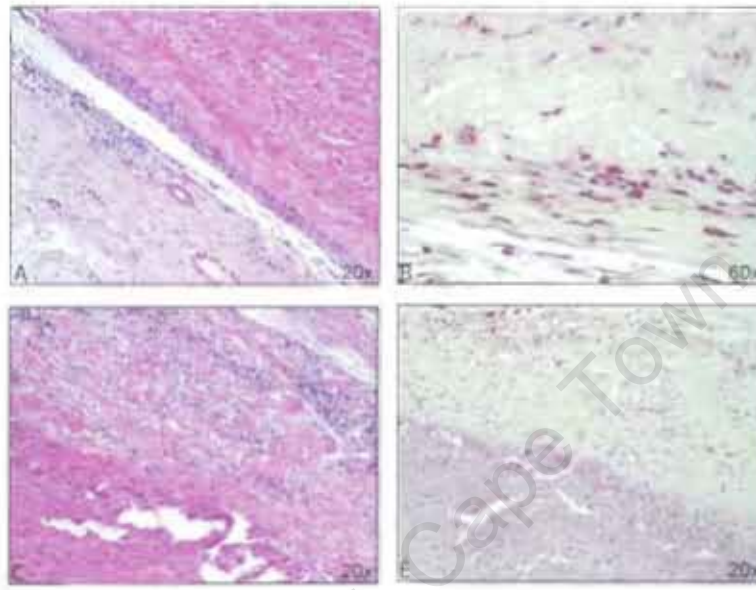

Figure C-25 Glutaraldehyde fixed porcine aorta coupons explanted from rats. A and B: intimal side, C and D: adventitial side. A and C: HE stain. B and D: BB stain.

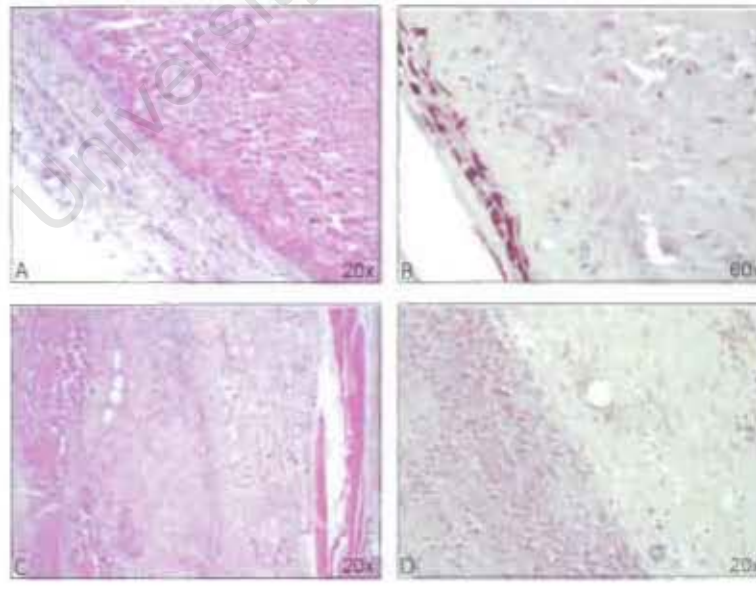

Figure C-26 Glutaraldehyde fixed porcine aorta coupons explanted from rats. A and B: intimal side. C and D: adventitial side. A and C: HE stain. B and D: BB stain.

Table 2 Summary of the inflammation of the different animal models

Model	Animal	Intima	Media	Adventitia
Circulatory	**Chacma baboon**	Ly, PMNs PCs, FBGCs, ECs	No inflammatory cells	PMNs, Eos, Mϕ, PCs, Ly, FBGCs
		Pannus	No Pannus	No Pannus
		IgG	No IgG	IgG
	Vervet monkey	Mϕ, FBGCs	No inflammatory cells	PMNs, Mϕ, Ly, PCs, FBGCs
		No Pannus	No Pannus	No Pannus
Subdermal	**Vervet monkey**	PMNs, Ly, Mϕ, FBGCs	Mϕ	PMNs, Mϕ, Ly, PCs, FBGCs
		IgG, C3	IgG, C3	C3
	New Zealand White rabbit	PMNs, PCs, Mϕ, FBGCs	No inflammatory cells	PMNs, Ly, PCs, Mϕ, FBGCs
		IgG, IgM	IgG, C3	IgG, IgM, C3
	Long Evans rat	Ly, Mϕ, PMNs	No inflammatory cells	Ly, Mϕ, PMNs

(Ly: Lymphocytes, PMNs: polymorphonuclear leukocytes, Eos: eosinophils, Mϕ: macrophages, PCs: plasma cells, FBGCs: foreign body giant cells, ECs: endothelial cells)

C1.2.D Summary

In this study we showed that different animal models all elicited an immune response to glutaraldehyde fixed porcine tissue. The response was further investigated in the Rabbit model. A smaller animal model which is more cost effective with less ethical consequences than using the primate species with a similar inflammation pattern to the primate species.

In different animal studies investigators had a few findings that may link inflammation and calcification. These findings were the following:

- Heterologous tissue calcifies more than homologous tissue[114]
- Grafts incubated in graft-specific serum before being implanted had three times more calcification[161]
- Tissue fixed in glutaraldehyde elicit both cellular and humoral responses[152], and
- Increasing the glutaraldehyde concentration to 3% to better mask the antigenicity lowered the calcification of the grafts[141, 144].

The circulatory model has an advantage over the noncirculatory model in that the tissue is exposed to the blood environment. The shear stress of the blood flow reduced adherence of inflammatory cells on the intimal side compared to the adventitial side. A similar pattern was seen in the noncirculatory model where more inflammatory cells adhere to the adventitial side of the coupons. This is clearly therefore not only the result of shear stress, but that the adventitial surface with its loose collagen has potentially more exposed and accessible antigens than the smooth compact surface of the intima. The inflammatory cells were similar in all the models, except in the rat model where the inflammatory cells were dominated by lymphocytes. In the other models the inflammatory cellular response was dominated by granulocytes and macrophages. The humoral response was observed in both the circulatory and noncirculatory models. Most of the inflammatory cells have Fc receptors and the presence of IgG opsonising the surface of the tissue may lead to a more specific response.

The rabbit subdermal model proved to be a good model to evaluate the inflammatory response, since it showed similar inflammatory cells to the two circulatory models. Even though it was a subdermal model without the shear stress of blood flow, the coupons subdermally implanted into the rabbit showed more inflammation on the adventitial side than on the intimal side. This is similar as to what was seen in the circulatory models. As a subdermal model the rabbit did not show any pannus, but there were foreign body giant cells present similar to the circulatory models. The rabbit is also a less expensive model to evaluate than both the baboon and vervet.

Although they provide a better estimate of the response in humans, ethical consideration restricts the use of primates in experimentation. Ethical considerations make the choice of animal model more complex and the researcher must consider the use of animal models carefully. Due to the complexity of the immune response [208] animal models, however, remain crucial to bioprosthetic research. The ideal is to use the rabbit as a screening model and the primate as the pre-clinical model.

C1.3. Acquired immune response in rabbits to porcine tissue

C1.3.A Immunisation of rabbits with porcine tissue

C1.3.A(1) Introduction

Rabbits were immunised with different porcine valve tissue preparations to investigate their potential to elicit an immune response. The sera of the animals immunised were used to compare IgG binding to fresh porcine aortic tissue treated with glutaraldehyde. Serum from rabbits before immunisation was used to evaluate the possibility of preformed antibodies with specificity or cross-reactivity for the porcine tissue used for immunisation.

Three preparations of porcine aortic tissue were used for immunisation:

- Fresh porcine aortic wall was used to evaluate the overall response to porcine aortic tissue.
- Decellularised porcine aortic tissue was used to evaluate the extent of immunogenicity of the extracellular as opposed to cellular components of the aortic tissue.
- Purified porcine fibronectin was selected, because it had previously been shown to elicit an immunoglobulin response in porcine aorta.

C1.3.A(2) Materials and methods

C1.3.A.2(i) Preparation of tissue for immunisation

Different homogenates for immunisation were prepared. The tissue of the porcine aortas was homogenised into a powder form to disturb the structure and render the epitopes more accessible for immune system recognition.

Fibronectin was isolated from the plasma of porcine blood. The structure of soluble plasma and insoluble cellular fibronectin appear to share similar common structural organisation [209]. It is reported that there are three regions with differences in the

polypeptides of plasma and cellular fibronectin. Plasma fibronectin does not result from posttranslational proteolytic modification of the cellular form [210]. They are however very similar or at least not distinguishable in immunological assays, amino acid and carbohydrate compositions, peptide maps, electrophoretic mobilities and spectrophotometric properties [210]. Thus, using plasma fibronectin would therefore elicit a similar response as cellular fibronectin.

Porcine aorta

Fresh porcine aortas were collected from the abattoir (see Appendix A3) and the aortic wall was divided into smaller fragments and frozen in liquid nitrogen.

Fresh porcine aortas collected from the abattoir were extensively washed in solutions with SDS and Triton X-100 detergents to remove cells from the tissue ideally leaving behind only the extracellular matrix. This process was performed by Medtronic's Heart Valve Division in Sante Ana, CA, USA (see Appendix A4). After receipt of the decellularised tissue, it was rinsed in PBS (pH 7.4) and the wall divided into smaller fragments and frozen in liquid nitrogen.

The frozen fresh porcine aortic wall and decellularised aortic wall fragments were homogenised (see Appendix A5) with a homogeniser. Small frozen tissue fragments were placed in an ice-cold stainless steel tube (cooled in liquid nitrogen) with two ice-cold stainless steel ball bearings (also cooled in liquid nitrogen). The tissue is shaken at high speed for only a few seconds to prevent the tissue from thawing. The tissue was pulverised into powder form. The powder was pooled in a mortar cooled with liquid nitrogen and mixed with a pestle into a homogenous mix. The homogenous powder of the two groups was stored separately at -80°C.

Fibronectin

Blood was collected from normal, healthy pigs and the plasma (see Appendix A2) was used for isolation of plasma fibronectin using affinity chromatography (see Appendix A11). Pig plasma (100 ml) was applied to a gelatin-agarose column (see Appendix A11b) and since fibronectin has a gelatin-binding domain, it was able to bind the gelatin ligand. All the other plasma constituents remained unbound and were eluted from the column. The fibronectin was finally eluted from the column using urea causing it to briefly denature. The pooled fractions of fibronectin were subsequently dialysed against double distilled water to remove the buffer salts and urea. The pure fibronectin was freeze-dried and finally stored at -80°C until use.

C1.3.A.2(ii) Preparation of emulsions for immunisation

Emulsions were prepared for immunisation from suspensions of the powdered tissue in sterile saline and Freund's incomplete adjuvant in a 1:1 ratio (see Appendix A6).

The porcine aorta homogenate and decellularised porcine aorta homogenate were prepared from 10 mg of the powder respectively. The powder was insoluble and mixed with sterile saline (0.5 ml) before adding the Freund's incomplete adjuvant (0.5 ml).

Fibronectin (1 mg) was first dissolved in sterile saline (0.5 ml) before adding the Freund's incomplete adjuvant (0.5 ml).

A final volume of 1 ml emulsion per animal was prepared from each immunogen preparation using Freund's incomplete adjuvant. The emulsions were stored in sterile injections at 4°C ready for immunisation.

C1.3.A.2(iii) Immunisation of the animals

Eight New Zealand White rabbits aged 5 weeks were used for immunisation. Four animals were immunised with porcine aorta homogenate, three animals were immunised with decellularised porcine aorta homogenate and one animal was immunised with fibronectin homogenate (see Figure C-27). The emulsions were injected subcutaneously at two sites (0.5 ml each) on the animal's back with each animal receiving a total dose of 10 mg.

Fibronectin was injected at four sites (0.25 ml each) with each animal receiving a total dose of only 1 mg.

After 14 and 21 days respectively the animals were administered booster immunisations of the same dose. Test blood (5 ml) was drawn from an ear vein immediately prior to immunisation and immediately prior to booster immunisations to monitor antibody production. The animals were killed after four weeks and a large volume of blood collected by cardiac puncture into blood collection tubes and sera were isolated (see Appendix A1).

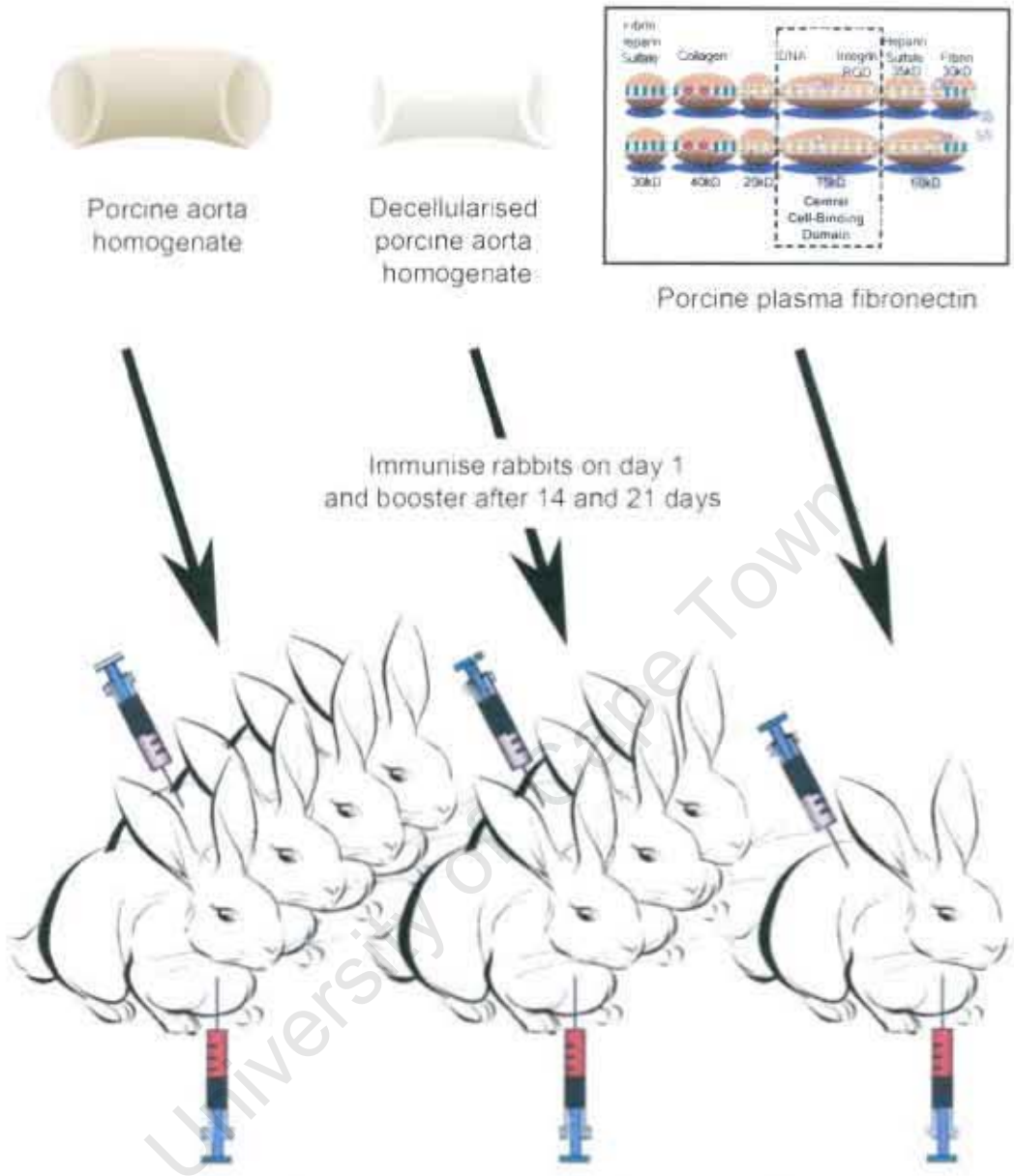

Figure C-27 Immunisation of rabbits with different porcine immunogens

Care of Animals

All anaesthetic and surgical procedures were approved by the animal ethics committee of the University of Cape Town and complied with the "Principals of Laboratory Care" and the guidelines for the care and use of laboratory animals.

C1.3.A.2(iv) Western blot detection of tissue specific antibodies

SDS PAGE electrophoresis is a size-based separation of proteins. SDS is an anionic detergent that binds to most soluble protein molecules in aqueous solution over a wide pH range. Polypeptide chains bind amounts of SDS proportional to the size of the molecules. The net negative charge of the proteins is strongly attracted towards the anode in an electrical field. The density of the polyacrylamide gel determines the migration rate of the protein with larger molecules migrating slower than smaller ones.

Western blotting involves electroblotting which uses a electric current to transfer the separated proteins from the gel onto the PVDF membrane which can be detected using labelled antibody. The PVDF membrane binds all proteins non-specifically based upon hydrophobic interactions, as well as charged interactions between the membrane and protein. The proteins move from the gel onto the PVDF membrane while maintaining the organisation of the proteins separated on the SDS polyacrylamide gel. The PVDF membrane has the ability to bind both the target proteins and antibodies. To prevent interactions between the membrane and the antibody used for detection the membrane was blocked for non-specific binding by placing the membrane in a dilute solution of protein such as a non-fat dry milk and a detergent such as Tween 20. The transferred proteins were used to detect antibody production in the serum of the animals immunised with porcine immunogens.

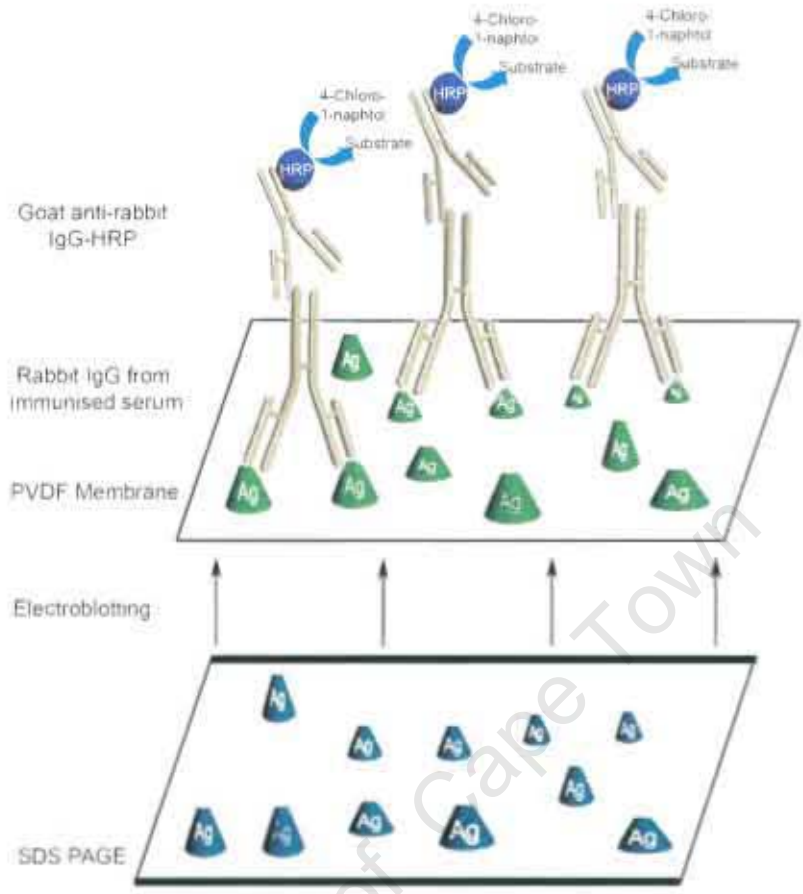

Figure C-28 The transfer of proteins to a PVDF membrane and Western Blot.

Fresh porcine aortic extract Western blot

A protein extract was prepared from homogenised unfixed porcine aortic wall tissue by overnight extraction in a denaturing buffer (see Appendix A7). The protein concentration of the extract supernatant was determined using a detergent compatible protein detection kit ((DC protein assay, Bio-Rad) (see Appendix A8)). The extract was electrophoretically separated on gradient SDS polyacrylamide gels (4-20%) to achieve good separation of high molecular weight proteins whilst avoiding loss of smaller proteins (see Appendix A9). The separated proteins were transferred onto a PVDF membrane and the membrane was blocked overnight in 5% milk powder in TTBS buffer at 4°C to prevent any non-specific binding of proteins and antibodies to the PVDF membrane. Western blot (See Appendix A10) was performed with the sera obtained from the immunised rabbits. The serum samples were diluted 1:100 in 5% milk powder TTBS buffer. For detection, the secondary

antibody goat anti-rabbit immunoglobulin conjugated to horseradish peroxidase (Bio-Rad, cat no 170-6515) was diluted 1:3000 and applied.

Fibronectin Western blot

Porcine fibronectin was dissolved in PBS and electrophoretically separated on gradient SDS polyacrylamide gels (4-20%) to separate the high molecular weight fibronectin (440 kD consisting of two 220 kD subunits) and any fragments thereof (see Appendix A9). The separated protein was blotted onto PVDF membranes and a similar Western blot (See Appendix A10) with the sera obtained from the immunised rabbits was performed (see above).

C1.3.A(3) Results

C1.3.A.3(i) Western blot detection of antibodies from immunised serum

The SDS extraction process of unfixed porcine aortic wall tissue showed a wide range of high and lower molecular weight proteins after separation on a gradient SDS polyacrylamide gel. The Western blots as shown in Figure C-29 and Figure C-30 clearly showed that the rabbits formed antibodies against the proteins extracted from porcine aortic wall and porcine fibronectin fragments. As shown in Figure C-29 and Figure C-30 these antibodies were not present in the sera collected from the rabbits before immunisation (control sera).

Fresh porcine aortic extract Western blot

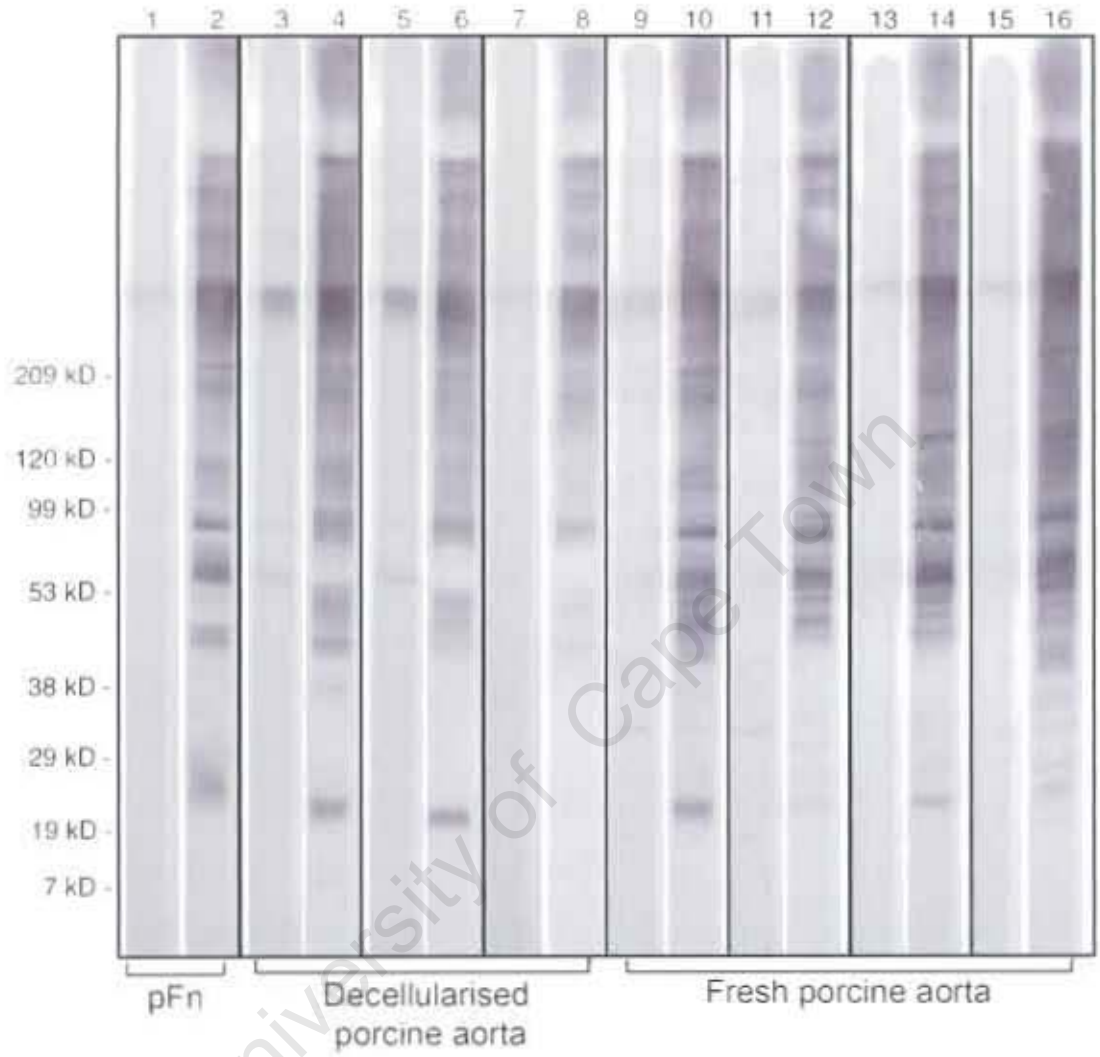

Figure C-29 Antigen: fresh porcine aorta extract. Lanes alternate: pre-immune serum and serum after immunisation. Lane 1 and 2: sera of one rabbit immunised against fibronectin; Lanes 3 to 8: sera of the three rabbits immunised against decellularised porcine aortic tissue; Lanes 9 to 16: sera of the four rabbits immunised against fresh porcine aortic wall tissue

Fibronectin Western blot

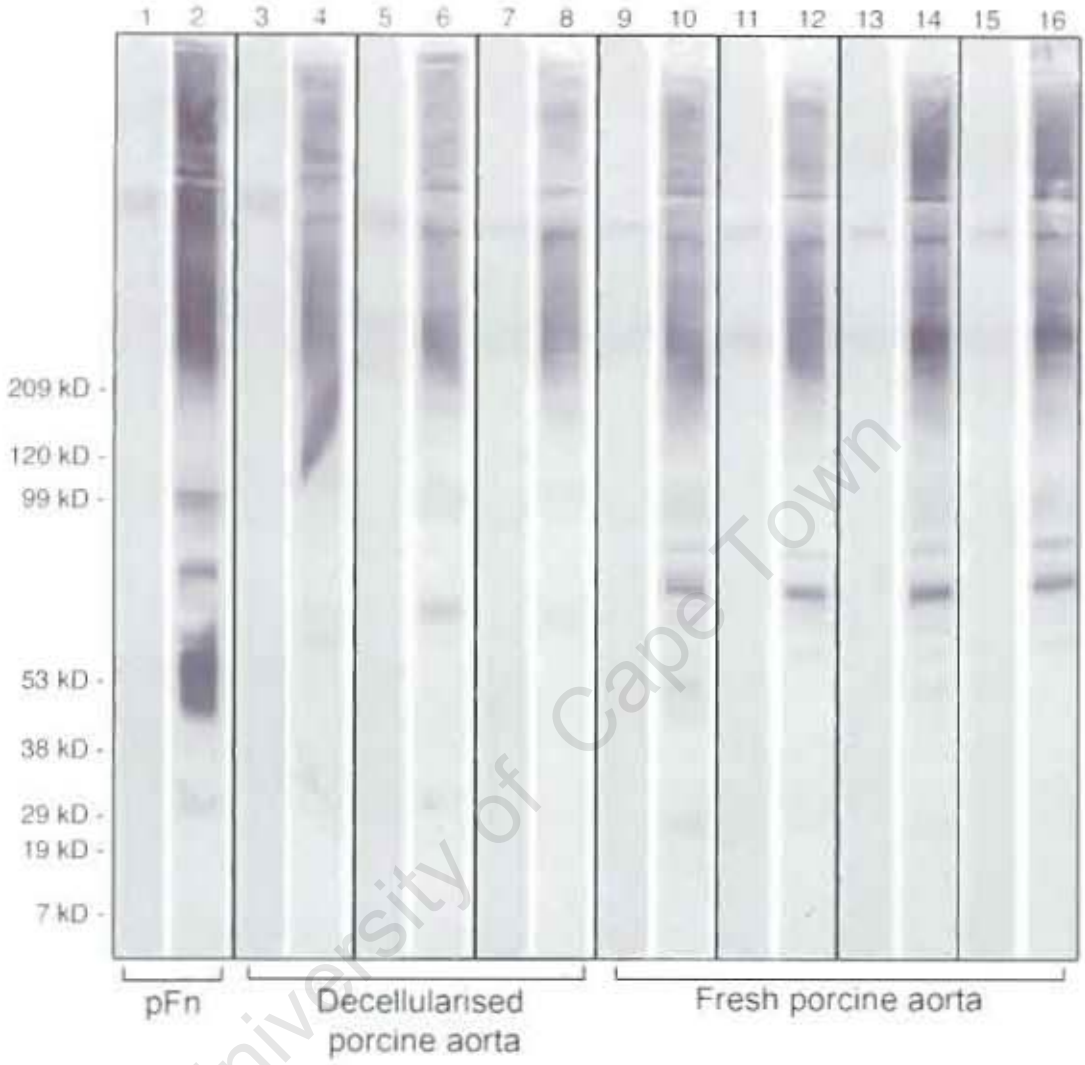

Figure C-30 Antigen: porcine fibronectin. Lanes alternate: pre-immune serum and serum after immunisation. Lane 1 and 2: sera of one rabbit immunised against fibronectin; Lanes 3 to 8: sera of the three rabbits immunised against decellularised porcine aortic tissue; Lanes 9 to 16: sera of the four rabbits immunised against fresh porcine aortic wall tissue.

C1.3.A(4) Summary

This study confirms the development of an immune response to porcine aortic valve tissue. There is also clear evidence that removal of the cells did not render the tissue non-immunogenic and that the extracellular matrix components continued to elicit a response in the animals immunised with decellularised porcine aortic valve tissue. The specific antigen, porcine plasma fibronectin, elicited a response and was specific for many antigens extracted from porcine aortic valve tissue as well as for the plasma porcine fibronectin and fragments thereof. Thus, the immunogenicity of porcine aortic valve tissue is not limited only to the cells but that the extracellular matrix components also play a role. The strategy to remove the cells from porcine aortic valves in order to render them non-immunogenic is not sufficient and will have to be combined with an additional strategy to mask the residual immunogenicity of the extracellular matrix. Fibronectin, a glycoprotein, is a major constituent of the basement membrane and therefore represents the first level contact with the host immune system. It was shown that fibronectin is a significant contributor to the immune response. A further study to identify the antigens present in the extracellular matrix of the porcine aorta will help to understand the immune response better and to find strategies to mask specific antigens.

C1.3.B Determine binding of immune sera to commercial bioprosthetic porcine tissue (0.2% glutaraldehyde)

C1.3.B(1) Introduction

It was important to demonstrate that the acquired immune response seen in the rabbits immunised with the different porcine tissue preparations was also specific for intact porcine bioprostheses. Treatment of porcine valves with 0.2% glutaraldehyde was used to replicate contemporary commercial bioprosthetic valves.

C1.3.B(2) Materials and methods

C1.3.B.2(i) Tissue preparation and fixation

Fresh porcine aortas were collected from the abattoir (see Appendix A3). The valves were fixed in 0.2% glutaraldehyde (see Appendix A11) and processed in 4% paraformaldehyde for immunohistology (see Appendix A18).

Fresh porcine aortic valve was fixed in 10% formalin (see Appendix A11) and processed for immunohistology (see Appendix A18). The ELMAS stain is a histochemical stain for collagen, elastin and muscle. This stain (see Appendix A20) was performed with fresh porcine aortic valve to identify the distribution of collagen and elastin.

C1.3.B.2(ii) Immunohistochemistry

The immune sera from the immunised groups were used to stain for IgG (see Figure C-31 on 0.2% glutaraldehyde fixed porcine aortic valves (see Appendix A19). The sera collected from animals before immunisation (control sera) were used to determine the baseline response of the animal before immunisation and to detect if any preformed antibodies against porcine aortic wall were present. Serum was applied to the sections at 1:100 dilutions in TTBS as the primary antibody. The secondary antibody goat anti-rabbit immunoglobulin conjugated to horseradish peroxidase (Bio-Rad, cat no 170-6515), was diluted 1:200 and applied to detect the rabbit IgG from the immune serum bound to the 0.2% glutaraldehyde fixed porcine aortic valve.

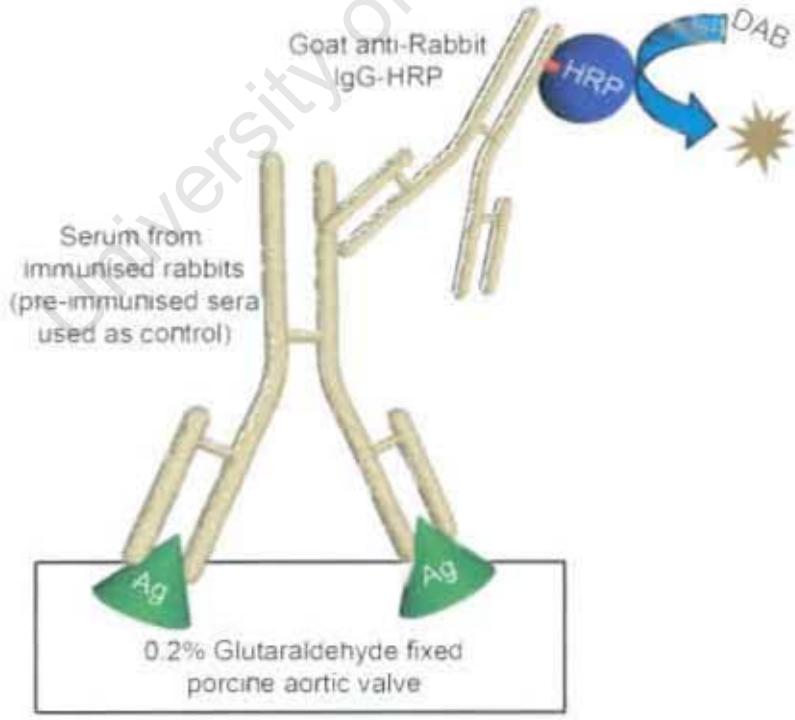

Figure C-31 The concept of immunohistology staining for IgG.

C1.3.B(3) Results

C1.3.B.3(i) Porcine aorta valve (ELMAS)

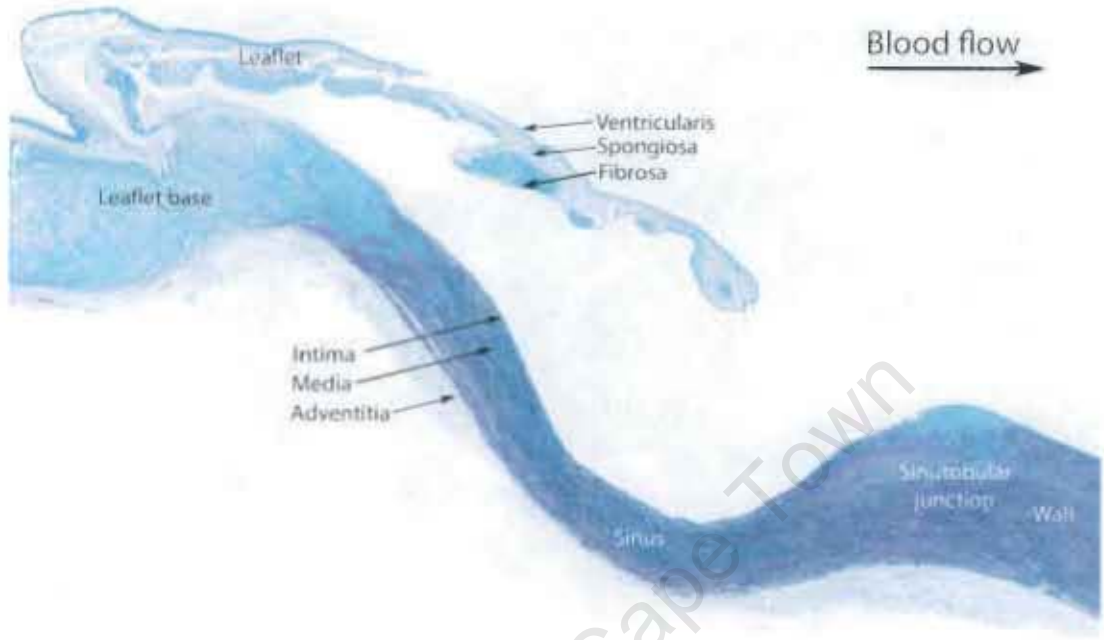

Figure C-32 Porcine aorta valve (leaflet, sinus and aortic wall) stained with ELMAS. The collagen stained blue and the elastin black.

The ELMAS stain (see Figure C-32) demonstrated that collagen was the major component of the leaflet's extracellular matrix whereas the elastin was the major extracellular matrix component of post-sinutubular junction aortic wall. The intimal surface of the aortic wall stained mostly blue for collagen and on the adventitial surface there was a loose arrangement of collagen. The media mostly showed staining of the elastin fibres throughout with collagen in between the fibres.

The leaflet stained predominantly for collagen. The fibrosa was composed of densely packed collagen with some elastin surrounding the collagen. The spongiosa showed mostly loosely arranged collagen without elastin staining. The ventricularis was also seen to be composed of dense collagen with elastin fibres but with a looser arrangement than that of the fibrosa. The correlation of the IgG stain with the distribution of elastin and collagen may indicate the contribution of these two major constituents of the extracellular matrix to the immunogenicity of the tissue.

C1.3.B.3(ii) Immunohistology (IgG stains)

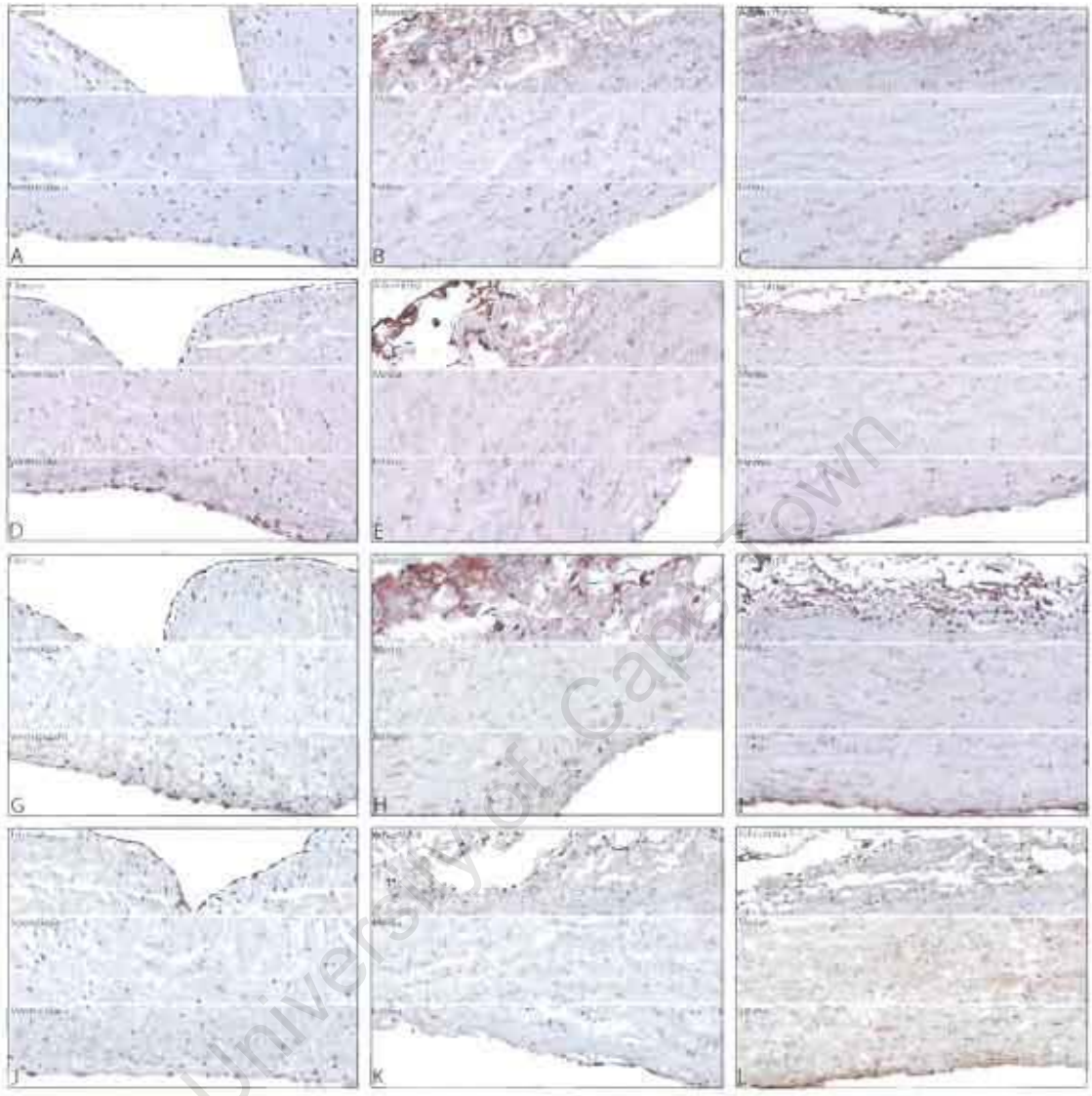

Figure C-33 0.2% Glutaraldehyde fixed porcine aorta stained for IgG using the different anti-sera. A, D, G, J: leaflet; B, E, H, K: sinus; C, F, I, L: wall; A-C: control sera, D-F: anti-fresh porcine aortic wall sera; G-I: anti-decellularised porcine aortic wall serum; J-L: anti-porcine plasma fibronectin sera (original magnification 10x). The lack of staining in tissue exposed to swine instead of rabbit sera (not shown) confirmed that staining was not an artefact due to the presence of native pig immunoglobulin.

A wide range of dilutions (1:50 to 1:20 000) of the labelled IgG was used to determine the optimum concentration for IgG staining to be sure no background staining was seen. All the sections were incubated with the same serum dilution

(1:100) and stained with the same concentration of labelled IgG (1:2000) to be able to compare the levels of IgG. All the sections stained for the different sera groups were done on the same day and the same run to have as little variability between the groups as possible. The sections were stained with only the labelled IgG as a negative control. All the negative control sections were negative.

In contrast, there was positive staining for all the serum groups used (see Figure C-33). The sera collected from the animals before immunisation had positive staining for IgG which made it difficult to compare the different post-immunisation sera with each other. The control sera resulted in background staining of the porcine aortic valve, suggesting that the animals had preformed antibodies capable of recognising epitopes present in the porcine aortic valve protein extract even before immunisation. This was not observed in the Western blotting experiments. The staining pattern for all the sera were very similar with only some intensity differences. The sera of the rabbits immunised against fresh porcine aortic wall tissue showed the most intense staining of the leaflet and the sinus area. The sera of the rabbit immunised against porcine fibronectin showed the most intense staining of the wall.

Control rabbit sera

Leaflet

There was IgG staining on the edges of the tissue on both the fibrosa and ventricularis side of the leaflet. There was some staining associated with the cells on the edge of the ventricularis side. There was no IgG positive staining in the spongiosa.

Sinus

Most of the staining was associated with the loose collagen on the adventitial side of the sinus area. There was not staining associated with the cells of the tissue. Throughout the media was a light stain that may be staining the extracellular matrix, but it was not as intense as the staining of the loose collagen on the edge of the adventitial side. The intima had the light staining similar to that of the media.

Wall

The staining of the loose collagen was very intense on the adventitial side (see Figure C-33). The staining was not associated with cells, but mostly the extracellular

Sera from rabbits immunised with fresh porcine aortic wall tissue

Leaflet

The fibrosa and ventricularis stained positive for IgG. The cells on the edge of the ventricularis stained positive and close to the edge the extracellular matrix stained positive. The spongiosa had a light positive stain of the extracellular matrix, but no staining was associated with the cells in the spongiosa.

Sinus

The staining was mostly associated with the loose collagen on the edge of the adventitial side and the extracellular matrix of the media but not with any cells. The cells on the edge of the intima stained positive for IgG.

Wall

There was staining on both the adventitial and the intimal side of the wall. The media stained lightly positive. The staining was mostly associated with the extracellular matrix and not with the cells.

Sera from rabbits immunised with decellularised porcine aortic wall tissue

Leaflet

There was no staining in the spongiosa, but the fibrosa and ventricularis both had positive staining. The ventricularis had most of the staining and it was associated with the cells.

Sinus

Only the loose collagen on the adventitial side showed intense staining. The media and intima were only lightly stained and which was associated with extracellular matrix.

Wall

Both the adventitial and intima had intense positive staining. The media had only light staining.

Sera from rabbits immunised with fibronectin isolated from pig plasma

Leaflet

The fibrosa and ventricularis had positive staining. The staining was associated with the cells on the ventricularis side of the leaflet. The spongiosa had light staining associated with the extracellular matrix becoming more intense towards the fibrosa and ventricularis sides.

Sinus

There was some staining of the loose collagen on the adventitial side. Some cells stained positive on the intimal side. The media was only lightly stained.

Wall

The adventitia, media and intima showed intense staining of the extracellular matrix. The intensity of the staining was the most dramatic for all the wall samples stained with post-immunisation sera.

C1.3.B(4) Summary

Pre-immunisation sera staining positive suggest that the rabbit had preformed antibodies against porcine aortic wall tissue. Thus, the extraction of proteins from the porcine aorta wall clearly did not extract all potential antigens as the Western blot did not stain positive with the pre-immunisation sera. In contrast, using immunohisotolgy sections of the porcine aorta made it difficult to distinguish between preformed antibodies and the antibodies acquired by immunisation. The pre-immunisation sera stained specifically the porcine aortic wall with less staining associated with the leaflet.

No clear pattern was seen associating IgG with specific distribution of the two major constituents, collagen and elastin, of the extracellular matrix. There was a similar pattern for all the post-immunisation sera with the blood surface and especially the adventitia of the porcine aortic wall presenting potential antigens to target. In all groups the most staining was associated with the loose collagen on the adventitial surface of the aortic wall.

The only observation was that the intensity of the stain was different for the post-immunisation sera groups. The most intense staining of the leaflet and sinus area was with the post-immunisation sera from animals immunised with fresh porcine

aortic wall tissue and the most intense staining of the aortic wall was with the post-immunisation sera from the animal immunised with porcine plasma fibronectin.

Animals immunised with the fresh porcine aortic wall tissue should be exposed to most of the possible different immunogens in porcine aortic tissue. Thus, one would expect the post-immunisation sera from this group to stain most of the porcine aortic wall. Porcine fibronectin (a major constituent of the basement membrane may be a major constituent of the extracellular matrix of the porcine aortic wall and thus the intense staining of the aortic wall with the post-immunisation sera of the animal immunised with porcine plasma fibronectin. Therefore it is clear that even with the background staining of preformed antibodies the animals immunised with the porcine tissue did acquire antibodies against porcine aortic tissue.

C1.3.C Specific antigen binding to porcine aortic tissue

C1.3.C(1) Introduction

Fibronectin is an immunogen that elicits a significant immune response in bioprosthetic porcine aortic tissue. To further investigate fibronectin, the IgG from the rabbit immunised against fibronectin was affinity purified and investigated with transmission electron microscopy (TEM). The objective was to use immunogold labelling to see where the antibody specifically binds in the glutaraldehyde-fixed porcine aortic wall tissue.

C1.3.C(2) Materials and methods

C1.3.C.2(i) Affinity purification of anti-fibronectin IgG from serum of rabbits immunised against porcine fibronectin

Sera from rabbits immunised against porcine plasma fibronectin was shown by western blot to contain moderate titres of specific antibody for fibronectin. Porcine fibronectin was used for affinity purification of these antibodies. Porcine fibronectin was covalently coupled to a solid medium which was agarose with activated cyanogen bromide (Sigma, cat no. C9210). Agarose provide an uncharged hydrophilic matrix and cyanogen bromide in basic solution (sodium hydroxide) reacts with –OH groups on agarose to form cyanate esters. These groups react readily with primary amines under very mild conditions resulting in a covalent coupling of a ligand (fibronectin) to the agarose matrix. The porcine fibronectin affinity column was prepared (see appendix A11c). The rabbit anti-porcine plasma fibronectin antisera were pooled and applied to the porcine fibronectin affinity column binding to the

porcine fibronectin coupled to the solid medium. This allowed antibodies specifically to porcine plasma fibronectin to bind to the column and all rabbit serum proteins, including immunglobulins to flow though the column. A low pH buffer (citrate buffer, pH 3.0) was used to elute the anti-porcine fibronectin antibody from the column and the eluted fractions were immediately adjusted to pH 7.4 to avoid degrading of the antibody at the otherwise low pH.

C1.3.C.2(ii) Transmission electron microscopy: Binding of specific antibodies to porcine aortic wall tissue

The pooled rabbit anti-porcine plasma fibronectin antiserum, rabbit anti-human fibronectin immunoglobulin (Sigma, cat no F3648) and affinity purified rabbit anti-porcine plasma fibronectin were used to study binding of specific antibodies to porcine glutaraldehyde-fixed tissue using immuno-gold labelling. The porcine tissue was fixed for TEM (see Appendix A22a) and prepared for immuno-gold labelling (see Appendix A22b). The anti-sera (1:100), the anti-human fibronectin (1:50) and the affinity purified anti-porcine fibronectin antibody (1:10) were applied to the tissue. For detection immuno-gold labelled goat anti-rabbit immunoglobulin was applied (see Appendix A22c). The grids were viewed with TEM.

C1.3.C(3) Results

C1.3.C.3(i) Gold labelling (TEM)

The anti-human fibronectin rabbit antibodies were associated with the elastin and the collagen. There was not obvious binding of the antibody to the nuclei of the cells.

The serum of rabbits immunised with porcine plasma fibronectin was associated with most of the porcine aortic wall constituents such as cells, collagen and elastin.

The affinity purified rabbit anti-porcine plasma fibronectin was mostly associated with the extracellular matrix constitutents namely collagen and elastin. There was little staining of the nuclei or cells of the tissue.

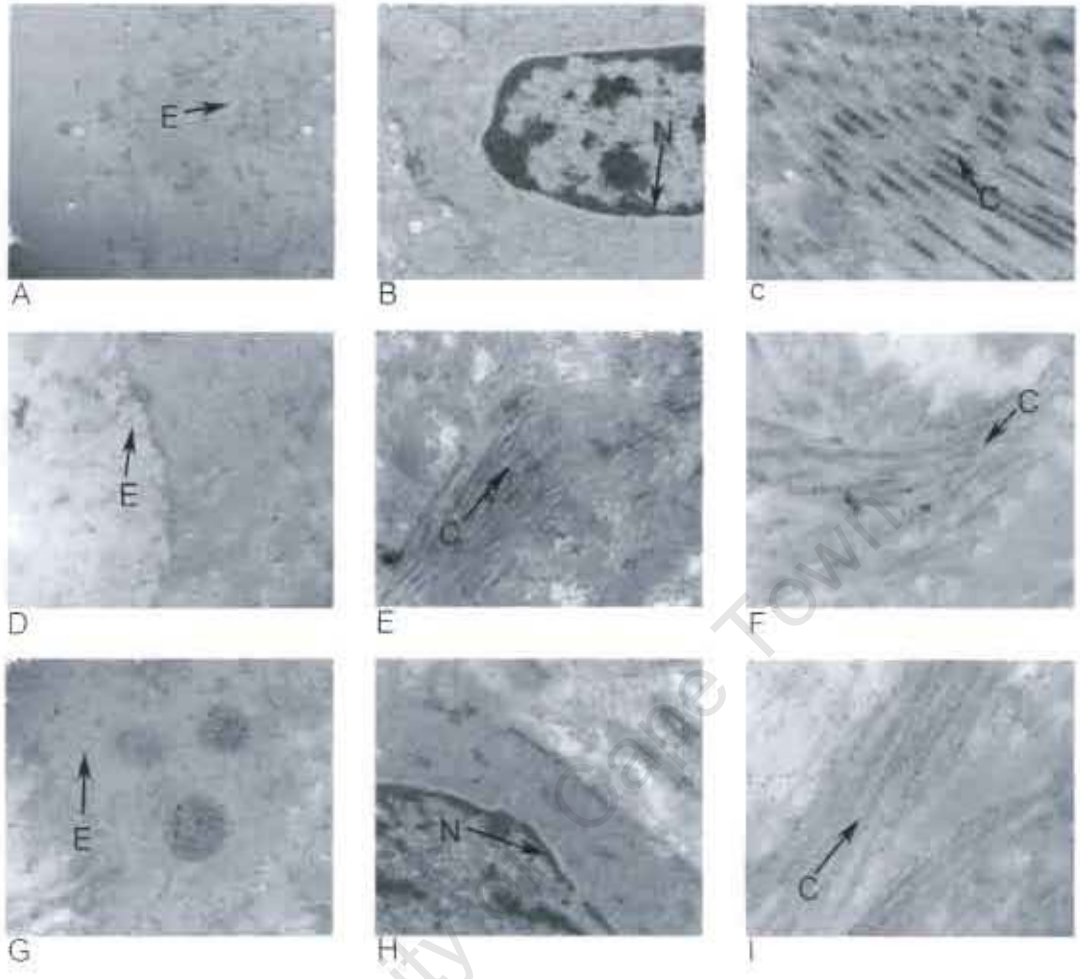

Figure C-34 TEM of the gold labelling of the different anti-fibronectin antibodies with glutaraldehyde-fixed porcine aortic wall tissue. A-C: rabbit anti-human fibronectin, D-F: rabbit anti-porcine fibronectin, G-I: affinity purified rabbit anti-porcine plasma fibronectin. A negative control which excluded application of a rabbit primary anti-sera did not demonstrate any gold labelling. (E – elastin, N – Nuclei, C – collagen)

C1.3.C(4) Summary

It is clear that the rabbits immunised with porcine plasma fibronectin produced antibodies that recognise porcine aortic wall tissue. It was not clear how specific the antibodies to fibronectin were because the pattern staining between the serum and the affinity purified antibody was similar. The only difference was that there was less staining of the nuclei using the affinity purified antibody. The staining seen for collagen may be due to fibronectin associated with collagen, since the labelling did not have a highly repetitive distribution that one may have expected if the sera were specific for collagen itself.

The gold labelling technique confirmed that porcine aortic wall tissue was immunogenic and the need to identify the specific antigens for masking would help with possible strategies to protect bioprosthetic tissue against immune response of the host.

C1.4. Mitigation of IgG binding by chemical modification of porcine aorta valves

C1.4.A Introduction

The masking of porcine aortic valve tissue fixed with 0.2% and 3% glutaraldehyde was investigated. The serum from rabbits immunised with fresh porcine tissue were used to compare the masking of the fresh porcine aortic valve tissue, porcine aortic wall tissue fixed with either 0.2% or 3% glutaraldehyde.

C1.4.B Materials and methods

C1.4.B(1) Chemical modification of porcine aortic valves

Fresh porcine aortas were collected from the abattoir (see Appendix A3). The valves were fixed in 10% formalin (fresh tissue), 0.2% glutaraldehyde, 3% glutaraldehyde (see Appendix A11) and processed in 4% paraformaldehyde for immunohistology (see Appendix A18).

C1.4.B(2) Binding of sera from rabbits immunised with fresh porcine aortic

The immune sera were used to stain the fresh porcine aortic valve, 0.2% glutaraldehyde and 3% glutaraldehyde fixed porcine aortic valves to compare the ability of the different fixation concentrations of glutaraldehyde to mask the antigens (see Appendix A19). Control sera were obtained from the animals before immunisation. The serum was applied to the sections at 1:100 dilutions in TTBS as the primary antibody. The secondary antibody goat anti-rabbit immunoglobulin conjugated to horseradish peroxidase (Bio-Rad, cat no 170-6515) was diluted 1:200 and applied to detect the rabbit IgG from the immune serum bound to the fresh, 0.2% and 3% glutaraldehyde fixed porcine aortic valve respectively.

C1.4.C Results

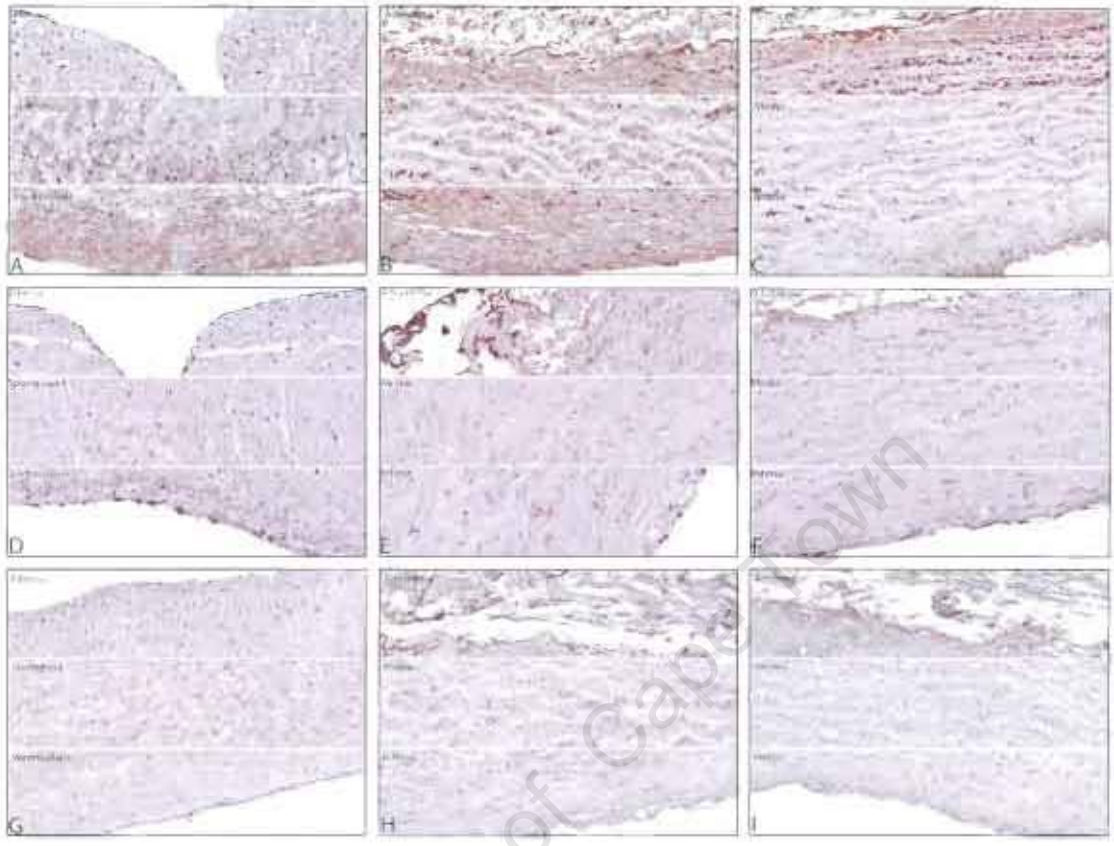

Figure C-35 The anti-sera from rabbits immunised with porcine aortic wall tissue was used to stain for IgG on porcine aortic valves not fixed, fixed with 0.2% and 3% glutaraldehyde respectively. A-C: porcine aortic valve not fixed; D-F: porcine aortic valve fixed with 0.2% glutaraldehyde; G-I: porcine aortic valve fixed with 3% glutaraldehyde. A, D, G: leaflet; B, E, H: sinus; C, F, I: wall. (Original magnification 10x)

C1.4.C(1) Fresh porcine aortic valve

Anti-whole porcine aorta IgG staining of the fibrosa and the spongiosa layers of the leaflet were mostly associated with the cells. The ventricularis stained intensely positive for IgG and the staining was associated with the cells and the extracellular matrix.

There was intense positive staining for IgG in all the layers of the sinus area. The staining was associated with the cells and the extracellular matrix.

The aortic wall adventitial side stained intensely positive for IgG. The media close to the adventitia also stained more than the rest of the media. The staining in the

media was mostly associated with the extracellular matrix. The intimal side had less staining.

C1.4.C(2) 0.2% glutaraldehyde fixed porcine aorta valve

The leaflet only had some staining on the ventricularis side of the cells lining the edge of the ventricularis and the area next to the ventricularis the extracellular matrix stained. The spongiosa had a light positive stain of the extracellular matrix, but no staining was associated with the cells in the spongiosa.

In the sinus area the staining was mostly associated with the loose collagen on the edge of the adventitial side and the extracellular matrix of the media but not with any cells. The cells on the edge of the intima stained positive for IgG.

There was staining on both the adventitial and the intimal side of the wall. The media stained light positive. The staining was mostly associated with the extracellular matrix and not with any cells.

C1.4.C(3) 3% glutaraldehyde fixed porcine aorta valve

The leaflet stained only lightly positive. A few cells on the fibrosa stained positive for IgG. The spongiosa and ventricularis had no staining associated with cells.

The loose collagen on the adventitial side in the sinus area stained positive for IgG. The extracellular matrix of the media stained lightly positive, but there was no positive staining on the intimal side of the sinus area.

The loose collagen on the adventitial side of the wall stained postive for IgG, but there was no staining of the media and only very light staining on the edge of the intimal side of the wall.

C1.4.D Summary

Work done by Zilla et al[141, 144] showed the influence of higher glutaraldehyde fixation on the calcification of bioprosthetic tissue and that increasing the glutaraldehyde concentration from 0.2% to 3% reduced calcification 34% in the sheep model. Fixation of porcine aortic wall with 3% glutaraldehyde resulted in less IgG staining, but the masking of the tissue was not complete. The 3% glutaraldehyde treatment is in any case not practical because it makes the tissue too tough to use. It is clear that additional masking is needed when 0.2% glutaraldehyde is used to mitigate the inflammatory response to bioprosthetic heart valves.

C2. Epitope masking by IgG fragments

C2.1. Confirmation of tissue specificity of sera collected from rabbits implanted with commercial bioprosthetic tissue

C2.1.A Introduction

Heart valves are fixed with glutaraldehyde to mask antigens and protect the valves from the inflammatory response of the recipient. The hypothesis that commercially used fixative for heart valves mask all the antigens of the porcine aortic tissue was investigated. Belgian hares and New Zealand White rabbits were implanted with porcine aortic wall coupons treated with different treatments used commercially for six weeks. We investigated the humoral inflammatory response specifically if any antibodies were formed during the implant period specific to porcine aortic tissue.

C2.1.B Materials and methods

C2.1.B(1) Collecting of rabbit serum

Rabbits were implanted with coupons treated with commercial fixatives and after 42 days killed under general anaesthesia. The serum was collected (see Appendix A1) and stored at -80°C until further fractionation.

C2.1.B(2) Western blot detection of tissue specific antibodies

Porcine aortas wall were collected from the abattoir (see Appendix A3). A protein extract were prepared from homogenised porcine aortic wall tissue (see Appendix A5) by overnight extraction in a denaturing buffer at 4°C (see Appendix A7). The protein concentration of the extract supernatant was determined using a detergent compatible protein detection kit ((DC Protein Assay, Bio-Rad) (see Appendix A8)). The extract was electrophoretically separated according to size using preparative SDS polyacrylamide gradient gels (4-20%) (see Appendix A9). The separated proteins were transferred onto a PVDF membrane and the membrane was blocked overnight in 5% milk powder TTBS buffer at 4°C to prevent non-specific binding of the detection antibody to the PVDF membrane.

A Western blot (see Appendix A10) was performed with serum from rabbits implanted with commercially fixed porcine bioprosthetic tissue as the primary antibody diluted 1:100. IgG antibody binding to the porcine aorta wall extract was detected with secondary antibody goat anti-rabbit immunoglobulin horseradish peroxidase conjugate (Bio-Rad, cat no 170-6515) diluted 1:3000.

C2.1.C Results

C2.1.C(1) Western blot detection of tissue specific antibodies

The Western blot with sera from Belgain Hare and New Zealand White rabbit implanted with porcine bioprosthetic tissue using proteins extracted from porcine aortic wall showed similar specificity to the tissue.

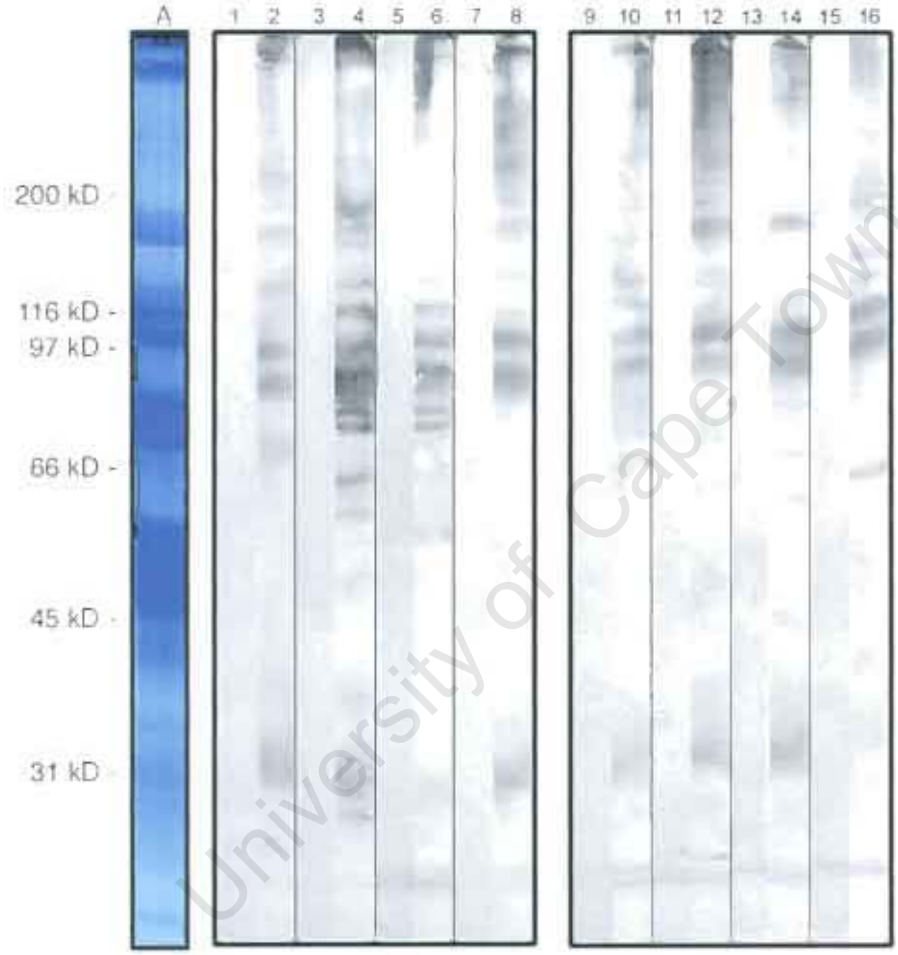

Figure C-36 Lane A is the protein separation of porcine aorta wall tissue extract on 4-20% SDS PAGE gradient gel under non-reducing conditions stained with Coomassie Brilliant Blue R-250 (Bio-Rad, UK). Western blot of porcine aortic wall tissue specific antibodies in the serum of animals implanted with commercially fixed porcine aorta wall after 42 days. Blood samples were taken from New Zealand White rabbits (lanes 1- 8) and Belgian Hares (lanes 9 – 16) before implant (lane 1, 3, 5, 7, 9, 11, 12 and 15) and after 42 days (lane 2, 4, 6, 8, 10, 12, 14 and 16).

C2.1.D Summary

Specific antibodies form in rabbits implanted with fixed bioprosthetic tissue used for heart valve replacement. There were no differences between the New Zealand White rabbits and Belgian hares. This made it possible to use sera from both species for further studies.

C2.2. Isolation of IgG isotype from rabbit serum

C2.2.A Introduction

Immunoglobulin is the most abundant in circulation and serum is the usual starting material for its isolation. The serum collected from the six New Zealand White rabbits, implanted with porcine aortic wall coupons treated with different treatments used commercially, was pooled for IgG isolation. Three different purification methods were compared to find a method that is easy to perform routinely, give a reasonable yield and does not inactivate or denature the IgG.

C2.2.B Materials and methods

C2.2.B(1) Different methods of isolating IgG from rabbit sera

C2.2.B.1(i) Protein A affinity chromatography

Affinity chromatography is a method of separating biochemical mixtures, such as a cell lysate, growth medium or blood serum, based on a highly specific biologic interaction such as that between antigen and antibody, enzyme and substrate, or receptor and ligand. The specific interaction between an insoluble ligand and soluble molecule renders the soluble molecule insoluble and allows it to be separated from soluble contaminants. The bonds between the ligand and the molecule can then be disrupted to yield soluble pure molecule. The basis for the purification is the specificity and reversibility of the binding of soluble molecule to insoluble ligand. Binding to the solid phase may be achieved by column chromatography, whereby the solid medium is packed onto a chromatography column, the initial mixture run through the column to allow binding, a wash buffer run through the column to wash the contaminants away and the elution buffer subsequently applied to the column to collect the pure molecule.

Protein A-Sepharose can be used to affinity purify antibodies from blood serum (see Appendix A11a). Protein A binds to the Fc portion of the immunoglobulin. Protein A is used as ligand to purify IgG from serum. The serum is allowed to bind to the

Protein A affinity matrix and washed from the solid medium. Antibodies bind stably under physiological conditions of salt concentration, temperature, and pH, but the binding is reversible as the bonds are non-covalent. The bound IgG is eluted by disrupting the non-covalent bonds with 0.1 M glycine HCl (pH 3.00). The disadvantage is that the IgG is exposed to denaturing conditions. After extremes of pH have been applied, the solution must be neutralised as quickly as possible and then dialysed into a neutral isotonic buffer so as not to permanently denature these antibodies.

C2.2.B.1(ii) Polyethylene glycol (PEG) precipitation

High molecular weight proteins have been purified by precipitation using the nonionic hydrophilic polymer polyethylene glycol (PEG) 6000. IgG was precipitated with PEG 6000 and isolated by high-speed centrifugation (see Appendix A13). Fractionation of plasma proteins with 15% PEG 6000 gave a precipitate containing mainly IgG and a supernatant containing mainly albumin.

The exact mechanism of PEG precipitation is poorly understood. It may linked to polymers ability to form coiled particles in solution and that protein molecules such as IgG may diffuse into the inter-polymer spaces between PEG molecules and precipitation may occur when they exceed their solubility.

C2.2.B.1(iii) Sodium sulphate

Sodium sulphate was used as a salt to precipitate to sediment the antibodies from serum (see Appendix A14). The antibodies were removed by centrifugation and dissolved in PBS.

C2.2.C Results

C2.2.C(1) Isolation of rabbit IgG

C2.2.C.1(i) Protein A sepharose affinity chromatography

The IgG eluted from the column was run on a SDS PAGE gel to determine if the product was pure and intact. The low pH for elution fragmented the IgG and a low yield of good quality IgG was obtained by this method (see Figure C-38).

Figure C-37 The graph of affinity chromatographic separation of rabbit IgG from rabbit serum using protein A sepharose affinity chromatography. The second peak was rabbit IgG eluted with elution buffer.

Figure C-38 The SDS PAGE of IgG isolated using protein A sepharose affinity chromatography. Lane 1 shows the serum used for isolating the IgG and lane 2 shows the IgG eluted from the column.

C2.2.C.1(ii) PEG 6000 and Sodium sulphate

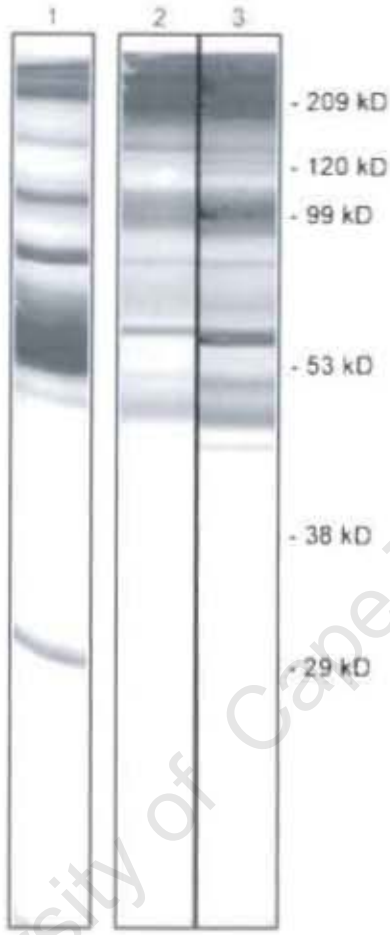

Figure C-39 The IgG isolated by using PEG 6000 (lane 2) and sodium sulphate (lane 3). Lane 1 shows the rabbit serum from which the IgG was isolated.

PEG 6000 and sodium sulphate were both easy, fast methods of isolating IgG. The PEG 6000 had a higher yield with less fragments.

C2.2.D Summary

After comparing the three methods of isolation, it was decided to use PEG 6000 method for isolating IgG. It was a quick and easy method to use giving a good product for further use.

C2.3. Digestion of rabbit IgG with proteolytic enzymes

C2.3.A Introduction

Three proteolytic enzymes were compared for preparing Fab or $F(ab')_2$ fragment from rabbit IgG by protease digestion. The following three enzymes were used to give different antibody fragments. Papain cleaves IgG at the amino-terminal side of the disulfide bonds and release the two arms as separate Fab fragments and the Fc fragment. Pepsin cleaves in the same general region but on the carboxy-terminal side of the disulfide bonds giving the $F(ab')_2$ fragment where the two binding arms remain linked and the remaining part is cut into several small fragments. Ficin has the ability to cleave IgG in either Fab or $F(ab')_2$ fragment in the presence of different L-cysteine concentrations (see Figure C-40).

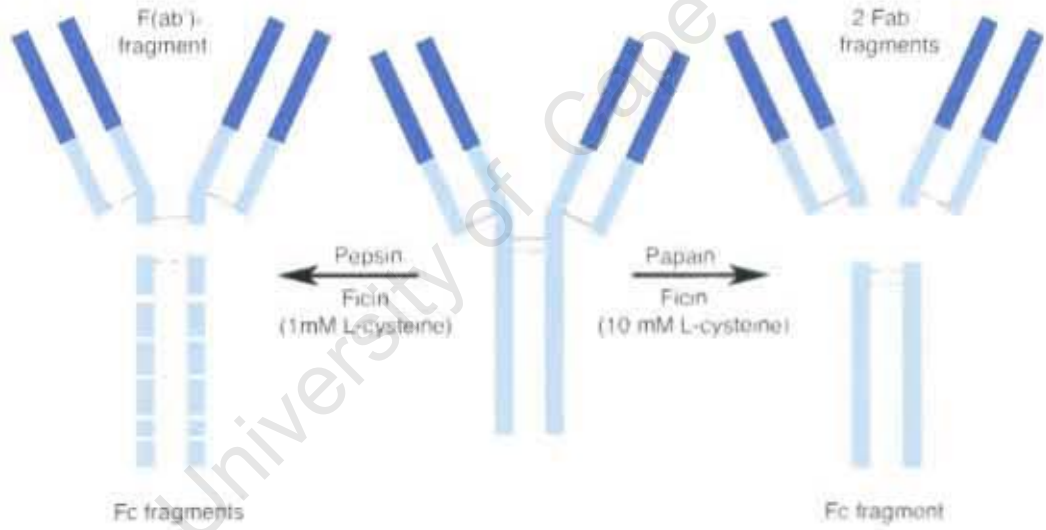

Figure C-40 Proteolytic enzymes can cleave IgG into Fab or $F(ab')_2$ fragments.

C2.3.B Materials and methods

C2.3.B(1) Different proteolytic enzymes

C2.3.B.1(i) Ficin (Fab and $F(ab')_2$ fragments)

Ficin is a thiol protease prepared from fig latex with a molecular weight of 25 kD. It has a broad pH working range and cleave IgG in the presence of the reducing agent L-cysteine at a concentration of 1 mM in $F(ab')_2$ fragments and at a concentration of 10 mM in Fab fragments. The fragments were purified by affinity chromatography (see Appendix A11a).

Ficin was used with both concentration of L-cysteine to prepare Fab and $F(ab')_2$ fragments (see Appendix A15). Samples were taken at different time intervals and run on a SDS PAGE to determine the optimum time for digesting IgG with Ficin.

C2.3.B.1(ii) Pepsin ($F(ab')_2$ fragments)

Pepsin, a member of the Peptidase A1 family, is the predominant digestive protease in the gastric juice of vertebrates with a molecular weight of 34 kD. Pepsin has optimal activity with native proteins at approximately pH 1.0, but with some denatured proteins the optimal activity is at approximately pH 1.5-3.5. Pepsin (see Appendix A16) was used in the preparation of $F(ab')_2$ fragments from antibodies. IgG was digested with pepsin, which cleaves the heavy chains near the hinge region. One or more of the disulfide bonds that join the heavy chains in the hinge region are preserved, so the two Fab regions of the antibody remain joined together, yielding a divalent molecule (containing two antibody binding sites), the $F(ab')_2$ fragment. The light chains remain intact and attached to the heavy chain. The Fc fragment is digested into small peptides. The fragments were purified by affinity chromatography (see Appendix A11a).

C2.3.B.1(iii) Papain (Fab fragments)

Papain is a cysteine protease prepared from latex from the fruit of the papaya tree with a molecular weight of 23 kD. Papain was used to cleave antibodies into two Fab fragments (see Appendix A17), which recognize the antigen specifically with their variable region, and one Fc fragment. It cleaves above the hinge region containing the disulfide bonds that join the heavy chains, but below the site of the disulfide bond between the light chain and heavy chain. This generates two separate monovalent (containing a single antibody binding site) Fab fragments and an intact Fc fragment. The fragments were purified by affinity chromatography (see Appendix A11a).

C2.3.B(2) Affinity chromatographic separation of antibody fragments

The Fab or $F(ab')_2$ fragments were separated from intact undigested IgG and Fc fragments by Protein A affinity chromatrography (see Appendix A11a). The intact IgG and Fc fragment binds to the protein A and the Fab or $F(ab')_2$ fragments are washed through the column, because they lack the Fc fragment that is recognized by protein A. The Fab or $F(ab')_2$ fragments were not exposed to the low pH needed to elute the IgG. 1 ml fractions of the unbound fragments (Fab and $F(ab')_2$ fragments)

were collected. The pooled Fab and $F(ab')_2$ fragments were dialysed against PBS (pH 7.4).

C2.3.C Results

C2.3.C(1) Cleave rabbit IgG with proteolytic enzymes

C2.3.C.1(i) Ficin

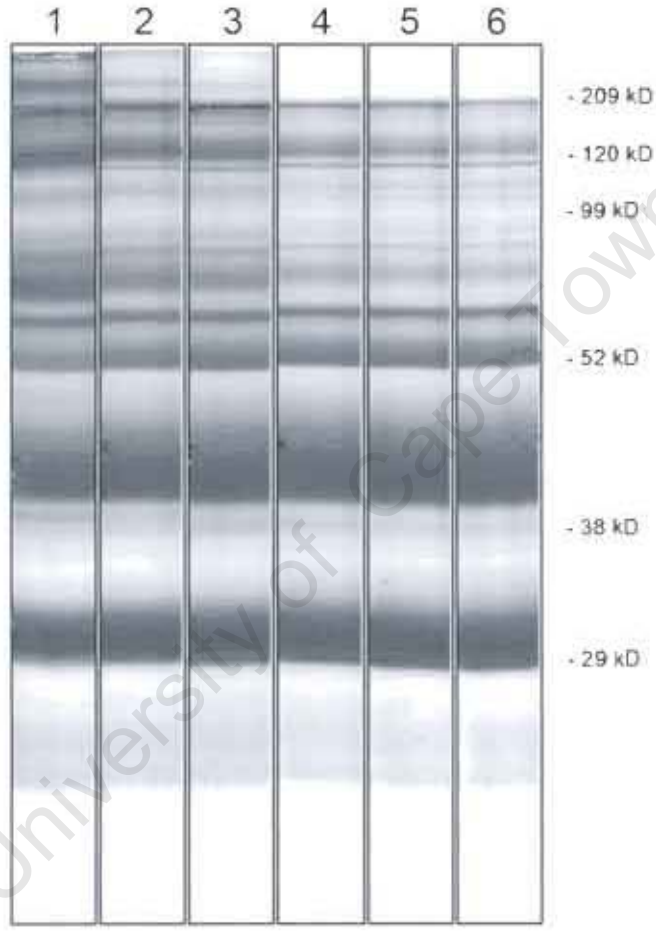

Figure C-41 SDS PAGE of ficin digestion mixture of IgG after hourly intervals with a L-cysteine concentration of 10 mM (lane 1 after 1 hour, lane 2 after 2 hours, lane 3 after 6 hours, lane 4 after 7 hours, lane 5 after 8 hours and lane 6 after 16 hours.

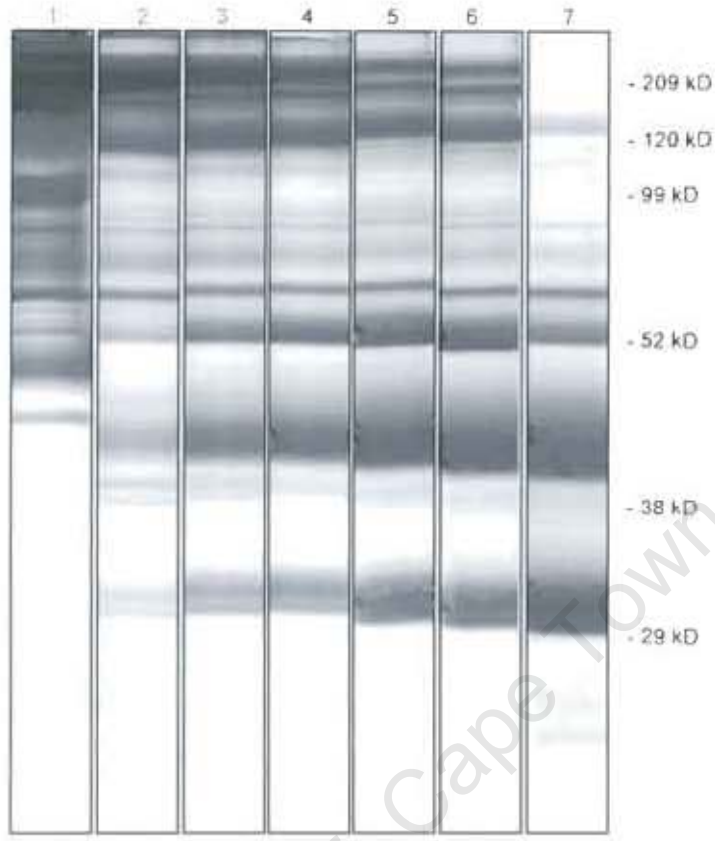

Figure C-42 SDS PAGE of ficin digestion mixture after hourly intervals using a L-cysteine concentration of 1 mM (lane 1 before starting, lane 2 after 1 hour, lane 3 after 2 hours, lane 4 after 6 hours, lane 5 after 7 hours, lane 7 after 8 hours and lane 8 after 16 hours.

Ficin digestion after 3 hours with L-cysteine concentration of 10 mM was the optimum condition with a good yield of Fab and/or $F(ab')_2$ fragments.

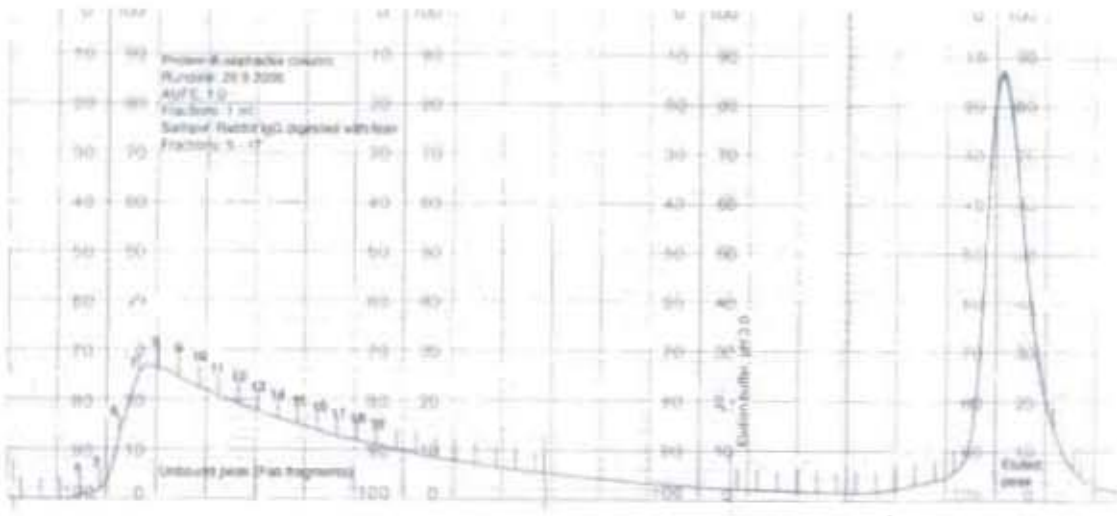

Figure C-43 Affinity chromatographic separation of fragments from rabbit IgG digested with ficin using protein A-sepharose column. The first peak is Fab and/or $F(ab')_2$ fragments.

C2.3.C.1(ii) Pepsin and Papain

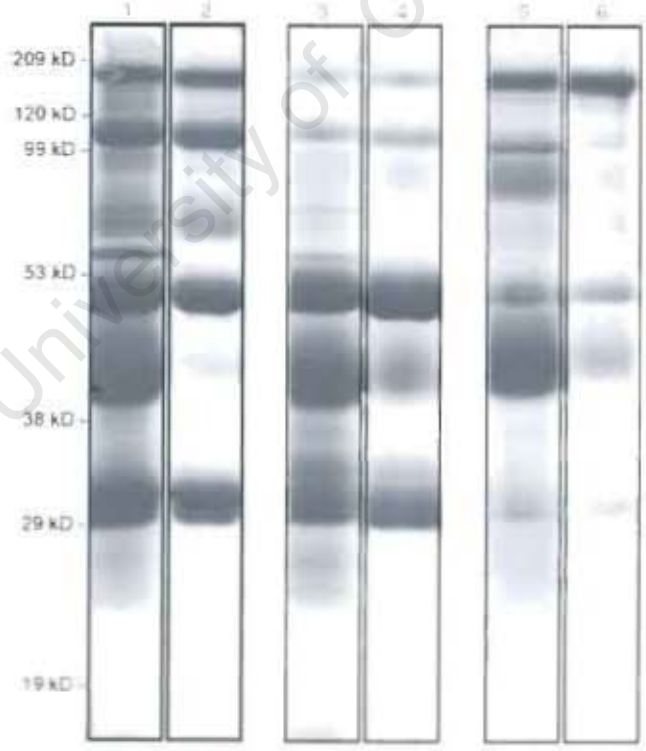

Figure C-44 SDS PAGE of the different proteolytic enzyme digests of rabbit IgG. Each group shows in the first lane the IgG dialysed against the buffer used and the

second lane the digestion mixture. Lane 1 and 2 shows Ficin digestion after 8 hours, lane 3 and 4 digestion with papain and lane 5 and 6 digestion with pepsin (pH 4.5).

C2.3.D Summary

It was decided to use Ficin digestion, because it was reliable and had a good yield of Fab and/or $F(ab')_2$ fragments after only 3 hours. The conditions for digestion were not as harsh as with pepsin (pH 4.5). It was also an attractive option because it was possible to get either Fab or $F(ab')_2$ fragments using the same enzyme and it was possible to evaluate both fragments as potential masking agents.

C2.4. Mask porcine aortic wall with IgG fragments

C2.4.A Introduction

It is essential that the immunoglobulin fragments are sufficient to mask the extent of epitopes exposed in the tissue which are capable of binding host antibody. Immunohistological staining will allow a visual confirmation of the quenching effect of Fab or $F(ab')_2$ fragments application to porcine aortic wall tissue. Comparison of masked versus non-masked slides with subsequent application of intact peroxidase conjugated IgG will provide confidence that the application of Fab or $F(ab')_2$ fragments are effective in masking immunogenic epitopes.

C2.4.B Materials and Methods

C2.4.B(1) Conjugate peroxidase to IgG

IgG isolated from rabbit sera was labelled with horseradish peroxidase (see Appendix A18). Peroxidase produced by horseradish root is a stable, highly active enzyme. Conjugation is achieved using glutaraldehyde to cross-link immunoglobulin to the enzyme.

C2.4.B(2) Binding of IgG fragments to porcine aorta wall

Immunohistological staining will allow a visual confirmation of the quenching effect of Fab or $F(ab')_2$ applicaton to porcine aorta tissue. Although the concentration of Fab or $F(ab')_2$ will be far in excess when applied to a histological slide, comparison of masked versus non-masked slides with subsequent application of labelled intact IgG will provide confidence that the application of Fab or $F(ab')_2$ is effective at masking immunogenic epitopes.

Porcine aorta wall was cut into 12mm coupons and fixed in 0.2% glutaraldehyde (see Appendix A12). The coupons were prepared for immunohistology (see Apendix A19). Fab fragments were used to mask the epitopes as primary. The peroxidase-conjugated IgG was used as the secondary and detection antibody. For the control group, the incubation with Fab fragments was excluded. The peroxidase conjugates were detected by reaction with DAB, which produced a brown insoluble product.

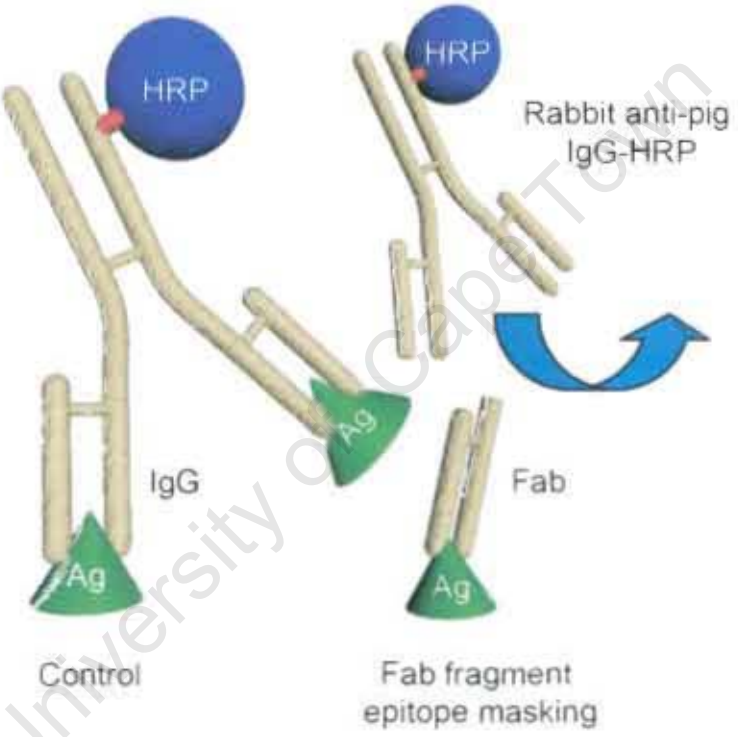

Figure C-45 The masking of epitopes with Fab fragments.

C2.4.C Results

C2.4.C(1) Binding of IgG fragments to porcine aorta wall

Figure C-46 0.2% glutaraldehyde fixed porcine aortic wall sections stained with conjugated rabbit anti porcine IgG-HRP

The IgG isolated and conjugated with HRP was specific for porcine aorta tissue (see Figure C-46).

C2.4.C(2) Ficin

Figure C-47 0.2% glutaraldehyde fixed porcine aortic wall sections were firstly masked with Fab and $F(ab')_2$ fragments prepared with ficin digestion of rabbit IgG. After masking the sections were stained with conjugated rabbit anti porcine IgG-HRP.

The Fab and $F(ab')_2$ fragments prepared with ficin digestion of rabbit IgG prevented staining of the sections with conjugated rabbit anti porcine IgG-HRP (see Figure C-47). Only a few cells stained positive for the IgG.

C2.4.C(3) Pepsin

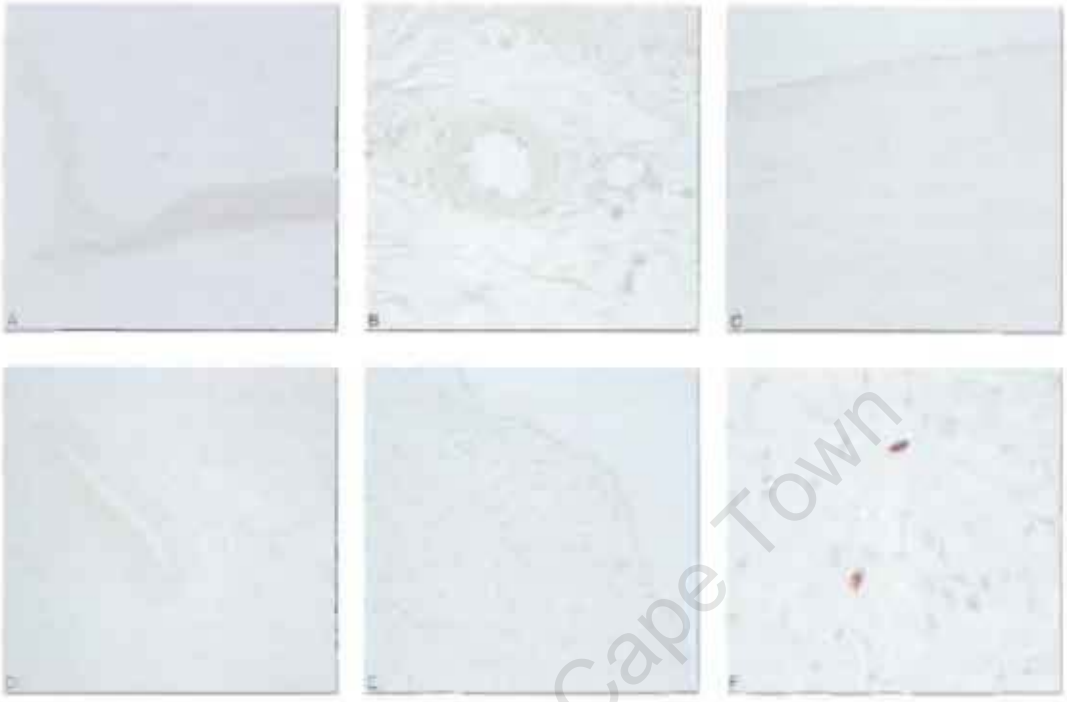

Figure C-48 0.2% glutaraldehyde fixed porcine aortic wall sections were firstly masked with $F(ab')_2$ fragments prepared with pepsin digestion of rabbit IgG. After masking the sections were stained with conjugated rabbit anti porcine IgG-HRP.

The Fab and $F(ab')_2$ fragments prepared with pepsin digestion of rabbit IgG prevented staining of the sections with conjugated rabbit anti porcine IgG-HRP (see Figure C-48). Only a few cells stained positive for the IgG.

C2.4.C(4) Papain

Figure C-49 0.2% glutaraldehyde fixed porcine aortic wall sections were firstly masked with Fab antibody fragments prepared with papain digestion of rabbit IgG. After masking the sections were stained with conjugated rabbit anti porcine IgG-HRP.

The Fab and $F(ab')_2$ fragments prepared with papain digestion of rabbit IgG prevented staining of the sections with conjugated rabbit anti porcine IgG-HRP (see Figure C-49). Only a few cells stained positive for the IgG.

C2.4.D Summary

Sera from animals implanted with porcine aortic tissue showed specificity for porcine aortic tissue. The sera from these animals were taken and the IgG isolated. The IgG Fc fragment was removed by proteolytic digestion to produce Fab and/or $F(ab')_2$ fragments. Intact IgG from the post-implant sera were labelled with horseradish peroxidase to be used to label the antigens present on the immunohistology sections of porcine aortic wall. The option to use commercially available protein G conjugated to horseradish peroxidase was not available because protein G binds to Fc fragment and Fab fragment of the antibody[211]

The concept is that the Fab and/or $F(ab')_2$ fragments would bind to the tissue first and block all the possible sites for the intact labelled IgG to bind. Applying either Fab and/or $F(ab')_2$ fragments to the porcine aortic tissue before applying the same sera from which the fragments were prepared, masked the porcine aortic tissue sufficiently to mitigate binding of the antibodies present in the sera. Therefore applying these fragments to porcine heart valve tissue before implanting it into an animal (or patient) has the potential to mask the antigens from antibodies binding. The removal of the Fc fragment from these fragments may prevent inflammatory cells with Fc receptors from binding to the tissue.

D. *In Vivo* Pilot Study to assess the anti-inflammatory efficacy of porcine bioprosthetic tissue masked with specific immunoglobulin fragments

D1. Introduction

Although the goal of this thesis was to provide *in vitro* proof of principle supporting the concept of immunoglobulin fragment masking of residual immunogen in contemporary bioprosthetic heart valves, a pilot *in vivo* study was nevertheless performed to identify potential, and to some extent, anticipated obstacles which might otherwise limit the successful implementation of this novel technique. In no means does this aspect of the work represent a definitive assessment of the success or otherwise of this technique.

Some anticipated problems relate to the anticipated variation in immunogenicity of the epitopes contained in the tissue and therefore the resulting avidity, masking potential and titre of the immunoglobulin fragments thus produced.

Aspects that have not been addressed here but which would also be important in the translation of this concept to the clinical arena include whether the use of 'xeno-immunoglobulin', that is which is produced in animals, would be appropriate or even desired. The concept of glutaraldehyde tethering of immunoglobulin fragments by fixation subsequent to their application, a process that is anyway necessitated in the production of bioprosthetic heart valves, is a convenient starting point as it ensures that bound immunoglobulin fragments, especially low avidity ones, are not lost from the tissue after implantation but may also hold the key to minimizing a host response to these foreign molecules themselves. Certainly, there are precedents for the use of xeno-antibodies in humans, including the widespread use of polyclonal rabbit anti-

thymocyte globulin (Fresenius) and mouse monoclonal anti-T3 (OKT3, Orthokline) in transplant patients, without an ensuing anaphylactic response.

D2. Materials and Methods

D2.1. Study design

New Zealand White rabbits were immunised with homogenates of porcine aortic wall tissue (4 animals). Immunoglobulin G was isolated from the serum of the immunised animals and used to treat porcine aortic wall tissue as well as decellularized porcine aortic wall tissue. Coupons punched from treated aortas were implanted subdermally into New Zealand White rabbits (6 animals) to compare the inflammatory response of Fab masked versus unmasked control groups.

D2.2. Immunisation

Preparation of tissue for immunisation

Fresh porcine aortas were collected in cold PBS (pH 7.4) at the local abattoir (Maitland, Cape Town) from normal, healthy pigs. They were cleaned and rinsed in PBS (pH 7.4). The porcine aortic wall was cut into smaller pieces and frozen in liquid nitrogen.

Homogenisation of tissue

A stainless steel vial and associated ball bearings, as well as a mortar, pestle and spatula, were first cleaned with 70% ethanol and cooled in liquid nitrogen. The frozen aortic wall samples were placed in the cooled stainless steel vial together with the ball bearings and homogenized for a few seconds. After all the aortic samples were roughly homogenized they were placed in the cooled mortar and frozen with liquid nitrogen and ground with the pestle to form a homogeneous mixture. The resulting powder was frozen in liquid nitrogen, freeze-dried overnight and then stored at -80°C.

Preparing of homogenates for immunisation

Sterile saline (0.5 ml) was added to porcine aorta homogenate (10 mg) and the mixture vortexed to suspend the powder. Freund's incomplete adjuvant was added to the saline mixture in a 1:1 ratio and mixed by passing the solution through two connected syringes to emulsify the immunogen.

Immunisation of the animals

Female New Zealand White rabbits were used for immunisation. Four animals were immunised using porcine aorta homogenate. The emulsions were injected subcutaneously bilaterally (0.5 ml at each site) on the animals back with a total dose of 10mg tissue. After 14 and 21 days the animals were each administered a booster immunisation of the same dose. Test blood was drawn immediately prior to immunisation and immediately prior to booster immunisation to monitor antibody production. Animals were killed under anaesthesia after four weeks. A maximum amount of blood was collected by cardiac puncture into uncoated Vacutainer™ glass tubes.

Isolation of serum from rabbit blood

The blood was allowed to clot at room temperature and centrifuged at 1260 xg for 45 minutes at 4°C. The serum was collected and stored at -80°C.

D2.2.A Western blot detection of tissue specific antibodies

A protein extract was prepared from homogenized porcine aortic wall tissue by overnight extraction in a denaturing buffer (50 mM Tris, 0.1% SDS, pH 7.4) at 4°C. The extract was separated by SDS polyacrylamide gradient (4-20%) gel electrophoresis.

The separated protein bands were transferred onto PVDF membranes using a semi-dry electroblotter (Biorad) after equilibration in Towbin transfer buffer (25 mM Tris, 192 mM glycine, 20% Methanol, 0.1% SDS, pH 8.3). The membrane was blocked overnight in 5% (w/v) milk powder (fat free) in Tween-Tris buffered saline (TTBS) (0.05% Tween-20 in 20 mM Tris-HCl, 500 mM sodium chloride, pH 7.5) overnight at 4°C. Sera collected from immunised rabbits were applied as 1:100 dilutions in 5% milk powder solution for 90 minutes at 37°C using a multiscreen device (Biorad). After TTBS washing, specific IgG antibody was detected by use of a goat anti-rabbit immunoglobulin horseradish peroxidase conjugate (Biorad) secondary antibody diluted in TTBS and applied for 60 minutes at 37°C. After the final TTBS wash, development of bound complex was performed using an Opti-4CN™ Substrate kit (Biorad).

D2.3. IgG fragment preparation

D2.3.A *Isolation of IgG from rabbit serum*

Two serum volumes of 0.01 M borate buffer, pH 8.6, were added to rabbit serum. Pulverized PEG (Mr 6000) was added to the mixture to give a final concentration of 15% (w/v). Once the PEG was dissolved the mixture was centrifuged at 12100 x g for 10 minutes at 4°C. The pellet was dissolved in two serum volumes of borate buffer, pH 8.6. Pulverized PEG was added to give a final concentration of 15% (w/v) and once dissolved the mixture was centrifuged at 12100 x g for 10 minutes at 4°C. The pellet was dissolved in half the original serum volume PBS (pH 7.4), containing 0.05% sodium azide and stored at 4°C.

D2.3.B *Preparation of Fab fragments*

IgG was dialysed against 50 mM Tris, 2 mM EDTA, pH 7.0. Ficin (Sigma) was added at a ratio of 1:30 (E/S) to IgG and activated by adding L-cysteine to a final concentration of 1 mM. The mixture was incubated at 37°C under gentle shaking and after 3 hours the reaction was ended by adding 1:10 (v/v) of a 100 mM N-ethyl-maleimide solution. The mixture was dialysed against PBS (pH 7.4).

D2.3.C *Affinity chromatographic separation of antibody fragments*

Protein A-Sepharose (Sigma) was re-suspended in 0.05 M sodium phosphate, 0.15 M sodium chloride, 0.005 M tri-sodium citrate, pH 7.4 (equilibration buffer). The suspension was degassed and packed in a column (1 cm x 10 cm) under gravity.

Using a protein A-sepharose low-pressure affinity chromatography column equilibrated at room temperature with a flow rate of 0.5 ml/min, the Ficin digestion mixture was applied and residual intact immunoglobulin separated from unbound immunoglobulin fragments. The eluate was monitored at a wavelength of 280 nm and samples (1 ml) collected in an automated fraction collector. Bound IgG was eluted with elution buffer (pH 3.0) between runs. Fab fragments were pooled and exhaustively dialysed against PBS (pH 7.4).

D2.3.D *SDS PAGE confirmation of Fab fragments*

The pooled Fab fragments were diluted 1:4 with non-reducing protein loading sample buffer (Biorad) and loaded on a 4-20% gradient SDS-polyacrylamide gel. SDS-PAGE was performed according to Laemmli. The proteins were stained with Coomassie Brilliant Blue R-250 (Biorad).

D2.4. Rabbit implants

D2.4.A *Tissue preparation*

Fresh porcine aorta walls were collected in cold PBS with 0.05% sodium azide (pH 7.4) at the local abattoir (Maitland, Cape Town). After rinsing in PBS the samples were transferred into cold PBS with 0.05% sodium azide (pH 7.4).

Decellularised porcine aortic wall tissue was prepared by Medtronic Inc. (Heart Valve Division, Santa Ana, CA, USA).

Circular coupons (12mm) were punched from the post-sinotubular ridge of porcine aortic wall from either fresh or decellularised porcine aortic wall tissue and immediately prepared according to their respective treatments.

Group 1: Porcine aortic wall treated with 0.2% glutaraldehyde

The coupons were transferred to HBS (pH 7.4) for 48 hours at 4°C before transferred to cold 0.2% glutaraldehyde in PBS (pH 7.4) After 7 days fixation at 4°C the samples were washed in high-volume HBS (with sodium azide. 4 x volume of fixative, 4°C) and stored in low-volume sterile filtered HBS (without sodium azide, 4°C).

Group 2: Decellularised porcine aortic wall treated with 0.2% glutaraldehyde

After 7 days of HBS washing the coupons were transferred to cold 0.2% glutaraldehyde in PBS (pH 7.4) for 7 days at 4°C. After fixation the samples were washed in high-volume HBS (with sodium azide. 4 x volume of fixative, 4°C) and stored in low-volume sterile filtered HBS (without sodium azide, 4°C).

Group 3: Porcine aortic wall with Fab fragments and treated with 0.2% glutaraldehyde

The coupons were transferred to sterile filtered Fab fragments in HBS (pH 7.4) for 48 hours at 4°C before transferred to cold 0.2% glutaraldehyde in PBS (pH 7.4) for 7 days at 4°C. After fixation the samples were washed in high-volume HBS (with sodium azide. 4 x volume of fixative, 4°C) and stored in low-volume sterile filtered HBS (without sodium azide, 4°C).

Group 4: Decellularised porcine aortic wall masked with Fab fragments and treated with 0.2% glutaraldehyde

After 7 days of HBS washing the coupons were transferred to sterile filtered fab fragments in HBS (pH 7.4) for 48 hours at 4°C before transferred to cold 0.2%

glutaraldehyde in PBS (pH 7.4) for 7 days at 4°C. After fixation the samples were washed in high-volume HBS (with sodium azide, 4 x volume of fixative, 4°C) and stored in low-volume sterile filtered HBS (without sodium azide, 4°C).

Prior to implantation, coupons were thoroughly rinsed by washing for two minutes in each of three basins containing sterile filtered HBS without sodium azide. After washing the coupons were kept in sterile filtered HBS without sodium azide (4°C) until implantation.

D2.4.B *Rabbit subdermal implant model*

Samples were implanted subdermally into pouches created by blunt dissection beneath the fascia on the back of anaesthetised New Zealand White rabbits. Aortic wall coupons were orientated with the adventitial surface facing towards the skin and their ablumenal surface towards the skeletal muscle. After six weeks of implantation the animals were killed and the implants retrieved by *en bloc* removal of the skin from the back of the animal with the coupons still adhering and encased in their fibrous capsules. The skin was immersed in 4% paraformaldehyde solution and stored overnight at 4 C.

D2.5. Histological processing of coupons

Following overnight fixation the coupons with the surrounding muscle and skin were cut from the skin for histology and immunohistochemistry (figure 1-1). The samples were cut into two halves longitudinally, further processed, embedded in wax and cut into sections. The sections were stained with haematoxylin and counterstained with eosin.

Figure D-1 Skin flap after *en bloc* removal and paraformaldehyde fixation with adhering aortic wall coupons prior to sectioning. This method served to preserve the otherwise fragile adherent inflammatory rim and fibrous capsule.

D2.6. Analysis of coupons

Histological examination of the stained sections was performed on a Eclipse 2000 light microscope (Nikon).

D3. Results

D3.1. Immunisation Response

An acquired immune response to the porcine tissue homogenates used to immunize New Zealand White rabbits was observed in each of the four animals (Figure 1-2). Although the identity of the individual bands was not determined, as it fell beyond the scope of this thesis, and may also represent different fragments of similar antigen in cases, an apparently strong broad spectrum response was evident with the bulk of immunoglobulin being specific for proteins ranging in size from as high as 500 kD to 19 kD.

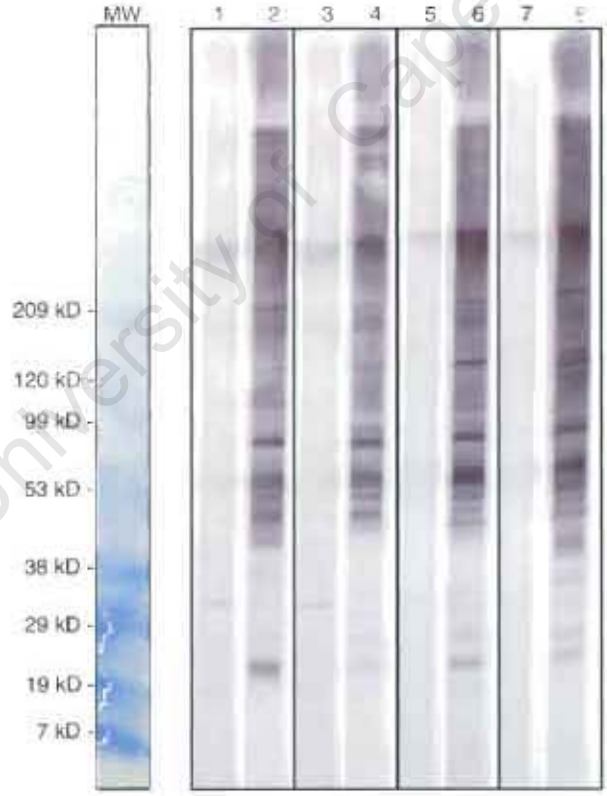

Figure D-2 Western blot showing tissue-specific antibody in serum from immunised New Zealand White rabbits. Lanes 1, 3, 5 and 7 correspond to pre-immunisation sera from the four immunised animals and lanes 2, 4, 6 and 8 correspond to the corresponding pre-termination, that is post-boost sera.

D3.2. Histology

One of the oversights identified in this study was the simultaneous implantation of all the defined groups in each of the recipient animals. Ordinarily, this method is practised when screening the calcification potential of bioprosthetic treatments in rat subdermal models and indeed this has not adversely affected analysis of glutaraldehyde treatments in terms of their inflammation potential as the response is always limited to a small environment adjacent to the implant site. Naturally, it is accepted that the response to one sample can carry over to another through the action of lymphokines and pro-inflammatory stimuli such as complement factors. However, it was rather the qualitative nature of the response rather than its quantitative magnitude that we wished to examine here.

It is important to note that valves implanted clinically typically undergo inflammation predominantly on the ablumenal surface. Indeed it is a fallacy that, at least in the case of non-vital tissue valves, the inflammatory response is blood borne. This is partly due to the shear stress experienced by the luminal surface, especially in the high flow aortic position. Admittedly, transanastomotic hyperplasia does indeed encroach along the blood surface from the anastomoses, both upstream and downstream, where smooth muscle from the media of the injured native vessel is able to cross the now severed internal elastic lamella and progress along the surface of the prosthesis. Frequently, this allows a layer of inflammatory cells, mostly macrophages and foreign body giant cells, as well as microthrombi, to persist between this hyperplastic tissue and the prosthesis itself. The resulting 'pannus' can lead to stenosis of the valve as it extends over the leaflet cusps and is often the site of extrinsic calcification. In the subdermal implant model, however, this phenomenon is for obvious reasons not observed. Nevertheless, although the shear stress scenario is absent in this position, the intimal (luminal) surface is less susceptible to inflammation and, for reasons given above, it is appropriate to evaluate the response to the adventitial (ablumenal) side instead.

Group 1: Porcine aortic wall treated with 0.2% glutaraldehyde

Here two patterns of inflammation are observed (Figure D-6). In (a), a large number of foreign body giant cells (FBGC) interspersed with granulocytes, both polymorph neutrophils (PMN) and eosinophils (EOS) but without lymphocytes (Ly) or plasma cells. In (b), PMN and EOS predominated with fewer FBGC and scanty Ly.

Group 2: Decellularised porcine aortic wall treated with 0.2% glutaraldehyde

In the GA treated decellularised tissue (Figure D-7), granulocyte predominance similar to that seen in the non-decellularised tissue (Group 1) was again evident with equal ratios of PMN and EOS in both (a) and (b). Macrophages (Mø) were seen in (b) and, in contrast to GA fixed non-decellularised tissue (Group 1), no Ly were detected. It is worth noting that, when decellularised tissue was not cross-linked, a sterile granulocyte pus has often observed consisting of apoptosed PMN and presumably EOS. The extent of PMN and EOS in this group of GA fixed decellularised tissue did not constitute pus, which is usually seen as closely packed cell remnant areas with clear fissures extending throughout.

Group 3: Porcine aortic wall with Fab fragments and treated with 0.2% glutaraldehyde

The results of Fab masking followed by GA tethering (Figure D-8) did not show any clear differences compared to non-masked tissue. FBGC were present in large numbers as was the typical PMN/EOS granulocyte response. In (a) even a few Mø were observed as well as scanty Ly. In (b), a number of plasma cells were seen clearly suggesting that a humoral response was still active.

Group 4: Decellularised porcine aortic wall masked with Fab fragments and treated with 0.2% glutaraldehyde

The response in the decellularised, Fab-masked, GA fixed tissue (Figure D-9) was again similar to that observed in the other groups. However, substantially fewer FBGC were observed - they were completely absent in (b) – and Mø were also completely absent. PMN and EOS were the predominant cell type of essentially a granulocytic, if not foreign body, response. In (a), a few plasma cells were nevertheless noted and in (b), the granulocyte response had developed into the beginnings of a sterile pus.

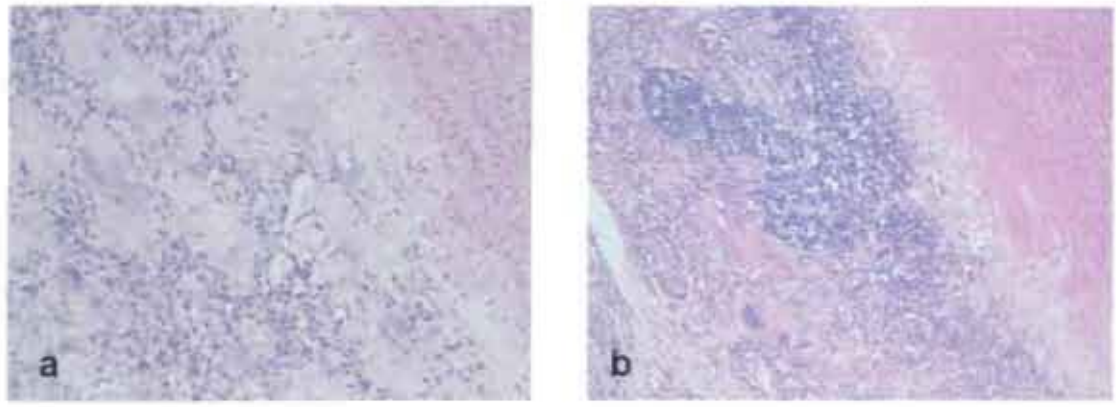

Figure D-3 Two replicates demonstrating the inflammatory rim associated with the adventitial surface of 0.2% GA fixed porcine aortic tissue. The media can be seen in the upper right.

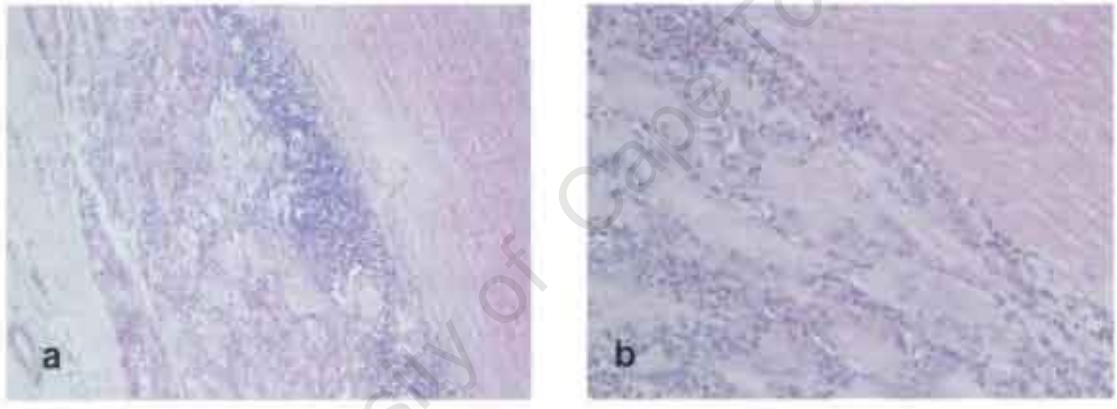

Figure D-4 Two replicates demonstrating the inflammatory rim associated with the adventitial surface of decellularised and subsequently 0.2% GA fixed porcine aortic tissue. The media devoid of smooth muscle cells can be seen in the upper right.

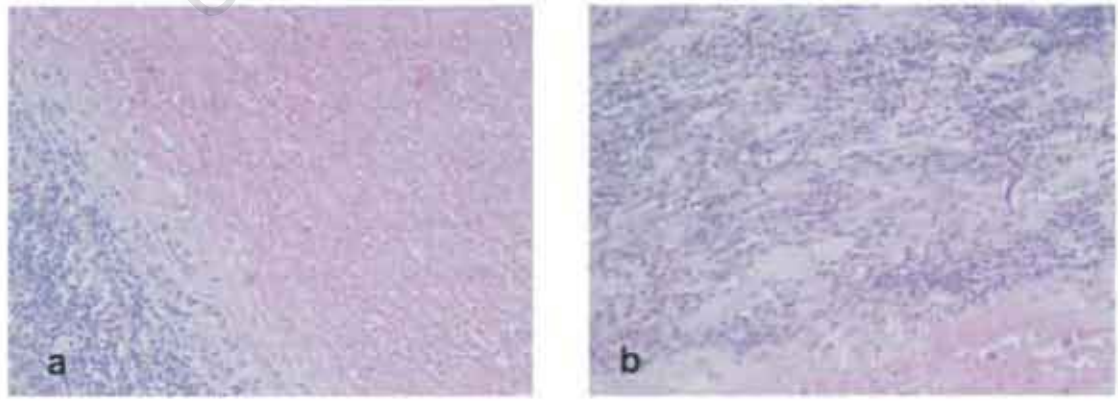

Figure D-5 Two replicates demonstrating the inflammatory rim associated with the adventitial surface of Fab masked and 0.2% GA fixed porcine aortic tissue.

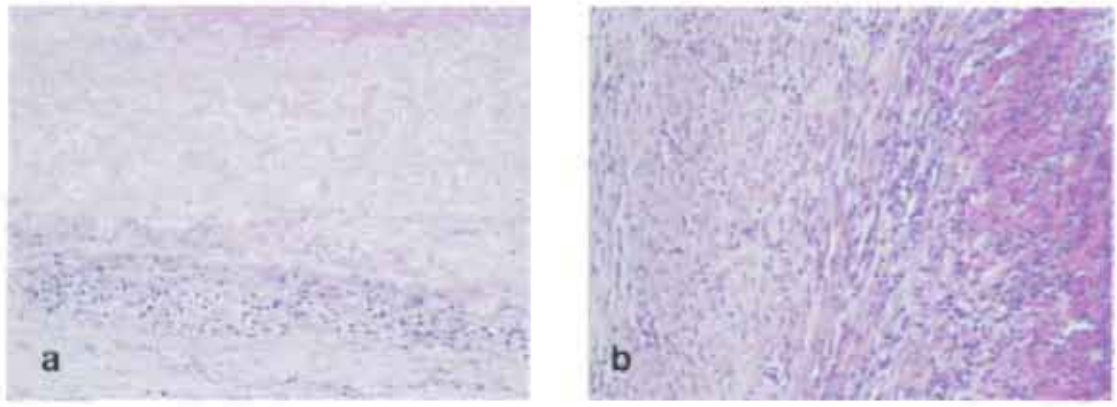

Figure D-6 Two replicates demonstrating the inflammatory rim associated with the adventitial surface of Fab masked decellularised and subsequently 0.2% GA fixed porcine aortic tissue.

D4. Summary

Although the concept of utilising immunoglobulin produced in response to immunogens which fixation treatments, such as GA cross-linking, are incapable of modifying or masking appears to hypothetically be a logical strategy at first glance. This was indeed confirmed by the *in vitro* aspect of this study. It is clear from this pilot *in vivo* study that the use of immunoglobulin fragments needs to be optimised to be of any value.

Part of the problem is likely due to the fact that the tissue itself is a heterogenous mix of proteins and proteoglycans which are capable of sensitising the host immune system in a dose-dependent manner. Some of these potential immunogens may be sufficiently hidden deep in the interior of the aortic wall or, alternatively, result in immunoglobulins with low avidity whereas others, which may be prevalent in only small quantities, may be much more accessible or result in high avidity antibody. It is likely therefore, that a cocktail of individually optimised antibody clones with defined specificity and which will also result in total masking of their respective targets is what will be required.

Another part of the problem is the very nature of the immune/inflammatory response itself and which has much redundancy built in. Simply blocking one aspect thereof may not prevent another from responding. Complement, for example acts through both antibody dependent and antibody independent pathways. Inflammatory cells such as macrophages and neutrophils have, in addition to their Fc receptors,

complement receptors which may be more effective at initiating a process of phagocytosis or, more likely with respect to highly cross-linked bioprosthetic tissue, a process of 'frustrated' phagocytosis.

Even the nature of the complement cascade itself introduces soluble proinflammatory factors which may thwart any attempt directed solely at inhibiting immunoglobulin binding in the quest to mitigate inflammatory demise of a valve bioprosthesis.

E. Discussion

Bioprosthetic heart valves have a limited average lifespan of 10 years[191-194] and patients younger than 60 years will likely need more than one redo operation in their lifetime. Therefore improvement of bioprosthetic heart valve durability is urgently needed. In this study the feasibility of using Fab fragments to quench inflammation of heart valve tissue through antigen masking was evaluated. This concept relies on additionally utilising the standard glutaraldehyde fixation process used in the manufacture of bioprosthetic heart valves in order to tether immunoglobulin fragments to the tissue prior to implant. Removal of the Fc fragment has the potential to prevent adherence of phagocytes and complement to the graft. Enzyme digestion of the immunoglobulin molecule potentially results in either Fab or $F(ab')_2$ fragments, however, the monovalent Fab fragments are smaller and hypothesized to penetrate the tissue deeper. The larger $F(ab')_2$ fragments have the potential to bind to more than one of their epitope targets and therefore with greater avidity to the antigen. Therefore, antibody fragments produced in rabbits immunised with different porcine heart valve tissue preparations were used to mask tissue representative of that seen in contemporary heart valve bioprostheses. Proof of concept was sought based on the potential for these fragments to mask histological sections *in vitro* and indeed clearly demonstrated high efficiency of masking against the binding of intact immunoglobulin to the tissue. To investigate whether this masking was capable of altering the inflammatory response *in vivo*, a pilot study was performed in a rabbit subdermal implant model. Here, in addition to evaluating the response to glutaraldehyde fixed porcine aortic wall tissue we also examined whether the method had potential with respect to decellularised aortic wall tissue where the antigen load was perhaps limited to largely extracellular matrix components. Both tissue groups were treated with antibody fragments tethered onto the tissue to avoid issues of premature release of these immunoglobulin caps. Although there was no clear difference observed between masked and control groups there was a hint that some mitigation of foreign body giant cell formation had resulted in the case of the decellularised tissue.

Faustman and Coe [212] first illustrated immunoprotection of xenografts using $F(ab')_2$ fragments to mask the donor major histocompatibility complex class I (MHC-1). Rejection of transplanted xenogeneic human pancreatic islets and liver in the mouse was circumvented by masking donor MHC-1 or tissue-specific epitopes with $F(ab')_2$

antibody fragments. This strategy eliminated the need for recipient immunosuppression and allowed islet xenograft survival beyond 200 days. This strategy was later applied for immunoprotection of neural xenografts by Pakzaban et al[213] who used monoclonal antibody $F(ab')_2$ fragments specific to porcine MHC-1 in an attempt to mask this complex on porcine fetal striatal cells transplanted into rat striata. The fragments enhanced survival of the xenografts significantly compared to non-immunosuppressed controls and thus were shown to have the potential for immunoprotection of neural xenografts.

In contrast, our study strove to mask not just one or two, but all potential residual immunogens in the highly complex bioprosthetic tissue in order to mitigate the host inflammatory response. Schussler et al[214] compared intravenous immunoglobulin (IVIg) (polyclonal human IgG prepared from pools of plasma from several thousand healthy blood donors) with $F(ab')_2$ fragments thereof with respect to the ability to minimize the response to bioprosthetic porcine heart valve tissue in a subcutaneous rat model. The treatment reportedly reduced the antigenicity as well as reduced the cellular response to the glutaraldehyde-fixed valves. Our study used serum from rabbits immunised with porcine aortic wall based preparations to achieve higher titres of antibodies directed against porcine heart valve tissue. In contrast, our study utlilised allogeneic immunoglobulin to prevent a xenogeneic response to the antibody fragments themselves. Immunoglobulin fragments were used based on the premise that this would prevent adherence of phagocytes via their Fc receptors.

A limitation of the study was that, except in the case of porcine fibronectin, most of the antigens targeted were unknown. An approach similar to the immunoproteomic identification of xenoantigens in bovine pericardium done by Griffiths group [215] should ideally also be performed for porcine bioprosthetic heart valve tissue. Their group identified thirty-one putative protein antigens which included cellular and matrix proteins.

We realised the importance of masking not just one but multiple xenoantigens, possibly with more than one epitope being targeted for each antigen. The consequence of immunising animals using a crude extract of porcine tissue is limited in that the response is dictated by the availability of antigen in the tissue. This clearly represents an imprecise approach but nevertheless provided an important insight in this early proof-of-concept phase. Future work should identify a library of highly immunogenic proteins present in bioprosthetic heart valve tissue and tailor a cocktail

of poly- or monoclonal antibody fragments to a selected number that would still achieve the desired effect.

The inflammatory response is a complicated network of responses triggered by a variety of molecules and it would be naïve to suggest that masking antigens with Fab and/or $F(ab')_2$ fragments would be sufficient to mitigate the response. Analysis of the response of our work and others clearly showed that the response to bioprosthetic heart valve tissue is largely a xenogenic response dominated by macrophages, neutrophils and foreign body giant cells. A large part of the research done in the bioprosthetic heart valve field is done using the subdermal rat model. It is a well-known fact, although mostly ignored, that in the rat model, inflammation is predominantly a lymphocyte response. Initially the response includes neutrophils and macrophages but the response quickly gives way to a mainly lymphocyte dominated one. In the primate as well as the rabbit, unlike the rat, a macrophage focussed response predominates and is thus a more representative model to use.

Neutrophils, macrophages and foreign body giant cells all have Fc receptors that recognise and will bind to the Fc fragment of IgG opsonised tissue. Fc receptors recognise specifically the Fc portion of the immunoglobulin molecule. This binding property of IgG antibodies has been shown to be independent of the Fab region of the antibody and requires only Fc interactions[216]. When binding to Fc receptors, antibodies effectively provide antigen specificity to a variety of cells, most of which are otherwise devoid of antigen recognition structures. The role of these receptors trigger effector responses such as cell activation, endocytosis, and phagocytosis. The nature of the responses depends primarily on the cell type[205]. Thus, removal of the Fc fragment of antibodies may prevent binding of cells relying on their Fc receptors to recognise antigens.

Activation of complement occurs by three different pathways: the classical pathway (triggered by IgM or IgG complexed with tissue), the lectin pathway (activated by binding mannose-binding lectin to mannose residues on the pathogen surface) and the alternative pathway (triggered by spontaneous C3 hydrolysis). The Fc region of the IgG or IgM contains a C1 binding site for C1q and binding of C1q to the IgM or IgG complexed with tissue activates the classical pathway[217]. Thus, mitigation with Fab and/or $F(ab')_2$ fragments may influence the classical pathway but may not be enough to mitigate the complement process.

The Fab and/or $F(ab')_2$ fragment treatment under investigation achieved encouraging results *in vitro* despite the lack of in depth optimisation of the polyclonal immunoglobulin preparation used to mask IgG binding to the tissue.

Most treatments of contemporary bioprosthetic heart valves focus on glutaraldehyde fixation of the tissue to prevent a host response and provide durability. As glutaraldehyde has been reported to be the main villain causing calcification, glutaraldehyde concentrations used are suboptimal in terms of their ability to render the tissue completely immunogen free. The drive behind alternative fixatives is largely geared towards avoiding mineralization of the bioprosthesis, especially in children although a decellularisation process is perhaps more focussed on minimizing the host response while at the same time offering a scaffold amenable to tissue ingrowth and remodelling. This is based on the misconception that cells alone are responsible for immunogenicity of bioprosthetic tissue and indeed there are studies confirming the significant role that the extracellular matrix plays in calcification[98] and inflammation[218, 219] of bioprosthetic heart valves.

Our study in fact confirmed that decellularised tissue substantially reduced the humoral immune response. Western blotting performed using sera obtained from rabbits immunised with decellularised tissue homogenates clearly showed a response against porcine aortic wall extract as well as porcine fibronectin. This provided support to the concept that cells alone are not responsible for the immunogenicity of porcine aortic tissue but that extracellular matrix components likewise contribute. Therefore, decellularised tissue, although possibly offering ingrowth potential falls short at fully avoiding the problem of immunogenicity. Indeed the massive granulocyte response observed in the *in vivo* study suggests that this is possibly due to incomplete antigen washout since bacterial contamination of the tissue was discounted (data not shown) and the tissue was also exhaustively washed to remove the anionic detergent SDS and other components used in the decellularisation process.

Although the scope of this thesis was to provide proof-of-concept with respect to the feasibility of applying immunoglobulin fragments to bioprosthetic tissue by masking remnant immunogenicity in contemporary bioprosthetic heart valves, an *in vivo* pilot study designed to investigate whether the concept had at least the potential to diminish the inflammatory response as well as identifying logistical problems should one endeavour to apply it in patients, was also performed.

Also outside of the scope of this thesis, but nevertheless an important consideration is the need or not to covalently tether immunoglobulin fragments to the tissue which otherwise may only persist for a short duration.

The source of antibody is of equal importance. Potentially these might involve either monoclonal antisera produced in mice or polyclonal ones produced in rabbits. Xenogeneic immunoglobulin sources may need to be better evaluated although there is a precedence for using animal derived IgG in patients in the clinical organ transplant field in the form of the immunosuppressive drug rabbit anti-thymocyte globulin (Fresenius)[220] produced in rabbits as well as in the murine monoclonal antibody OKT3 (Orthokline) also called Muromonab[221].

Nevertheless, the possibility exists that fragments could, for example be modified through a pegylation process whereby polyethylene glycol (PEG) bound to immunoglobulin fragments would both serve the purpose of delaying their clearance from the blood as well as possibly masking any antigen the pegylated antibody binds to with greater efficacy.

No clear difference was seen between the different groups in the *in vivo* study although the fact that, at least anecdotally, Fab treatment in the decellularised group presented with fewer foreign body giant cells. This may be that the as yet suboptimal Fab preparation may nevertheless be partly capable of masking the less immunogenic decellularised tissue and thereby reduce the response.

Appendix A Materials and Methods

A1. Isolation of serum

Animal blood was collected BD Vactuatiner® tubes (cat no 367955) and allowed to clot at room temperature. The clotted blood was centrifuged at 1260 xg for 45 minutes at room temperature and serum collected and stored at -80°C.

A2. Isolation of plasma

Blood were collected in a sterile glass container with the anticoagulant EDTA (0.2 mg/ml blood) at the local abattoir (Maitland, Cape Town). The blood was centrifuged at 1810 xg for 20 minutes at room temperature, and the plasma collected. The plasma was sterile filtered (0.22 µm).

A3. Collect porcine aorta

Table 3 Phosphate Buffered Saline (PBS)

Constituent	Supplier
137 mM sodium phosphate	Sigma
3 mM potassium chloride	Sigma
2 mM potassium dihydrogen phosphate	Sigma
8 mM sodium phosphate	Sigma
pH 7.4	

Fresh porcine aortas were collected in cold PBS (Table 3) at the local abattoir (Maitland, Cape Town, South Africa) from normal, healthy pigs. They were processed within five minutes of slaughter. After rough dissection, the valves were cleaned and rinsed in PBS (Table 3). On arrival at the laboratory the porcine aortas were transferred to sterile filtered PBS.

A4. Decellularise process (Medtronic)

Table 4 Wash solution

Constituent	Supplier
0.3% sodium chloride (w/v)	Sigma
0.05% sodium azide (w/v)	Sigma
20 mM $Na_2EDTA.2H_2O$	Sigma
Protease inhibitor cocktail (1 ml / 1.5 l)	Sigma
pH 7.4	
173 mOsm/kg	

Protease inhibitor cocktail was prepared by adding 10 ml deionised water to the protease inhibitor cocktail bottle (Sigma, cat. no. P2714).

Table 5 Decellularise solution

Constituent	Supplier
0.3% sodium chloride (w/v)	Sigma
0.05% sodium azide (w/v)	Sigma
0.5% SDS (w/v)	Sigma
0.5% Triton X-100 (v/v)	Sigma
pH 7.4	
130 mOsm/kg	

Table 6 Rinse solution

Constituent	Supplier
0.3% sodium chloride (w/v)	Sigma
0.05% sodium azide (w/v)	Sigma
pH 7.0	
110 mOsm/kg	

Table 7 Sterile solution

Constituent	Supplier
0.3% sodium chloride (w/v)	Sigma
0.25% CPC (w/v)	Sigma
1% IPA (v/v)	Sigma
20 mM $Na_2EDTA.2H_2O$	Sigma
pH 7.4	
296 mOsm/kg	

Table 8 Storage solution

Constituent	Supplier
0.6% Sodium chloride (w/v)	Sigma
0.25% Sodium Azide (w/v)	Sigma
10 mM HEPES	Sigma
20 mM $EDTA.2H_2O$	Sigma
pH 7.4	
282 mOsm/kg	

Porcine aortas collected from the abbatoir (see Appendix A3) were cleaned from any fat and washed with rolling (60 rpm) for 24 hours at room temperature in wash solution (Table 4). The solution was changed from the wash solution to the decellularise solution (Table 5). The aortas were washed with rolling (60 rpm) in the decellularise solution for 144 hours (6 days) at room temperature. The decellularise solution was changed every 24 hours. After decellularising the aortas the solution was changed to rinse solution (Table 6). The aortas were washed with rolling (60 rpm) in the rinse solution for another 144 hours, changing the solution every 0.5 to 1 hour (at least 40 times). The aortas were sterilised in sterile solution (Table 7) with rolling (30 rpm) for 3 hours at room temperature. After sterilisation the aortas were stored in storage solution (Table 8) at room temperature until needed.

A5. Homogenise tissue

A stainless steel vial and two bearing balls, as well as a mortar, a pestle and a spatula, were cleaned with 70% ethanol and cooled in liquid nitrogen. The tissue were cut into smaller pieces and frozen in liquid nitrogen. The frozen tissue pieces were placed in the cooled stainless steel vial, with two bearing balls and homogenised in a homogeniser for a few seconds (the tissue must stay frozen). After all the pieces were homogenised, they were placed in the cooled mortar. Liquid nitrogen was added and the frozen homogenised powder was mixed and ground with the pestle to form a homogeneous mixture. The homogenous powder was frozen in liquid nitrogen, freeze-dried overnight and stored at -80°C.

A6. Immunisation solutions

Sterile saline was added to the homogenous powder and vortexed to suspend the powder. The Freund's incomplete adjuvant was slowly added to the saline mixture in a 1:1 ratio. The two solutions were mixed, using two syringes connected with a small tube, to form an emulsion. The thick, white, creamy emulsion was stored at 4°C before immunisation.

A7. Protein extract

Table 9 Protein extraction Buffer

Constituent	**Supplier**
50 mM Tris	Sigma
0.1% (w/v) sodium dodecylsulfate (SDS)	Sigma
pH 7.4	

Freeze-dried homogenise tissue were weighed and protein extraction buffer (Table 9) was added in ratio of 100 µl buffer for 1 mg tissue. The mixture was incubated overnight at 4°C. After incubation it was centrifuged at 1260 xg for 15 minutes at 4°C and the supernatant was stored at -20°C.

A8. DC Protein Assay

The Bio-Rad DC protein assay is a calorimetric assay for protein concentration. The assay is based on the reaction of protein and copper in an alkaline medium and the subsequent reduction of Folin reagent by the copper-treated protein. A characteristic blue colour develops with maximum absorbance at 750 nm.

A protein standard (1 mg/ml BSA) (Sigma) was used for the standard curve. Doubling dilution series of the protein standard was prepared from 0.625 mg/ml to 1 mg/ml in the same buffer as the sample. A doubling dilution series (1 to 64) of the sample was also prepared. 100 µl of the standard dilutions and sample dilutions were pipetted into clean, dry test tubes. 500 µl reagent A (an alkaline copper tartrate solution) (Bio-Rad, UK) was added to each tube and vortex. 4 ml reagent B (Folin reagent) (Bio-Rad, UK) was added and vortex immediately. After 15 minutes the absorbance was read at 750 nm. The standard dilutions series of the known protein concentrations of the BSA sample was used to set up a standard curve. The absorbance of the samples was used to calculate the concentration of the samples using the standard curve.

A9. SDS Polyacrylamide Gel Electrophoresis (SDS PAGE)

Table 10 Sample buffer

Constituent	**Supplier**
62.5 mM Tris-HCl	Sigma
20% glycerol	Sigma
2% (w/v) SDS	Sigma
pH 6.8	

Table 11 Electrode running buffer

Constituent	Supplier
25mM Tris	Sigma
192 mM glycine	Sigma
0.1% (w/v) SDS	Sigma
pH 8.3	

Table 12 Formulation of SDS-PAGE separation and stacking gels.

	Separation Gel		Stacking gel
Monomer concentration	**4%**	**20%**	**4%**
acrylamide/bisacrylamide	1.3 ml	6.6 ml	1.3 ml
Distilled water	6.1 ml	0.7 ml	6.1 ml
1.5M Tris-HCL, pH 8.8	2.5 ml	2.5 ml	-
0.5M Tris-HCL, pH 6.8	-	-	2.5 ml
10% (w/v) SDS	100 µl	100 µl	100 µl
10% (w/v) ammonium persulfate	50 µl	50 µl	50 µl
TEMED	5 µl	5 µl	10 µl

A9a Mini-PROTEAN® 3 system:

SDS Page Separation gel solutions for 4% and 20% were prepared (Table 12). The gradient gel was poured with the 20% gel solution, while it was diluted with the 4% gel solutions. The separation gel was allowed to polymerise before pouring the 4% stacking gel. The comb was inserted before the stacking gel was polymerised. After the stacking gel was polymerised the comb was removed leaving wells for applying the protein samples to the gel. Every gel was run with a molecular weight marker to use as a reference for the protein weights.

The mini-PROTEAN® 3 system (Bio-Rad, UK) was used for separating proteins. The electrode running buffer (Table 11) was diluted 1:5 with distilled water and poured into the upper and bottom buffer chamber. Protein samples were diluted 1:4 in

sample buffer (Table 10) and applied to the gel. The mini-gel was run under constant voltage (200 V) at room temperature for 45 minutes.

A10. Western Blot

Table 13 Towbin transfer buffer

Constituent	Supplier
25 mM Tris	Sigma
192 mM glycine	Sigma
20% (v/v) methanol	Merck
0.1% (w/v) SDS	Sigma
pH 8.3	

Table 14 Tween Tris buffered saline (TTBS)

Constituent	Supplier
20 mM Tris-HCl	Sigma
500 mM sodium chloride	Sigma
0.05% (v/v) Tween-20	Sigma
pH 7.5	

The SDS-PAGE gel after the electrophoresis run was equilibrated in Towbin transfer buffer (Table 13) for an hour. The PVDF membrane was first activated in 100% methanol for a few seconds and then equilibrated with the filter paper in Towbin transfer buffer (Table 13). After equilibration the protein was blotted onto PVDF membrane using a semi-dry electroblotter (Bio-Rad, UK). The membrane and SDS-PAGE gel were sandwiched between filter paper. The semi-dry electroblotter was run under constant voltage (20 V) for 30 minutes. The membrane was blocked in 5% (w/v) milk powder (fat free) TTBS (Table 14) overnight at 4°C with agitation. The primary antibody was diluted in 5% (w/v) milk powder (fat free) TTBS (Table 14) and the membrane incubated in the milk powder solution for 90 minutes at 37°C. After incubation with the primary antibody the membrane was washed three times for 15 minutes in TTBS (Table 14). The membrane was incubated in horseradish peroxidase conjugate secondary antibody diluted in TTBS (Table 14) for 60 minutes

at 37°C. After the final three TTBS (Table 14) 15 minutes washes, development of bound complex was with Opti-4CN™ Substrate kit (Bio-Rad, UK). The 4-chloro-1-naphtol forms a brown insoluble chromogenic substrate in the presence of hydrogen peroxide.

A11. Protein affinity chromatography

Packing of the column

The amount of filtration medium needed to fill the column plus an extra 10% was equilibrated with twice the column volume of the equilibration buffer. The medium was allowed to swell overnight at 4°C. The suspension was degassed for 2 hours with periodic swirling. The buffer volume was increased to five times the volume and allowed to stand. After the majority of the beads settled the supernatant was aspirated to one and half times the settled volume. The column was packed by allowing the beads to settle under gravity without air bubbles. One volume of equilibration buffer was run through the column.

Sample application and elution

Equilibration buffer was added to the sample in a 1:1 ratio and applied to the column. After washing the unbound fractions from the column with equilibration buffer, the sample was eluted with elution buffer at room temperature with a flow rate of 0.5ml/min. 1ml fractions were collected and monitored for its absorbance at 280 nm (proteins). The eluted fractions with sample were pooled.

A11a Protein A-Sepharose column

Table 15 Equilibration buffer (sodium citrate)

Constituent	Supplier
50 mM sodium phosphate	Sigma
150 mM sodium chloride	Sigma
5 mM tri-sodium citrate	Sigma
pH 7.4	

Table 16 Rabbit IgG elution buffer

Constituent	Supplier
200 mM sodium phosphate	Sigma
100 mM citric acid	Sigma
pH 3.0	

Protein A-Sepharose (Sigma) was re-suspended in equilibration buffer (Table 15). The suspension was degassed and packed in a column (1 cm x 10 cm) (see – packing of the column). Sample was applied to the column (see - sample application and elution) and IgG was eluted with elution buffer (Table 16). The eluted fractions were neutralised with a sodium hydroxide solution to a pH in the region of 7.0-7.4. The fractions were pooled and dialysed against PBS (Table 3) overnight at 4°C.

A11b Gelatin-agarose column

Table 17 Sodium phosphate equilibration buffer

Constituent	Supplier
0.05 M sodium phosphate	Sigma
0.15 M sodium chloride	Sigma
0.005 M tri-sodium citrate	Sigma
pH 7.4	

Table 18 Urea elution buffer

Constituent	Supplier
4 M urea	Sigma
0.05 M Tris-HCl	Sigma
pH 7.5	

Gelatin immobilized on cross-linked 4% beaded agarose (Sigma), was re-suspended in sodium phosphate buffer (Table 17). The suspension was degassed and packed in a column (1 cm x 20 cm) (see – packing of the column). Sample was applied to the column (see sample application and elution) and fibronectin was eluted with elution

buffer (Table 16) at room temperature with a flow rate of 0.5 ml/min. The fractions were pooled and dialysed against double distilled water overnight at 4°C.

A11c Fibronectin affinity column

Prepare fibronectin affinity column

Table 19 Coupling buffer

Constituents	**Suppliers**
0.1 M $NaHCO_3$	Sigma
0.5 M sodium chloride	Sigma
pH 8.3	

Table 20 Blocking solution

Constituents	**Suppliers**
0.2 M glycine	Sigma
Coupling buffer (Table 19)	
pH 8.0	

Table 21 Acetate buffer

Constituents	**Suppliers**
0.1 M sodium acetate	Sigma
0.5 M sodium chloride	Sigma
pH 4.0	

The cyanogen bromide activated sepharose (Sigma, cat no C9210) was washed with cold 1 mM hydrochloric acid to remove lactose from the resin and allowed to swell for an hour. The resin was washed with double distilled water to remove the lactose necessary to stabilise the beads during storage but would interfere with binding if it was present during the coupling. After the wash, the resin was activated in the coupling buffer (Table 19). Pig plasma fibronectin dissolved in the coupling buffer

(Table 19) was added to the resin at a ratio of 10 mg protein per 1 ml of gel. The mixture was incubated for 16 hours at 4°C. After incubation the resin was washed with the resin activation solution (Table 19). The groups that did not react were blocked with blocking solution (Table 20) for 16 hours at 4°C. After blocking the resin wash extensively washed five times alternating coupling buffer (Table 19) and acetate buffer (Table 21). The resin was degassed and packed in a column (1 cm x 10 cm) (see packing of the column). The column was equilibrated with equilibration buffer (sodium citrate) (Table 15). Equal volume equilibration buffer (sodium citrate) (Table 15) was added to rabbit anti-sera. The mixture was applied to the porcine fibronectin column (see sample application and elution). After washing with the equilibration buffer, the rabbit IgG was eluted with rabbit IgG elution buffer (Table 16), at room temperature with a flow rate of 0.5 ml/min. The column output was monitored at a wavelength of 280 nm and fractions of 1.0 ml were collected. Sodium hydroxide solution was added to the mixture to neutralize the fractions (pH 7.0-7.4). The pooled fractions were dialyzed against PBS (Table 3) overnight at 4°C.

A12. Fixation of tissue in glutaraldehyde

Fresh porcine aortic valves were stored in PBS for 48 hours at 4°C.

Fresh tissue

The valves were deposited fixed in 10% formalin and processed for histology (see Appendix A18).

0.2% Glutaraldehyde

The valves were deposited into cold 0.2% (v:v) glutaraldehyde prepared in PBS (Table 3). After 7 days at 4°C the valves were washed in high volume PBS (30 ml/g. 37°C). The tissue was placed in cold PBS for low volume storage at 4°C until needed.

3% Glutaraldehyde

The valves were deposited into 3% (v:v) glutaraldehyde prepared in PBS (Table 3). After 7 days at 4°C the valves were washed in high volume PBS (30 ml/g. 37°C). The tissue was placed in cold PBS for low volume storage at 4°C until needed.

A13. Isolation of IgG with PEG 6000

Table 22 Borate buffer

Constituent	Supplier
10 mM boric acid	Merck
7.5 mM hydrochloric acid	Merck
37.5 mM sodium chloride	Sigma
pH 8.6	

Two serum volumes of borate buffer (Table 22) were added to rabbit serum. Pulverised PEG (Mr 6000) was added to the mixture to give a final concentration of 15% (w/v). Once the PEG was dissolved the mixture was centrifuged at 12100 g for 10 minutes at 4°C. The pellet was dissolved in two serum volumes borate buffer, pH 8.6. Pulverised PEG was added to give a final concentration of 15% (w/v) and once dissolved the mixture was centrifuged at 12100 g for 10 minutes at 4°C. The pellet was dissolved in half the original serum volume PBS (Table 3), containing 0.05% sodium azide and stored at 4°C.

A14. Isolation of IgG with sodium sulphate

4% (w/v) sodium sulphate in PBS (Table 3) was added drop wise with stirring to rabbit serum in a 1:1 ratio. After 30 minutes of stirring at room temperature the mixture was centrifuged at 2000 g for 30 minutes at room temperature. The pellet was dissolved in two serum volumes 2% (w/v) sodium sulphate in PBS (Table 3). After 30 minutes of stirring at room temperature the mixture was centrifuged at 2000 g for 30 minutes at room temperature. The pellet was dissolved in half the original serum volume PBS (Table 3), and stored at 4°C.

A15. Digestion of IgG with Ficin

Table 23 Ficin digestion buffer

Constituent	Supplier
50 mM Tris	Sigma
2 mM EDTA	Sigma
pH 7.0	

IgG was dialysed against Ficin digestion buffer (Table 23). Ficin (Sigma) was added in a ratio of 1:30 (E/S) to IgG and activated by adding L-cysteine to a final concentration of either 1 mM (Fab fragments) or 10 mM ($F(ab')_2$ fragments). The mixture was incubated at 37°C under gentle shaking and after 3 hours the reaction was stopped by adding 1:10 (v/v) of a 100 mM N-ethyl-maleimide solution. The mixture was dialysed against PBS (Table 3).

A16. Digestion of IgG with Pepsin

Table 24 Acetate buffer

Constituent	Supplier
100 mM sodium acetate	Sigma
pH 4.5	

IgG was dialysed against acetated buffer (Table 24). Pepsin (Sigma) was added in a ratio of 1:20 (E/S) to the rabbit IgG. The mixture was incubated for 8 hours at 37°C under gentle shaking and after 8 hours the reaction was stopped by adding 1:10 (v/v) of 1 M Tris buffer, pH 8.0. The digestion mixture was dialyzed at 4°C against PBS (Table 3).

A17. Digestion of IgG with Papain

Table 25 Papain digestion buffer

Constituent	Supplier
100 mM sodium phosphate	Sigma
2 mM EDTA	Sigma
pH 7.0	

IgG was dialysed against papain digestion buffer (Table 25). Papain (Sigma) was added in a ratio of 1:60 (E/S) to IgG and activated by adding L-cysteine tot a final concentration of 1 mM. The mixture was incubated for 8 hours at 37°C under gentle shaking and then dialysed at 4°C against PBS (Table 3)

A18. Conjugate peroxidase to IgG

IgG was dialysed against PBS (Table 3) without sodium azide (inactivate peroxidase). Horseradish peroxidase was added in a ratio of 1:5 (E/S) to the IgG. 0.02% Glutaraldehyde in PBS, pH 7.4, was added to the mixture to give a final concentration of 0.01% Glutaraldehyde and mixed for 1 hour at room temperature.

Sephadex G-100 (Sigma) was re-suspended in PBS (pH 7.4.) The suspension was degassed and packed in a column (1 cm x 30 cm) under gravity (see paragraph A11 - packing of the column).

The IgG peroxidase mixture was applied to the Sephadex G-100 column and eluted with PBS (pH 7.4.). 1 ml fractions were collected and monitored at a wavelength of 280 nm. The peroxidase-IgG conjugate fractions were pooled and stored at 4°C.

A19. Blocking and processing of samples

Table 26 Paraformaldehyde

Constituent	Supplier
4% paraformaldehyde (w/v)	Merck
10 M sodium hydroxide	Sigma

Preparation for 4% paraformaldehyde

4g paraform was dissolve in 100 ml PBS (Table 3). The solution was heated to 58°C and a few drops 10 M sodium hydroxide was added to clear the solution. The solution was cooled to room temperature and the pH was adjusted to 7.4.

Fixing and preparation of sample

Samples were immersed in 4% paraformaldehyde for 24 hours at room temperature to properly fix the tissue. The samples were cut for embedding in wax.

Wax processing

The sample was placed in histology cassette and the cassettes were placed into wire mesh baskets. The samples were dehydrated through graded alcohols (70%, 80%, 90% and three solutions of 100% ethanol) for an hour in each solution. The samples were cleared in three changes of iso-octane for an hour each time. The samples were placed in three changes of paraffin wax at 60°C for an hour in each and 2 hours in the last change of paraffin wax.

Embedding

The cassette with the sample was removed from the hot paraffin wax and opened. The orientation of the sample was determined to correctly embed the sample for cutting. The sample was embedded in hot waxed and placed on a cold plate to set for 5 to 10 minutes.

Sectioning of wax block

The blocks were kept on ice before cutting on a Microtome. The sections were cut 3µm thickness. The sections were transferred to a 56°C water bath from where it was placed on APES coated slides. The slides were incubated overnight at 37°C to dry any water between the sections and slide.

Dewax sections for staining

After incubation at 60°C for 30 minutes, the sections were washed three times for 10 minutes each in 100% xylene changes and three times in 100% alcohol, two times 96% alcohol and two times in 70% alcohol. After the washes the sections were rinsed in fresh tap water.

A20. Immunohistochemistry

Staining of sections with antibodies conjugated to Horseradish Peroxidase (HRP)

Table 27 0.5% Hydrogen peroxide

Constituent	Supplier
4 ml hydrogen peroxide	UnivAR
200 ml methanol	Sigma

The sections were treated with 0.5% hydrogen peroxide (Table 27) in methanol for 10 minutes to block endogenous peroxide in the tissue, washed in fresh tap water and placed in TTBS (Table 14). All incubations were done in a humidity chamber to prevent drying out of the section. The sections were incubated for 1 hour at room temperature with primary antibody. Unbound antibody was washed off with TTBS (Table 14) for 10 minutes. The sections were incubated with secondary antibody for 1 hour at room temperature. The unbound antibody was washed off with TTBS (Table 14) for 10 minutes. The sections were incubated with tertiary detection antibody conjugated to peroxidase for 30 minutes at room temperature. The unbound antibody was washed off with TTBS (Table 14) for 10 minutes. Freshly prepared DAB (DAKO) solution was added to visualise the bound conjugated antibody (brown) and the nuclei were counter-stained with Haematoxylin (blue).

Mount sections

The sections were washed in fresh tap water, dehydrated in 100% alcohol and cleared in 100% xylene. The sections were mounted in a drop of Entellan on the cover slip placed over the section and allowed to dry.

A21. Histology

Haematoxylin and eosin stain

Table 28 Mayers haemotoxylin

Constituent	Supplier
2 g haematoxylin	Merck
50 g potassium alum	SAARCHEM
0.2 g sodium iodate	Sigma
1 l double distilled water	
1 g citric acid	SAARCHEM
50 g chloral hydrate	SAARCHEM

The first four constituents in Table 28 were added and gently heated in a warm bath at 37°C. The rest of the constituents were added and boiled for 5 minutes. The solution was cooled and filtered and stored in a glass bottle at room temperature.

Table 29 Acid alcohol

Constituent	Supplier
1% concentrated hydrochloric acid	Merck
70% ethanol	Merck

Table 30 Eosin

Constituent	Supplier
1 g Eosin	Merck
1 l double distilled water	
Few drops acetic acid	Sigma

The sections were placed in the haematoxylin solution (Table 28) for 5 minutes and then 5 minutes in running tap water to stain the nuclei blue. The acid alcohol (Table 29) was used to differentiate the haematoxylin. The sections were placed in the eosin (Table 30) for 30 seconds and dipped in distilled water before mounting the sections (see mount sections).

Brown and Brenn stain

The sections was placed in 1% Crystal violet for 5 minutes and washed in tap water to remove the excess crystal violet. The sections were stained in Grams iodine for 5 minutes and washed in tap water to remove the excess iodine. The slides were differentiated in acetone two times for a second and washed in tap water to remove acetone. The sections were placed in working basic Fuchsinf or 5 minutes and briefly washed in water. The sections were placed in Gallego's solution for 5 minutes and washed in tap water. After the sections were washed the sections were dipped three times in acetone, three times in Picric acid/acetone, three times in acetone, five times in half acetone/xylene, ten times in xylene and finally left for 1 minute in xylene. The sections were mounted in DPX. Gram-positive bacteria stained red and Gram-negative bacteria stain purple.

ELMAS (Elastic Masson Trichrome)

Table 31 Verhoeffs solution

Constituent	**Supplier**
10% Alcoholic Haem	
10% ferric chloride	
100% iodine	
100% Alcohol	Merck

All the constituents from Table 31 were added in equal quantities.

Table 32 Acid Fuchsin solution

Constituent	**Supplier**
0.5 g Acid Fuchsin	
0.5 ml glacial acetic acid	Sigma
100 ml double distiller water	

Table 33 Phosphomolybdic acid solution

Constituent	Supplier
1g phosphomolybdic acid	
100ml double distilled water	

Table 34 Light green solution

Constituent	Supplier
2% Light green	
1% acetic acid	Merck

The sections were mordanted in Bouins fixative for 20 minutes and washed in running water for 15 minutes. The sections were covered with Verhoeffs solution (Table 31) for 15 minutes and rinsed in water. The sections were differentiate in 2% ferric chloride until the excess black was removed, leaving only the elastin stained black. The sections were stained with Acid Fuchsin solution (Table 32) for 5 minutes and rinsed in water. The sections were stained in phosphomolybdic acid solution (Table 33) for 5 minutes and rinsed in water. The sections were lastly stained with Light green solution (Table 34) for 2 minutes and rinsed in water before mounting (see mount sections). The muscle tissue stained red, the collagen stained blue and the elastin stained black.

A22. Transmission electron microscopy

A22a Fixation of tissue

Cut the tissue in 2 x 2 x 2 mm and place the tissue in 2.5 % glutaraldehyde (prepared in 0.1 M PBS, pH 7.4 (Table 3)). The tissue was fixed overnight at 4°C or 1 to 4 hours at room temperature and after fixation the tissue was stored at least overnight in PBS at 4°C. The tissue was fixed in 2% osmium for 1 to 2 hours in the fume hood and rinsed with distilled water for 5 minutes.

A22b Sample preparation

The tissue was dehydrated in each of the ethanol solutions for 15 minutes. Firstly in 50% ethanol, 70% ethanol, 80% ethanol, 90% ethanol and then two times for 20

minutes in 100% ethanol. The tissue was then dehydrated twice in 100% acetone solutions for 20 minutes each.

Table 35 Spurr resin

Constituent	Supplier
10 g vinyl cyclohexene dioxide	Sigma
6 g digilycidyl ether	Sigma
26 g nonenyl succinic anhydride	Sigma
0.4 g dimethylaminoethanol	Sigma

The tissue was prepared for embedding in Spurr resin (Table 35) with different Spurr resin ratio solutions in acetone. The tissue was placed in each solution for a hour at room temperature. The ratio's (Spurr resin: Acetone) of the solutions were 1:2, 1:1 and 2:1. The last solution was 100% Spurr resin with two times for 1 hour at room temperature. The tissue was embedded in Spur resin in a mould and allowed to polymerise overnight at 70°C.

A22c Immuno-Gold labelling

Ultra thin sections were cut for gold labelling with an ultramicrotome using a diamond knife. The sections where cut 120 nm thin, stretched with choloform vapour and collected on 200 to 300 mesh nickel-coated grids. The sections were dried overnight before staining. All the solutions and buffers were filterer before use.

The sections were etched in saturated aqua solution of sodium metaperiodate for 20 minutes. The grids were washed in distilled water and drained. The grids were blocked with normal serum similar to the host species of the secondary antibody (gold-labelled) diluted 1:30 in PBS (Table 3) for 30 minutes.

Table 36 Washing buffer

Constituent	Supplier
PBS (Table 3)	
0.1% BSA	Sigma
0.01% Tween 20	Sigma
pH 8.2	

The grids were washed in washing buffer (Table 36) for 5 minutes and in distilled water. The grids were incubated in primary antibody optimally diluted overnight at 4°C. After incubation the grids were washed with PBS, pH 7.2 and were washed three times with washing buffer for 5 minutes. The grids were then incubated in the secondary goat anit-rabbit immunoglobulin conjugated with gold diluted 1:50 with the washing buffer for 1 to 2 hours at room temperature. After incubation the grids were washed in large quantities washing buffer, rinsed in PBS, pH 7.2 and then in distilled water. The grids were drained on filter paper and ready for counterstain.

Table 37 Uranyl acetate

Constituent	**Supplier**
2% uranyl acetate dihydrate	Sigma
50% ethanol	Sigma

Store the solution in a dark bottle at 4°C.

Table 38 Lead citrate

Constituent	**Supplier**
2.66 g lead nitrate	Sigma
3.52 g trisodium citrate	Sigma
60 ml distilled water	
16 ml of 10N sodium hydroxide (4 g in 100 ml distilled water)	Sigma
Make up to 100 ml with distilled water	

The solution was mixed and filtered before it was stored at 4°C.

The tissue was stained with uranyl acetate (Table 37) for 10 minutes and afterwards with lead citrate (Table 38) for 2 minutes. After staining the grid was immersed in a drop of 10% aqua glacial acetic acid for 1 minute and rinsed in distilled water. The grid was ready for viewing on the TEM.

12. Schoen FJ. Cardiac valves and valvular pathology: update on function, disease, repair, and replacement. *Cardiovasc Pathol.* 2005;14(4):189-194.

13. Rabkin-Aikawa E, Mayer JE, Jr., Schoen FJ. Heart valve regeneration. *Adv Biochem Eng Biotechnol.* 2005;94:141-179.

14. Pupello DF, Bessone LN, Hiro SP, Lopez-Cuenca E, Glatterer MS, Jr., Angell WW, Brock JC, Alkire MJ, Izzo EG, Sanabria G, et al. Bioprosthetic valve longevity in the elderly: an 18-year longitudinal study. *Ann Thorac Surg.* 1995;60(2 Suppl):S270-274; discussion S275.

15. Harken DE, Taylor WJ, Lefemine AA, Lunzer S, Low HB, Cohen ML, Jacobey JA. Aortic valve replacement with a caged ball valve. *Am J Cardiol.* 1962;9:292-299.

16. Starr A, Edwards ML. Mitral replacement: clinical experience with a ball-valve prosthesis. *Ann Surg.* 1961;154:726-740.

17. Ross DN. Homograft replacement of the aortic valve. *Lancet.* 1962;2:487.

18. Binet JP, Duran CG, Carpenter A, Langlois J. Heterologous aortic valve transplantation. *Lancet.* 1965;2(7425):1275.

19. Turina J, Hess OM, Turina M, Krayenbuehl HP. Cardiac bioprostheses in the 1990s. *Circulation.* 1993;88(2):775-781.

20. Gallo I, Nistal F, Blasquez R, Arbe E, Artinano E. Incidence of primary tissue valve failure in porcine bioprosthetic heart valves. *Ann Thorac Surg.* 1988;45(1):66-70.

21. Jamieson WR, Rosado LJ, Munro AI, Gerein AN, Burr LH, Miyagishima RT, Janusz MT, Tyers GF. Carpentier-Edwards standard porcine bioprosthesis: primary tissue failure (structural valve deterioration) by age groups. *Ann Thorac Surg.* 1988;46(2):155-162.

22. Horstkotte D. Prosthetic valves or tissue valves--a vote for mechanical prostheses. *Z Kardiol.* 1985;74 Suppl 6:19-37.

23. Vongpatanasin W, Hillis LD, Lange RA. Prosthetic heart valves. *N Engl J Med.* 1996;335(6):407-416.

24. Morsi YS, Birchall IE, Rosenfeldt FL. Artificial aortic valves: an overview. *Int J Artif Organs.* 2004;27(6):445-451.

25. Butany J, Fayet C, Ahluwalia MS, Blit P, Ahn C, Munroe C, Israel N, Cusimano RJ, Leask RL. Biological replacement heart valves. Identification and evaluation. *Cardiovasc Pathol.* 2003;12(3):119-139.

26. Butany J, Ahluwalia MS, Munroe C, Fayet C, Ahn C, Blit P, Kepron C, Cusimano RJ, Leask RL. Mechanical heart valve prostheses: identification and evaluation. *Cardiovasc Pathol.* 2003;12(1):1-22.

27. Hopkins R. From cadaver harvested homograft valves to tissue-engineered valve conduits. *Prog Ped Card.* 2006;21(2):137-152.

28. Rabkin E, Schoen FJ. Cardiovascular tissue engineering. *Cardiovasc Pathol.* 2002;11(6):305-317.

29. Sapirstein JS, Smith PK. The "ideal" replacement heart valve. *Am Heart J.* 2001;141(5):856-860.

30. Aslam AK, Aslam AF, Vasavada BC, Khan IA. Prosthetic heart valves: Types and echocardiographic evaluation. *Int J Cardiol.* 2007.

31. Nassar AH, Hobeika EM, Abd Essamad HM, Taher A, Khalil AM, Usta IM. Pregnancy outcome in women with prosthetic heart valves. *Am J Obstet Gynecol.* 2004;191(3):1009-1013.

32. Borger MA, Ivanov J, Armstrong S, Christie-Hrybinsky D, Feindel CM, David TE. Twenty-year results of the Hancock II bioprosthesis. *J Heart Valve Dis.* 2006;15(1):49-55; discussion 55-46.

33. Edwards TJ, Livesey SA, Simpson IA, Monro JL, Ross JK. Biological valves beyond fifteen years: the Wessex experience. *Ann Thorac Surg.* 1995;60(2 Suppl):S211-215.

34. Hammermeister K, Sethi GK, Henderson WG, Grover FL, Oprian C, Rahimtoola SH. Outcomes 15 years after valve replacement with a mechanical versus a

bioprosthetic valve: final report of the Veterans Affairs randomized trial. *J Am Coll Cardiol.* 2000;36(4):1152-1158.

35. Holper K, Wottke M, Lewe T, Baumer L, Meisner H, Paek SU, Sebening F. Bioprosthetic and mechanical valves in the elderly: benefits and risks. *Ann Thorac Surg.* 1995;60(2 Suppl):S443-446.

36. Dunn JM. Porcine valve durability in children. *Ann Thorac Surg.* 1981;32(4):357-368.

37. Kutsche LM, Oyer P, Shumway N, Baum D. An important complication of Hancock mitral valve replacement in children. *Circulation.* 1979;60(2 Pt 2):98-103.

38. Sanders SP, Levy RJ, Freed MD, Norwood WI, Castaneda AR. Use of Hancock porcine xenografts in children and adolescents. *Am J Cardiol.* 1980;46(3):429-438.

39. Fann JI, Miller DC, Moore KA, Mitchell RS, Oyer PE, Stinson EB, Robbins RC, Reitz BA, Shumway NE. Twenty-year clinical experience with porcine bioprostheses. *Ann Thorac Surg.* 1996;62(5):1301-1311; discussion 1311-1302.

40. Thandroyen FT, Whitton IN, Pirie D, Rogers MA, Mitha AS. Severe calcification of glutaraldehyde-preserved porcine xenografts in children. *Am J Cardiol.* 1980;45(3):690-696.

41. Ross DN. Homograft replacement of the aortic and mitral valves with a pulmonary autograft. *Lancet.* 1967:956-958.

42. Elkins RC, Knott-Craig CJ, Ward KE, Lane MM. The Ross operation in children: 10-year experience. *Ann Thorac Surg.* 1998;65(2):496-502.

43. Stelzer P, Weinrauch S, Tranbaugh RF. Ten years of experience with the modified Ross procedure. *J Thorac Cardiovasc Surg.* 1998;115(5):1091-1100.

44. Turrentine MW, Ruzmetov M, Vijay P, Bills RG, Brown JW. Biological versus mechanical aortic valve replacement in children. *Ann Thorac Surg.* 2001;71(5 Suppl):S356-360.

45. Bohm JO, Botha CA, Horke A, Hemmer W, Roser D, Blumenstock G, Uhlemann F, Rein JG. Is the Ross operation still an acceptable option in children and adolescents? *Ann Thorac Surg.* 2006;82(3):940-947.

46. Phillips JR. Long-term outcomes of the Ross operation in children and adults. *Progress in Pediatric Cardiology.* 2003;16(2):149-154.

47. Elkins RC, Lane MM, McCue C. Pulmonary autograft reoperation: incidence and management. *Ann Thorac Surg.* 1996;62(2):450-455.

48. Chambers JC, Somerville J, Stone S, Ross DN. Pulmonary autograft procedure for aortic valve disease: long-term results of the pioneer series. *Circulation.* 1997;96(7):2206-2214.

49. Elkins RC, Lane MM, McCue C. Ross operation in children: late results. *J Heart Valve Dis.* 2001;10(6):736-741.

50. Bohm JO, Botha CA, Hemmer W, Roser D, Starck CT, Blumenstock G, Rein JG. The ross operation in 225 patients: a five-year experience in aortic root replacement. *J Heart Valve Dis.* 2001;10(6):742-749.

51. Fischlein T, Schutz A, Haushofer M, Frey R, Uhlig A, Detter C, Reichart B. Immunologic reaction and viability of cryopreserved homografts. *Ann Thorac Surg.* 1995;60(2 Suppl):S122-125; discussion S125-126.

52. McGiffin DC, O'Brien MF, Stafford EG, Gardner MA, Pohlner PG. Long-term results of the viable cryopreserved allograft aortic valve: continuing evidence for superior valve durability. *J Card Surg.* 1988;3(3 Suppl):289-296.

53. O'Brien MF, McGiffin DC, Stafford EG, Gardner MA, Pohlner PF, McLachlan GJ, Gall K, Smith S, Murphy E. Allograft aortic valve replacement: long-term comparative clinical analysis of the viable cryopreserved and antibiotic 4 degrees C stored valves. *J Card Surg.* 1991;6(4 Suppl):534-543.

54. O'Brien MF, Stafford EG, Gardner MA, Pohlner PG, McGiffin DC. A comparison of aortic valve replacement with viable cryopreserved and fresh allograft valves, with a note on chromosomal studies. *J Thorac Cardiovasc Surg.* 1987;94(6):812-823.

55. Baskett RJ, Nanton MA, Warren AE, Ross DB. Human leukocyte antigen-DR and ABO mismatch are associated with accelerated homograft valve failure in children: implications for therapeutic interventions. *J Thorac Cardiovasc Surg.* 2003;126(1):232-239.

56. Hawkins JA, Hillman ND, Lambert LM, Jones J, Di Russo GB, Profaizer T, Fuller TC, Minich LL, Williams RV, Shaddy RE. Immunogenicity of decellularized cryopreserved allografts in pediatric cardiac surgery: comparison with standard cryopreserved allografts. *J Thorac Cardiovasc Surg.* 2003;126(1):247-252; discussion 252-243.

57. Hogan P, Duplock L, Green M, Smith S, Gall KL, Frazer IH, O'Brien MF. Human aortic valve allografts elicit a donor-specific immune response. *J Thorac Cardiovasc Surg.* 1996;112(5):1260-1266; discussion 1266-1267.

58. Rajani B, Mee RB, Ratliff NB. Evidence for rejection of homograft cardiac valves in infants. *J Thorac Cardiovasc Surg.* 1998;115(1):111-117.

59. Shaddy RE, Hunter DD, Osborn KA, Lambert LM, Minich LL, Hawkins JA, McGough EC, Fuller TC. Prospective analysis of HLA immunogenicity of cryopreserved valved allografts used in pediatric heart surgery. *Circulation.* 1996;94(5):1063-1067.

60. Hoekstra FM, Witvliet M, Knoop CY, Wassenaar C, Bogers AJ, Weimar W, Claas FH. Immunogenic human leukocyte antigen class II antigens on human cardiac valves induce specific alloantibodies. *Ann Thorac Surg.* 1998;66(6):2022-2026.

61. Lang SJ, Giordano MS, Cardon-Cardo C, Summers BD, Staiano-Coico L, Hajjar DP. Biochemical and cellular characterization of cardiac valve tissue after cryopreservation or antibiotic preservation. *J Thorac Cardiovasc Surg.* 1994;108(1):63-67.

62. O'Brien MF, Stafford G, Gardner M, Pohlner P, McGiffin D, Johnston N, Brosnan A, Duffy P. The viable cryopreserved allograft aortic valve. *J Card Surg.* 1987;2(1 Suppl):153-167.

63. Hoekstra F, Knoop C, Aghai Z, Jutte N, Mochtar B, Bos E, Weimar W. Stimulation of immune-competent cells in vitro by human cardiac valve-derived

endothelial cells. *Ann Thorac Surg.* 1995;60(2 Suppl):S131-133; discussion S133-134.

64. Oei FB, Stegmann AP, van der Ham F, Zondervan PE, Vaessen LM, Baan CC, Weimar W, Bogers AJ. The presence of immune stimulatory cells in fresh and cryopreserved donor aortic and pulmonary valve allografts. *J Heart Valve Dis.* 2002;11(3):315-324; discussion 325.

65. Salomon RN, Friedman GB, Callow AD, Payne DD, Libby P. Cryopreserved aortic homografts contain viable smooth muscle cells capable of expressing transplantation antigens. *J Thorac Cardiovasc Surg.* 1993;106(6):1173-1180.

66. Christenson JT, Vala D, Sierra J, Beghetti M, Kalangos A. Blood group incompatibility and accelerated homograft fibrocalcifications. *J Thorac Cardiovasc Surg.* 2004;127(1):242-250.

67. Abd-Elfattah AS, Messier RH, Jr., Domkowski PW, Jones JL, Aly HM, Crescenzo DG, Wallace RB, Hopkins RA. Inhibition of adenosine deaminase and nucleoside transport. Utility in a model of homograft cardiac valve preimplantation processing. *J Thorac Cardiovasc Surg.* 1993;105(6):1095-1105.

68. Messier RH, Jr., Domkowski PW, Aly HM, Abd-Elfattah AS, Crescenzo DG, Wallace RB, Hopkins RA. High energy phosphate depletion in leaflet matrix cells during processing of cryopreserved cardiac valves. *J Surg Res.* 1992;52(5):483-488.

69. Tavakkol Z, Gelehrter S, Goldberg CS, Bove EL, Devaney EJ, Ohye RG. Superior durability of SynerGraft pulmonary allografts compared with standard cryopreserved allografts. *Ann Thorac Surg.* 2005;80(5):1610-1614.

70. Cheung DT, Nimni ME. Mechanism of crosslinking of proteins by glutaraldehyde II. Reaction with monomeric and polymeric collagen. *Connect Tissue Res.* 1982;10(2):201-216.

71. Okamura K, Chiba C, Iriyama T, Itoh T, Maeta H, Ijima H, Mitsui T, Hori M. Antigen depressant effect of glutaraldehyde for aortic heterografts with a valve, with special reference to a concentration right fit for the preservation of grafts. *Surgery.* 1980;87(2):170-176.

72. Villa ML, De Biasi S, Pilotto F. Residual heteroantigenicity of glutaraldehyde-treated porcine cardiac valves. *Tissue Antigens.* 1980;16(1):62-69.

73. Dahm M, Husmann M, Eckhard M, Prufer D, Groh E, Oelert H. Relevance of immunologic reactions for tissue failure of bioprosthetic heart valves. *Ann Thorac Surg.* 1995;60(2 Suppl):S348-352.

74. Jayakrishnan A, Jameela SR. Glutaraldehyde as a fixative in bioprostheses and drug delivery matrices. *Biomaterials.* 1996;17(5):471-484.

75. Ionescu MI, Pakrashi BC, Holden MP, Mary DA, Wooler GH. Results of aortic valve replacement with frame-supported fascia lata and pericardial grafts. *J Thorac Cardiovasc Surg.* 1972;64(3):340-353.

76. Golomb G, Schoen FJ, Smith MS, Linden J, Dixon M, Levy RJ. The role of glutaraldehyde-induced cross-links in calcification of bovine pericardium used in cardiac valve bioprostheses. *Am J Pathol.* 1987;127(1):122-130.

77. Schoen FJ, Tsao JW, Levy RJ. Calcification of bovine pericardium used in cardiac valve bioprostheses. Implications for the mechanisms of bioprosthetic tissue mineralization. *Am J Pathol.* 1986;123(1):134-145.

78. David TE, Ropchan GC, Butany JW. Aortic valve replacement with stentless porcine bioprostheses. *J Card Surg.* 1988;3(4):501-505.

79. David TE, Pollick C, Bos J. Aortic valve replacement with stentless porcine aortic bioprosthesis. *J Thorac Cardiovasc Surg.* 1990;99(1):113-118.

80. David TE, Feindel CM, Scully HE, Bos J, Rakowski H. Aortic valve replacement with stentless porcine aortic valves: a ten-year experience. *J Heart Valve Dis.* 1998;7(3):250-254.

81. Reul GJ, Jr., Cooley DA, Duncan JM, Frazier OH, Hallman GL, Livesay JJ, Ott DA, Walker WE. Valve failure with the Ionescu-Shiley bovine pericardial bioprosthesis: analysis of 2680 patients. *J Vasc Surg.* 1985;2(1):192-204.

82. Teoh KH, Ivanov J, Weisel RD, Darcel IC, Rakowski H. Survival and bioprosthetic valve failure. Ten-year follow-up. *Circulation.* 1989;80(3 Pt 1):I8-15.

83. Vesely I, Boughner D, Song T. Tissue buckling as a mechanism of bioprosthetic valve failure. *Ann Thorac Surg.* 1988;46(3):302-308.

84. Bortolotti U, Milano A, Mossuto E, Mazzaro E, Thiene G, Casarotto D. Porcine valve durability: a comparison between Hancock standard and Hancock II bioprostheses. *Ann Thorac Surg.* 1995;60(2 Suppl):S216-220.

85. Ruel M, Kulik A, Rubens FD, Bedard P, Masters RG, Pipe AL, Mesana TG. Late incidence and determinants of reoperation in patients with prosthetic heart valves. *Eur J Cardiothorac Surg.* 2004;25(3):364-370.

86. Vesely I, Barber JE, Ratliff NB. Tissue damage and calcification may be independent mechanisms of bioprosthetic heart valve failure. *J Heart Valve Dis.* 2001;10(4):471-477.

87. Carpentier A, Lemaigre G, Robert L, Carpentier S, Dubost C. Biological factors affecting long-term results of valvular heterografts. *J Thorac Cardiovasc Surg.* 1969;58(4):467-483.

88. Milano A, Bortolotti U, Talenti E, Valfre C, Arbustini E, Valente M, Mazzucco A, Gallucci V, Thiene G. Calcific degeneration as the main cause of porcine bioprosthetic valve failure. *Am J Cardiol.* 1984;53(8):1066-1070.

89. Thiene G, Bortolotti U, Valente M, Milano A, Calabrese F, Talenti E, Mazzucco A, Gallucci V. Mode of failure of the Hancock pericardial valve xenograft. *Am J Cardiol.* 1989;63(1):129-133.

90. Jamieson WR, Janusz MT, Burr LH, Ling H, Miyagishima RT, Germann E. Carpentier-Edwards supraannular porcine bioprosthesis: second-generation prosthesis in aortic valve replacement. *Ann Thorac Surg.* 2001;71(5 Suppl):S224-227.

91. Butany J, Leong SW, Cunningham KS, D'Cruz G, Carmichael K, Yau TM. A 10-year comparison of explanted Hancock-II and Carpentier-Edwards supraannular bioprostheses. *Cardiovasc Pathol.* 2007;16(1):4-13.

92. Schoen FJ, Hobson CE. Anatomic analysis of removed prosthetic heart valves: causes of failure of 33 mechanical valves and 58 bioprostheses, 1980 to 1983. *Hum Pathol.* 1985;16(6):549-559.

93. Butany J, Leask R. The failure modes of biological prosthetic heart valves. *J Long Term Eff Med Implants.* 2001;11(3-4):115-135.

94. Manji RA, Zhu LF, Nijjar NK, Rayner DC, Korbutt GS, Churchill TA, Rajotte RV, Koshal A, Ross DB. Glutaraldehyde-fixed bioprosthetic heart valve conduits calcify and fail from xenograft rejection. *Circulation.* 2006;114(4):318-327.

95. Schoen FJ, Levy RJ. Calcification of tissue heart valve substitutes: progress toward understanding and prevention. *Ann Thorac Surg.* 2005;79(3):1072-1080.

96. Schoen FJ, Levy RJ, Nelson AC, Bernhard WF, Nashef A, Hawley M. Onset and progression of experimental bioprosthetic heart valve calcification. *Lab Invest.* 1985;52(5):523-532.

97. Simionescu DT. Prevention of calcification in bioprosthetic heart valves: challenges and perspectives. *Expert Opin Biol Ther.* 2004;4(12):1971-1985.

98. Bailey MT, Pillarisetti S, Xiao H, Vyavahare NR. Role of elastin in pathologic calcification of xenograft heart valves. *J Biomed Mater Res A.* 2003;66(1):93-102.

99. Schoen FJ, Hirsch D, Bianco RW, Levy RJ. Onset and progression of calcification in porcine aortic bioprosthetic valves implanted as orthotopic mitral valve replacements in juvenile sheep. *J Thorac Cardiovasc Surg.* 1994;108(5):880-887.

100. Kim KM. Cellular mechanism of calcification and its prevention in glutaraldehyde treated vascular tissue. *Z Kardiol.* 2001;90 Suppl 3:99-105.

101. Valente M, Bortolotti U, Thiene G. Ultrastructural substrates of dystrophic calcification in porcine bioprosthetic valve failure. *Am J Pathol.* 1985;119(1):12-21.

102. Schoen FJ, Levy RJ. Heart valve bioprostheses: antimineralization. *Eur J Cardiothorac Surg.* 1992;6 Suppl 1:S91-93; discussion S94.

103. Vyavahare PNR, Chen PW, Joshi PRR, Lee PC-H, Hirsch PD, Levy PJ, Schoen MDPFJ, Levy MDRJ. Current Progress in Anticalcification for Bioprosthetic and Polymeric Heart Valves. *Cardiovascular Pathology.* 1997;6(4):219-229.

104. Canet D, Forge V, Guillain F, Mintz E. Ca2+ translocation across sarcoplasmic reticulum ATPase randomizes the two transported ions. *J Biol Chem.* Vol 271. UNITED STATES; 1996:20566-20572.

105. Mintz E, Guillain F. Ca2+ transport by the sarcoplasmic reticulum ATPase. *Biochim Biophys Acta.* Vol 1318. NETHERLANDS; 1997:52-70.

106. Nimni ME, Myers D, Ertl D, Han B. Factors which affect the calcification of tissue-derived bioprostheses. *J Biomed Mater Res.* 1997;35(4):531-537.

107. Cunanan CM, Cabiling CM, Dinh TT, Shen SH, Tran-Hata P, Rutledge JH, 3rd, Fishbein MC. Tissue characterization and calcification potential of commercial bioprosthetic heart valves. *Ann Thorac Surg.* 2001;71(5 Suppl):S417-421.

108. Riddle JM, Magilligan DJ, Jr., Stein PD. Surface morphology of degenerated porcine bioprosthetic valves four to seven years following implantation. *J Thorac Cardiovasc Surg.* 1981;81(2):279-287.

109. Trantina-Yates AE, Human P, Bracher M, Zilla P. Mitigation of bioprosthetic heart valve degeneration through biocompatibility: in vitro versus spontaneous endothelialization. *Biomaterials.* 2001;22(13):1837-1846.

110. Bernacca GM, Gibson SA, Wilkinson R, Wheatley DJ. Confocal laser scanning microscopy of calcified bioprosthetic heart valves. *J Heart Valve Dis.* 1994;3(2):205-211.

111. Golomb G, Ezra V. Prevention of bioprosthetic heart valve tissue calcification by charge modification: effects of protamine binding by formaldehyde. *J Biomed Mater Res.* 1991;25(1):85-98.

112. Anderson HC. Mineralization by matrix vesicles. *Scan Electron Microsc.* 1984(Pt 2):953-964.

113. Levy RJ, Schoen FJ, Sherman FS, Nichols J, Hawley MA, Lund SA. Calcification of subcutaneously implanted type I collagen sponges. Effects of formaldehyde and glutaraldehyde pretreatments. *Am J Pathol.* 1986;122(1):71-82.

114. Vincentelli A, Latremouille C, Zegdi R, Shen M, Lajos PS, Chachques JC, Fabiani JN. Does glutaraldehyde induce calcification of bioprosthetic tissues? *Ann Thorac Surg.* 1998;66(6 Suppl):S255-258.

115. Simionescu DT, Lovekamp JJ, Vyavahare NR. Extracellular matrix degrading enzymes are active in porcine stentless aortic bioprosthetic heart valves. *J Biomed Mater Res A.* 2003;66(4):755-763.

116. Webb CL, Nguyen NM, Schoen FJ, Levy RJ. Calcification of allograft aortic wall in a rat subdermal model. Pathophysiology and inhibition by Al3+ and aminodiphosphonate preincubations. *Am J Pathol.* 1992;141(2):487-496.

117. Vyavahare N, Ogle M, Schoen FJ, Levy RJ. Elastin calcification and its prevention with aluminum chloride pretreatment. *Am J Pathol.* 1999;155(3):973-982.

118. Isenburg JC, Simionescu DT, Vyavahare NR. Elastin stabilization in cardiovascular implants: improved resistance to enzymatic degradation by treatment with tannic acid. *Biomaterials.* 2004;25(16):3293-3302.

119. Hance KA, Tataria M, Ziporin SJ, Lee JK, Thompson RW. Monocyte chemotactic activity in human abdominal aortic aneurysms: role of elastin degradation peptides and the 67-kD cell surface elastin receptor. *J Vasc Surg.* 2002;35(2):254-261.

120. Mochizuki S, Brassart B, Hinek A. Signaling pathways transduced through the elastin receptor facilitate proliferation of arterial smooth muscle cells. *J Biol Chem.* 2002;277(47):44854-44863.

121. Vyavahare N, Jones PL, Tallapragada S, Levy RJ. Inhibition of matrix metalloproteinase activity attenuates tenascin-C production and calcification of implanted purified elastin in rats. *Am J Pathol.* 2000;157(3):885-893.

122. Lee JS, Basalyga DM, Simionescu A, Isenburg JC, Simionescu DT, Vyavahare NR. Elastin calcification in the rat subdermal model is accompanied by

up-regulation of degradative and osteogenic cellular responses. *Am J Pathol.* 2006;168(2):490-498.

123. Simionescu D, Iozzo RV, Kefalides NA. Bovine pericardial proteoglycan: biochemical, immunochemical and ultrastructural studies. *Matrix.* 1989;9(4):301-310.

124. Hunter GK. Role of proteoglycan in the provisional calcification of cartilage. A review and reinterpretation. *Clin Orthop Relat Res.* 1991(262):256-280.

125. Chen CC, Boskey AL. The effects of proteoglycans from different cartilage types on in vitro hydroxyapatite proliferation. *Calcif Tissue Int.* 1986;39(5):324-327.

126. Simionescu DT, Lovekamp JJ, Vyavahare NR. Glycosaminoglycan-degrading enzymes in porcine aortic heart valves: implications for bioprosthetic heart valve degeneration. *J Heart Valve Dis.* 2003;12(2):217-225.

127. Hynes RO, Yamada KM. Fibronectins. Multifunctional modular glycoproteins. *J. Cell Biol. .* 1982;95:369 - 377.

128. Potts JR, Campbell ID. Structure and function of fibronectin modules. *Matrix Biol.* 1996;15(5):313-320; discussion 321.

129. Romberger DJ. Fibronectin. *Int J Biochem Cell Biol.* 1997;29(7):939-943.

130. Ingram RT, Clarke BL, Fisher LW, Fitzpatrick LA. Distribution of noncollagenous proteins in the matrix of adult human bone: evidence of anatomic and functional heterogeneity. *J Bone Miner Res.* 1993;8(9):1019-1029.

131. Gura TA, Wright KL, Veis A, Webb CL. Identification of specific calcium-binding noncollagenous proteins associated with glutaraldehyde-preserved bovine pericardium in the rat subdermal model. *J Biomed Mater Res.* 1997;35(4):483-495.

132. Shen M, Marie P, Farge D, Carpentier S, De Pollak C, Hott M, Chen L, Martinet B, Carpentier A. Osteopontin is associated with bioprosthetic heart valve calcification in humans. *C R Acad Sci III.* 1997;320(1):49-57.

133. Srivatsa SS, Harrity PJ, Maercklein PB, Kleppe L, Veinot J, Edwards WD, Johnson CM, Fitzpatrick LA. Increased cellular expression of matrix proteins that

regulate mineralization is associated with calcification of native human and porcine xenograft bioprosthetic heart valves. *J Clin Invest.* 1997;99(5):996-1009.

134. Steitz SA, Speer MY, McKee MD, Liaw L, Almeida M, Yang H, Giachelli CM. Osteopontin inhibits mineral deposition and promotes regression of ectopic calcification. *Am J Pathol.* 2002;161(6):2035-2046.

135. O'Brien ER, Garvin MR, Stewart DK, Hinohara T, Simpson JB, Schwartz SM, Giachelli CM. Osteopontin is synthesized by macrophage, smooth muscle, and endothelial cells in primary and restenotic human coronary atherosclerotic plaques. *Arterioscler Thromb.* 1994;14(10):1648-1656.

136. Grabenwoger M, Sider J, Fitzal F, Zelenka C, Windberger U, Grimm M, Moritz A, Bock P, Wolner E. Impact of glutaraldehyde on calcification of pericardial bioprosthetic heart valve material. *Ann Thorac Surg.* 1996;62(3):772-777.

137. Gong G, Ling Z, Seifter E, Factor SM, Frater RW. Aldehyde tanning: the villain in bioprosthetic calcification. *Eur J Cardiothorac Surg.* 1991;5(6):288-299; discussion 293.

138. Levy RJ, Schoen FJ, Levy JT, Nelson AC, Howard SL, Oshry LJ. Biologic determinants of dystrophic calcification and osteocalcin deposition in glutaraldehyde-preserved porcine aortic valve leaflets implanted subcutaneously in rats. *Am J Pathol.* 1983;113(2):143-155.

139. Kim KM, Herrera GA, Battarbee HD. Role of glutaraldehyde in calcification of porcine aortic valve fibroblasts. *Am J Pathol.* 1999;154(3):843-852.

140. Maranto AR, Schoen FJ. Effect of delay between tissue harvest and glutaraldehyde pretreatment on mineralization of bovine pericardium used in bioprosthetic heart valves. *J Biomed Mater Res.* 1988;22(9):819-825.

141. Zilla P, Weissenstein C, Bracher M, Zhang Y, Koen W, Human P, von Oppell U. High glutaraldehyde concentrations reduce rather than increase the calcification of aortic wall tissue. *J Heart Valve Dis.* 1997;6(5):502-509.

142. Huang-Lee LL, Cheung DT, Nimni ME. Biochemical changes and cytotoxicity associated with the degradation of polymeric glutaraldehyde derived crosslinks. *J Biomed Mater Res.* 1990;24(9):1185-1201.

143. Grabenwoger M, Grimm M, Eybl E, Leukauf C, M¸ller MM, Plenck H, Jr., B^ck P. Decreased tissue reaction to bioprosthetic heart valve material after L-glutamic acid treatment. A morphological study. *J Biomed Mater Res.* 1992;26(9):1231-1240.

144. Zilla P, Weissenstein C, Human P, Dower T, von Oppell UO. High glutaraldehyde concentrations mitigate bioprosthetic root calcification in the sheep model. *Ann Thorac Surg.* 2000;70(6):2091-2095.

145. Zilla P, Zhang Y, Human P, Koen W, von Oppell U. Improved ultrastructural preservation of bioprosthetic tissue. *J Heart Valve Dis.* 1997;6(5):492-501.

146. Dower T, Adler U, Davids L, Zilla P. Increasing cross-linking efficiency mitigates macrophage activation on bioprosthetic tissue. *Cardiovasc Pathol.* 1998;7:295.

147. Human P, Bracher M, Zilla P. The immune response to bioprosthetic tissue - influence of cross-link density. *Cardiovasc Pathol.* 1998;7:334.

148. Silver MM, Pollock J, Silver MD, Williams WG, Trusler GA. Calcification in porcine xenograft valves in children. *Am J Cardiol.* 1980;45(3):685-689.

149. Root AW, Harrison HE. Recent advances in calcium metabolism. I. Mechanisms of calcium homeostasis. *J Pediatr.* 1976;88(1):1-18.

150. Kuzela DC, Huffer WE, Conger JD, Winter SD, Hammond WS. Soft tissue calcification in chronic dialysis patients. *Am J Pathol.* 1977;86(2):403-424.

151. Carpentier SM, Monier MH, Shen M, Carpentier AF. Do donor or recipient species influence calcification of bioprosthetic tissues? *Ann Thorac Surg.* 1995;60(2 Suppl):S328-330; discussion S330-321.

152. Dahm M, Lyman WD, Schwell AB, Factor SM, Frater RW. Immunogenicity of glutaraldehyde-tanned bovine pericardium. *J Thorac Cardiovasc Surg.* 1990;99(6):1082-1090.

153. Nimni ME, Cheung D, Strates B, Kodama M, Sheikh K. Chemically modified collagen: a natural biomaterial for tissue replacement. *J Biomed Mater Res.* 1987;21(6):741-771.

154. Salgaller ML, Bajpai PK. Immunogenicity of glutaraldehyde-treated bovine pericardial tissue xenografts in rabbits. *J Biomed Mater Res.* 1985;19(1):1-12.

155. Chen R, Duncan JM, Nihill M, Cooley DA. Early degeneration of porcine xenograft valves in pediatric patients who have undergone apico-aortic bypass. *Tex Heart Inst J.* 1982;9(1):41-47.

156. Spray TL, Roberts WC. Structural changes in porcine xenografts used as substitute cardiac valves. Gross and histologic observations in 51 glutaraldehyde-preserved Hancock valves in 41 patients. *Am J Cardiol.* 1977;40(3):319-330.

157. Rocchini AP, Weesner KM, Heidelberger K, Keren D, Behrendt D, Rosenthal A. Porcine xenograft valve failure in children: an immunologic response. *Circulation.* 1981;64(2 Pt 2):II162-171.

158. Levy RJ, Schoen FJ, Howard SL. Mechanism of calcification of porcine bioprosthetic aortic valve cusps: role of T-lymphocytes. *Am J Cardiol.* 1983;52(5):629-631.

159. Liao K, Frater RW, LaPietra A, Ciuffo G, Ilardi CF, Seifter E. Time-dependent effect of glutaraldehyde on the tendency to calcify of both autografts and xenografts. *Ann Thorac Surg.* 1995;60(2 Suppl):S343-347.

160. Magilligan DJ, Jr., Lewis JW, Jr., Heinzerling RH, Smith D. Fate of a second porcine bioprosthetic valve. *J Thorac Cardiovasc Surg.* 1983;85(3):362-370.

161. Human P, Zilla P. Characterization of the immune response to valve bioprostheses and its role in primary tissue failure. *Ann Thorac Surg.* 2001;71(5 Suppl):S385-388.

162. Stein PD, Wang CH, Riddle JM, Magilligan DJ, Jr. Leukocytes, platelets, and surface microstructure of spontaneously degenerated porcine bioprosthetic valves. *J Card Surg.* 1988;3(3):253-261.

163. Eishi K, Ishibashi-Ueda H, Nakano K, Kosakai Y, Sasako Y, Kobayashi J, Yutani C. Calcific degeneration of bioprosthetic aortic valves in patients receiving steroid therapy. *J Heart Valve Dis.* 1996;5(6):668-672.

164. Ferrans VJ, Boyce SW, Billingham ME, Jones M, Ishihara T, Roberts WC. Calcific deposits in porcine bioprostheses: structure and pathogenesis. *Am J Cardiol.* 1980;46(5):721-734.

165. Ishihara T, Ferrans VJ, Boyce SW, Jones M, Roberts WC. Structure and classification of cuspal tears and perforations in porcine bioprosthetic cardiac valves implanted in patients. *Am J Cardiol.* 1981;48(4):665-678.

166. Thubrikar MJ, Deck JD, Aouad J, Nolan SP. Role of mechanical stress in calcification of aortic bioprosthetic valves. *J Thorac Cardiovasc Surg.* 1983;86(1):115-125.

167. Sabbah HN, Hamid MS, Stein PD. Mechanical stresses on closed cusps of porcine bioprosthetic valves: correlation with sites of calcification. *Ann Thorac Surg.* 1986;42(1):93-96.

168. Nimni ME, Ertl D, Villanueva J, Nimni BS. Inhibition of ectopic calcification of glutaraldehyde crosslinked collagen and collagenous tissues by a covalently bound diphosphonate (APD). *Am J Cardiovasc Pathol.* 1990;3(3):237-245.

169. Gasser AB, Fleisch H. The influence of a diphosphonate on calcium metabolism in rats. *Calcif Tissue Res.* 1970:Suppl:96-97.

170. Levy RJ, Hawley MA, Schoen FJ, Lund SA, Liu PY. Inhibition by diphosphonate compounds of calcification of porcine bioprosthetic heart valve cusps implanted subcutaneously in rats. *Circulation.* 1985;71(2):349-356.

171. Levy RJ, Schoen FJ, Flowers WB, Staelin ST. Initiation of mineralization in bioprosthetic heart valves: studies of alkaline phosphatase activity and its inhibition by AlCl3 or FeCl3 preincubations. *J Biomed Mater Res.* 1991;25(8):905-935.

172. Webb CL, Schoen FJ, Flowers WE, Alfrey AC, Horton C, Levy RJ. Inhibition of mineralization of glutaraldehyde-pretreated bovine pericardium by AlCl3.

Mechanisms and comparisons with FeCl3, LaCl3, and Ga(NO3)3 in rat subdermal model studies. *Am J Pathol.* 1991;138(4):971-981.

173. Pathak YV, Boyd J, Levy RJ, Schoen FJ. Prevention of calcification of glutaraldehyde pretreated bovine pericardium through controlled release polymeric implants: studies of Fe3+, Al3+, protamine sulphate and levamisole. *Biomaterials.* 1990;11(9):718-723.

174. Bailey M, Xiao H, Ogle M, Vyavahare N. Aluminum chloride pretreatment of elastin inhibits elastolysis by matrix metalloproteinases and leads to inhibition of elastin-oriented calcification. *Am J Pathol.* 2001;159(6):1981-1986.

175. Clark JN, Ogle MF, Ashworth P, Bianco RW, Levy RJ. Prevention of calcification of bioprosthetic heart valve cusp and aortic wall with ethanol and aluminum chloride. *Ann Thorac Surg.* 2005;79(3):897-904.

176. Hirsch D, Drader J, Thomas TJ, Schoen FJ, Levy JT, Levy RJ. Inhibition of calcification of glutaraldehyde pretreated porcine aortic valve cusps with sodium dodecyl sulfate: preincubation and controlled release studies. *J Biomed Mater Res.* 1993;27(12):1477-1484.

177. Flameng W, Meuris B, Yperman J, De Visscher G, Herijgers P, Verbeken E. Factors influencing calcification of cardiac bioprostheses in adolescent sheep. *J Thorac Cardiovasc Surg.* 2006;132(1):89-98.

178. Jones M, Eidbo EE, Hilbert SL, Ferrans VJ, Clark RE. Anticalcification treatments of bioprosthetic heart valves: in vivo studies in sheep. *J Card Surg.* 1989;4(1):69-73.

179. Lee CH, Vyavahare N, Zand R, Kruth H, Schoen FJ, Bianco R, Levy RJ. Inhibition of aortic wall calcification in bioprosthetic heart valves by ethanol pretreatment: biochemical and biophysical mechanisms. *J Biomed Mater Res.* 1998;42(1):30-37.

180. Vyavahare N, Hirsch D, Lerner E, Baskin JZ, Schoen FJ, Bianco R, Kruth HS, Zand R, Levy RJ. Prevention of bioprosthetic heart valve calcification by ethanol preincubation. Efficacy and mechanisms. *Circulation.* 1997;95(2):479-488.

181. Isenburg JC, Simionescu DT, Vyavahare NR. Tannic acid treatment enhances biostability and reduces calcification of glutaraldehyde fixed aortic wall. *Biomaterials.* 2005;26(11):1237-1245.

182. Human P, Bezuidenhout D, Torrianni M, Hendriks M, Zilla P. Optimization of diamine bridges in glutaraldehyde treated bioprosthetic aortic wall tissue. *Biomaterials.* 2002;23(10):2099-2103.

183. Jee KS, Kim YS, Park KD, Kim YH. A novel chemical modification of bioprosthetic tissues using L-arginine. *Biomaterials.* 2003;24(20):3409-3416.

184. Weissenstein C, Human P, Bezuidenhout D, Zilla P. Glutaraldehyde detoxification in addition to enhanced amine cross-linking dramatically reduces bioprosthetic tissue calcification in the rat model. *J Heart Valve Dis.* 2000;9(2):230-240.

185. Zilla P, Fullard L, Trescony P, Meinhart J, Bezuidenhout D, Gorlitzer M, Human P, von Oppell U. Glutaraldehyde detoxification of aortic wall tissue: a promising perspective for emerging bioprosthetic valve concepts. *J Heart Valve Dis.* 1997;6(5):510-520.

186. Chen W, Schoen FJ, Levy RJ. Mechanism of efficacy of 2-amino oleic acid for inhibition of calcification of glutaraldehyde-pretreated porcine bioprosthetic heart valves. *Circulation.* 1994;90(1):323-329.

187. Chen W, Kim JD, Schoen FJ, Levy RJ. Effect of 2-amino oleic acid exposure conditions on the inhibition of calcification of glutaraldehyde cross-linked porcine aortic valves. *J Biomed Mater Res.* 1994;28(12):1485-1495.

188. Girardot MN, Torrianni M, Girardot JM. Effect of AOA on glutaraldehyde-fixed bioprosthetic heart valve cusps and walls: binding and calcification studies. *Int J Artif Organs.* 1994;17(2):76-82.

189. Fyfe BS, Schoen FJ. Pathological analysis of nonstented Freestyle aortic root bioprostheses treated with amino oleic acid. *Semin Thorac Cardiovasc Surg.* 1999;11(4 Suppl 1):151-156.

190. Fradet G, Bleese N, Busse E, Jamieson E, Raudkivi P, Goldstein J, Metras J. The mosaic valve clinical performance at seven years: results from a multicenter prospective clinical trial. *J Heart Valve Dis.* 2004;13(2):239-246; discussion 246-237.

191. Bach DS, Kon ND, Dumesnil JG, Sintek CF, Doty DB. Ten-Year Outcome After Aortic Valve Replacement with the Freestyle Stentless Bioprosthesis. *The Annals of Thoracic Surgery.* 2005;80(2):480-487.

192. Butany J, Collins MJ, Nair V, Leask RL, Scully HE, Williams WG, David TE. Morphological findings in explanted Toronto stentless porcine valves. *Cardiovasc Pathol.* 2006;15(1):41-48.

193. Carrier M, Pellerin M, Perrault LP, Page P, Hebert Y, Cartier R, Dyrda I, Pelletier LC. Aortic valve replacement with mechanical and biologic prosthesis in middle-aged patients. *Ann Thorac Surg.* 2001;71(5 Suppl):S253-256.

194. David TE, Armstrong S, Sun Z. The Hancock II bioprosthesis at ten years. *Ann Thorac Surg.* 1995;60(2 Suppl):S229-234.

195. Aderem A, Underhill DM. Mechanisms of phagocytosis in macrophages. *Ann Rev Immunol.* 1999;17(1):593-623.

196. Lee WL, Harrison RE, Grinstein S. Phagocytosis by neutrophils. *Microb Infect.* 2003;5(14):1299-1306.

197. Watts C, Amigorena S. Phagocytosis and antigen presentation. *Semin Immunol.* 2001;13(6):373-379.

198. Anderson JM, Rodriguez A, Chang DT. Foreign body reaction to biomaterials. *Semin Immunol.* 2008;20(2):86-100.

199. Henson PM. The Immunologic Release of Constituents from Neutrophil Leukocytes: II. Mechanisms of Release During Phagocytosis, and Adherence to Nonphagocytosable Surfaces. *J Immunol.* 1971;107(6):1547-1557.

200. Henson PM. Mechanisms of exocytosis in phagocytic inflammatory cells. Parke-Davis Award Lecture. *Am J Pathol.* 1980;101(3):494-511.

201. Logan MR, Odemuyiwa SO, Moqbel R. Understanding exocytosis in immune and inflammatory cells: The molecular basis of mediator secretion. *J All Clin Immunol.* 2003;111(5):923-932.

202. Butany J, Zhou T, Leong SW, Cunningham KS, Thangaroopan M, Jeggatheeswaran A, Feindel C, David TE. Inflammation and infection in nine surgically explanted Medtronic Freestyle stentless aortic valves. *Cardiovasc Pathol.* 2007;16(5):258-267.

203. Chen RH, Kadner A, Mitchell RN, Adams DH. Fresh porcine cardiac valves are not rejected in primates. *J Thorac Cardiovasc Surg.* 2000;119(6):1216-1220.

204. Konakci KZ, Bohle B, Blumer R, Hoetzenecker W, Roth G, Moser B, Boltz-Nitulescu G, Gorlitzer M, Klepetko W, Wolner E, Ankersmit HJ. Alpha-Gal on bioprostheses: xenograft immune response in cardiac surgery. *European Journal of Clinical Investigation.* 2005;35(1):17-23.

205. Daeron M. Fc receptor biology. *Ann Rev Immunol.* 1997;15(1):203-234.

206. Trantina-Yates A, Weissenstein C, Human P, Zilla P. Stentless bioprosthetic heart valve research: sheep versus primate model. *Ann Thorac Surg.* 2001;71(5 Suppl):S422-427.

207. Abolhoda A, Yu S, Oyarzun JR, Allen KR, McCormick JR, Han S, Kemp FW, Bogden JD, Lu Q, Gabbay S. No-react detoxification process: a superior anticalcification method for bioprostheses. *Ann Thorac Surg.* 1996;62(6):1724-1730.

208. Silliman CC, Wang M. The merits of in vitro versus in vivo modeling in investigation of the immune system. *Environ Tox Pharm.* 2006;21(2):123-134.

209. Akiyama SK, Yamada KM. Comparisons of evolutionarily distinct fibronectins: evidence for the origin of plasma and fibroblast cellular fibronectins from a single gene. *J Cell Biochem.* 1985;27(2):97-107.

210. Goto T, Wong KS, Brunette DM. Observation of Fibronectin Distribution on the Cell Undersurface Using Immunogold Scanning Electron Microscopy. *J. Histochem. Cytochem.* 1999;47(11):1487-1494.

211. Aybay C. Differential binding characteristics of protein G and protein A for Fc fragments of papain-digested mouse IgG. *Immunol Lett.* 2003;85(3):231-235.

212. Faustman D, Coe C. Prevention of xenograft rejection by masking donor HLA class I antigens. *Science.* 1991;252(5013):1700-1702.

213. Pakzaban P, Deacon TW, Burns LH, Dinsmore J, Isacson O. A novel mode of immunoprotection of neural xenotransplants: masking of donor major histocompatibility complex class I enhances transplant survival in the central nervous system. *Neuroscience.* 1995;65(4):983-996.

214. Schussler O, Shen M, Shen L, Carpentier SM, Kaveri S, Carpentier A. Effect of human immunoglobulins on the immunogenicity of porcine bioprostheses. *Ann Thorac Surg.* 2001;71(5 Suppl):S396-400.

215. Griffiths LG, Choe LH, Reardon KF, Dow SW, Christopher Orton E. Immunoproteomic identification of bovine pericardium xenoantigens. *Biomaterials.* 2008;29(26):3514-3520.

216. Ravetch JV, Bolland S. IgG Fc receptors. *Annu Rev Immunol.* 2001;19:275-290.

217. Schmidt RE, Gessner JE. Fc receptors and their interaction with complement in autoimmunity. *Immunol Lett.* 2005;100(1):56-67.

218. Allaire E, Bruneval P, Mandet C, Becquemin JP, Michel JB. The immunogenicity of the extracellular matrix in arterial xenografts. *Surgery.* 1997;122(1):73-81.

219. Wilhelmi MH, Mertsching H, Wilhelmi M, Leyh R, Haverich A. Role of inflammation in allogeneic and xenogeneic heart valve degeneration: immunohistochemical evaluation of inflammatory endothelial cell activation. *J Heart Valve Dis.* 2003;12(4):520-526.

220. Call SK, Kasow KA, Barfield R, Madden R, Leung W, Horwitz E, Woodard P, Panetta JC, Baker S, Handgretinger R, Rodman J, Hale GA. Total and Active Rabbit Antithymocyte Globulin (rATG;Thymoglobulin®) Pharmacokinetics in Pediatric

Patients Undergoing Unrelated Donor Bone Marrow Transplantation. *Biol Blood Marrow Transpl.* 2009;15(2):274-278.

221. Karsten Midtvedt PFBLAHDABLBTLIBB. Individualized T cell monitored administration of ATG versus OKT3 in steroid-resistant kidney graft rejection. *Clinical Transplantation.* 2003;17(1):69-74.